Title: The Physics of Unification

Author: Steven Howard Snyder

Email: steveinternetemail@yahoo.com

Abstract:

To date, a unification is needed with the application of Planck units which unifies not only the force of Newtonian gravity with the electromagnetic force and the strong and weak nuclear forces, but also one which includes quantum field theory and relativity. Herein, a unification as such is accomplished in which the mathematical terms of the conventional fields and the corresponding forces are unified into one general function in Planck units, and the geometry (including internal structure) and functionality of certain aspects of the respective unified field constructed therefrom are described. Accordingly, the geometry and functionality of the unified field are applied for describing certain aspects of electromagnetic, gravitational, and nuclear interaction along with certain aspects of elementary particles (including antiparticles), atoms, molecules, and, at the macroscopic scale, astronomical bodies.

GENERAL FUNCTION OF THE UNIFIED FIELD:

A general function of a unified field is formulated herein complemented by a theoretical internal structure which has been constructed for the posited unified field unlike the functions of the conventional forces of Newtonian gravity, the electromagnetic force, the strong and weak nuclear forces, and the functions of conventional relativistic spacetime. Wherein, first, equation (1A), which was designed especially for the purposes of the theory herein, is rewritten as a general exponential function which has the form shown in equation (1B):

$$f = z = \pm e^{\frac{1}{N}[n_1 \pm x + n_2 \pm y]}$$

Eq. (1A)

$$f = z = \pm e^{\left[\frac{1}{N}n_1 \pm x + \frac{1}{N}n_2 \pm y\right]}$$

Eq. (1B)

In which case, 1/N is a constant such that N=1, 2, 3,…; and n_1 and n_2 are constants such that $1< n_1 <2$ and $1>n_2>0$.

Now, substituting $\dfrac{2\pi(qvr)}{h_q}$ and $\dfrac{2\pi(mvr)}{h}$ for (x) and (y), respectively, in equation (1B) results in the following more specific function:

$$f = \pm e^{\left[\frac{1}{N}n_1\frac{\pm 2\pi(qvr)}{h_q} + \frac{1}{N}n_2\frac{\pm 2\pi(mvr)}{h}\right]}.$$ Eq. (2)

Here, (q) is charge, (v) is velocity, (r) is radius, (m) is mass, (π) is pi, and (h) is Planck's constant as applied for the mass aspect of the unified field, and (h_q) is a variation of sorts on Planck's constant which is applied theoretically for the charge aspect of the unified field as will be described more so below.

Equation (2) is expressed as follows when v=c:

$$f = \pm e^{\left[\frac{1}{N}n_1\frac{\pm 2\pi(qcr)}{h_q} + \frac{1}{N}n_2\frac{\pm 2\pi(mcr)}{h}\right]}.$$ Eq. (3A)

The (x) and (y) terms in the exponent (neglecting signs) can each be made approximately equal to a dimensionless value of one when using terms which include Planck units in both variables of the exponent, when h=2πmcr, and when applying the following charge to mass ratio in the (x) variable of the exponent:

$$\frac{\dfrac{(q_p)}{(m_p)}}{\dfrac{(q_p)}{(m_p)}} = \frac{\dfrac{(1.8755x10^{-18}C)}{(2.1765x10^{-8}kg)}}{\dfrac{(1.8755x10^{-18}C)}{(2.1765x10^{-8}kg)}} = 1.$$

Wherein, $\dfrac{2\pi(qcr)}{h_q} = \dfrac{2\pi(mcr)}{h}$ as shown by figures (1A) and (1B) as follows:

$$x = \frac{2\pi(qcr)}{hq} = \frac{2\pi(2.1765x10^{-8}kg)\dfrac{(1.8755x10^{-18}C)}{(2.1765x10^{-8}kg)}\dfrac{(1.6162x10^{-35}m)}{(5.3911x10^{-44}s)}(1.6162x10^{-35}m)}{\dfrac{(1.6162x10^{-35}m)^2(2.1765x10^{-8}kg)\dfrac{(1.8755x10^{-18}C)}{(2.1765x10^{-8}kg)}(5.3911x10^{-44}s)}{(5.3911x10^{-44}s)^2}} \approx 1$$

FIG. 1A

$$y = \frac{2\pi(mcr)}{h} = \frac{2\pi(2.1765x10^{-8}kg)\dfrac{(1.6162x10^{-35}m)}{(5.3911x10^{-44}s)}(1.6162x10^{-35}m)}{\dfrac{(1.6162x10^{-35}m)^2(2.1765x10^{-8}kg)(5.3911x10^{-44}s)}{(5.3911x10^{-44}s)^2}} \approx 1$$

FIG. 1B

Here, the (x) variable of the exponent in equation (3A) is made to represent the "charge" aspect of the function with the application of the respective charge to mass ratio, and, as will be shown later, the ratio will be useful for constructing an expression for theoretical and conventional electromagnetic potentials, etc.

Now, equation (3A) is made into unified field function (4A) by first taking equation (3A)

$$f = \pm e^{\left[\frac{1}{N}n_1\frac{\pm 2\pi(qcr)}{h_q} + \frac{1}{N}n_2\frac{\pm 2\pi(mcr)}{h}\right]}$$
Eq. (3A)

and rewriting it as Eq. (3B)

$$f = {}^{\pm}e^{\left[\frac{1}{N}n_1\frac{\pm 2\pi(qcr)}{h_q}\right]} * {}^{\pm}e^{\left[\frac{1}{N}n_2\frac{\pm 2\pi(mcr)}{h}\right]},$$
Eq. (3B)

and then reflecting the (x) variable (which relates to charge) while treating (c) and 1/N as constants, such that

$$f = {}^{\pm} c\frac{1}{N} * \ln\left[\frac{\pm n_1 * 2\pi(qr)}{h_q}\right] * {}^{\pm} e^{\left[\frac{1}{N} n_2 \frac{*\pm 2\pi(mcr)}{h}\right]}.$$

Finally, equation (4A) is produced as follows upon taking one partial derivative by keeping the exponential portion of the function which relates to the (y) variable (mass) constant:

$$f_x(x, y) = {}^{\pm}\frac{1}{N}\frac{h_q c}{n_1 * 2\pi(qr)} * {}^{\pm} e^{\left[\frac{1}{N} n_2 \frac{*\pm 2\pi(mcr)}{h}\right]}.$$
Eq. (4A)

In result, equation (4A) is a general unified field function which provides families of functions for the potential

of the unified field presented herein, and can be related to the conventional strong, weak, electromagnetic, and gravitational fields. Note that the forgoing reflection of the function, and the subsequent partial derivative thereof, is considered to be a mathematical representation of an important physical aspect of the oscillatory trajectory of the flow of mass-energy in the unified field as will be indicative later.

Equation (4A) can be applied to describe both theoretical and conventional nuclear, electromagnetic, and gravitational potentials. However, the essential difference between the function of equation (4A) and the functions of conventional Newtonian and Coulombic potentials resides in the presence of the exponential term.

In convention, the exponential term is present along with the inverse function in the function which describes nuclear potential (e.g., the Yukawa potential). In which case, the exponential term in the function of conventional nuclear potential is considered to approach a value of one as the mass in the exponent approaches a value of zero. While, the exponential term is absent in the functions which conventionally describe Newtonian gravitational potential and Coulombic electrostatic potential.

However, to the contrary, the exponential term is applied with the inverse function in the unified field function herein, and thus is included in the definition of not only the theoretical nuclear potential, but also included in the definition of the theoretical electromagnetic and gravitational potentials (effectively including modified forms of Newtonian and Coulombic potentials). Wherein, in the present theory, the exponential term only approaches a value of zero in expressions for electromagnetic and gravitational potentials (i.e., the potential is not normalized for the nuclear region as in convention). While, in physical terms, the exponential term plays an important role in the unified field function in allowing for the three dimensional spatial aspect of the function (i.e., the three dimensional spatial aspect of the oscillatory trajectory of the flow of mass-energy in the unified field) as will be indicative more so later.

Next, a generic theoretical unified field potential is achieved by first taking the absolute value of the function of equation (4A), and then taking the negative of the function for convention as shown in equation (4B) below:

$$f = - \left| \frac{\pm}{} \frac{1}{N} \frac{h_q c}{n_1 * 2\pi(qr)} * \pm e^{\left[\frac{1}{N} \frac{n_2 * \pm 2\pi(mcr)}{h} \right]} \right|.$$ Eq. (4B)

Then, a theoretical unified field potential representing a portion of the unified field is achieved in equation (4C) by applying the following member functions from the families of functions in equation (4B)

$$f = - \left| \frac{+}{} \frac{1}{N} \frac{h_q c}{n_1 * 2\pi(qr)} * + e^{\left[\frac{1}{N} \frac{n_2 * - 2\pi(mcr)}{h} \right]} \right|,$$

or

$$f = - \frac{1}{N} \frac{h_q c}{n_1 * 2\pi(qr)} * e^{\left[\frac{1}{N} \frac{n_2 * - 2\pi(mcr)}{h} \right]}.$$ Eq. (4C)

Note that the signs used for the families of functions in equation (4A) pertain to the signs on the axes which relate to the functions, while the sign of the function as a whole in equation (4C) relates to the direction of potential in conventional terms.

Next, the value of the theoretical unified potential function in equation (4C) approximately equals $-\frac{1}{2}c^2$ when 1/N is considered equal to one, and $n_1 \approx 2$ and $n_2 \approx 0$, such that

$$ f = \frac{{}^-h_q c}{\approx 4\pi(qr)} * e^{\left[\frac{\approx {}^- 0 * 2\pi(mcr)}{h}\right]} \approx {}^-\frac{1}{2}c^2 , $$

or

$$ f = \frac{{}^-h_q c}{\approx 4\pi(qr)} * e^{\left[\frac{\approx {}^- 0\pi(mcr)}{h}\right]} \approx {}^-\frac{1}{2}c^2 . \qquad \text{Eq. (4D)} $$

Wherein, equation (4D) is considered to represent one half of one portion of the unified field potential functions when $n_1 \approx 2$ and $n_2 \approx 0$, as will be elaborated upon later.

Now, since $\dfrac{2\pi qcr}{h_q} = \dfrac{2\pi mcr}{h} \approx 1$, then $\dfrac{q}{h_q} = \dfrac{m}{h}$ and $\dfrac{h_q}{q} = \dfrac{h}{m}$. Wherein, after taking the gradient of equation (4D), breaking the result down into perpendicular vector components, and then substituting $\dfrac{h}{m}$ for

$\dfrac{h_q}{q}$ in one component, equation (4D) can be made into equation (5A) in terms of the sum of the squares of the electromagnetic (electric charge) and gravitational (mass) gradient components of the respective unified field gradient of the given portion of the unified field (when $n_1 \approx 2$ and $n_2 \approx 0$):

$$\left(\frac{1}{\sqrt{2}}\frac{^-h_q c}{\approx 4\pi(qr^2)} * e^{\left[\frac{\approx^- 0\pi(mcr)}{h}\right]}\right)^2 + \left(\frac{1}{\sqrt{2}}\frac{^-hc}{\approx 4\pi(mr^2)} * e^{\left[\frac{\approx^- 0\pi(mcr)}{h}\right]}\right)^2 = \left(\frac{^-h_q c}{\approx 4\pi(qr^2)} * e^{\left[\frac{\approx^- 0\pi(mcr)}{h}\right]}\right)^2 ,$$

Eq. (5A)

or, according to the Pythagorean theorem, one half of the negative of the gradient (i.e., one half of the negative of the negative gradient) of the respective unified field portion can be written in equation (5B) as:

$$\frac{^-1}{\approx 2}\nabla\varphi \text{ (unified field gradient portion)} = ^-\sqrt{\left(\frac{1}{\sqrt{2}}\frac{^-h_q c}{\approx 4\pi(qr^2)} * e^{\left[\frac{\approx^- 0\pi(mcr)}{h}\right]}\right)^2 + \left(\frac{1}{\sqrt{2}}\frac{^-hc}{\approx 4\pi(mr^2)} * e^{\left[\frac{\approx^- 0\pi(mcr)}{h}\right]}\right)^2} =$$

$$\frac{^-h_q c}{\approx 4\pi(qr^2)} * e^{\left[\frac{\approx^- 0\pi(mcr)}{h}\right]}.$$

Eq. (5B)

Here (∇) is gradient, and $\varphi = \dfrac{^-h_q c}{2\pi(qr)} * e^{\left[\frac{\approx^- 0\pi(mcr)}{h}\right]} = \dfrac{^-K_T q}{r} * e^{\left[\frac{\approx^- 0\pi(mcr)}{h}\right]}$. Wherein, K_T is a theoretical precursor to the conventional electrostatic constant K_c as will be described more so later.

The theoretical gravitational gradient component of the unified field can be related to, for example, the conventional Newtonian gravitational potential. Wherein, in terms of the respective theoretical gravitational

potential, $\dfrac{^{-}hc}{\approx 4\pi(mr)} * e^{\left[\frac{\approx^{-}0\pi(mcr)}{h}\right]} \approx ^{-}\dfrac{1}{2}c^2$ when

$h = 2\pi mcr \approx 2\pi(2.1765x10^{-8})\left(\dfrac{1.6162x10^{-35}}{5.3911x10^{-44}}\right)(1.6162x10^{-35}) = 6.6258x10^{-34}$, such that $e^{\left[\frac{\approx^{-}0\pi(mcr)}{h}\right]} \approx 1$ and

the units in $e^{\left[\frac{\approx^{-}0\pi(mcr)}{h}\right]}$ cancel, in which case the exponential term can be dropped, and such that

$\dfrac{^{-}hc}{\approx 4\pi(mr)} = \dfrac{^{-}2\pi mc^2 r}{\approx 4\pi(mr)} \approx ^{-}\dfrac{1}{2}c^2$. Also, figure (2A) shows the production of approximately one half of the

conventional gravitational potential, i.e., $\approx ^{-}\dfrac{1}{2}G_T * \dfrac{m}{r}$, after the cancellation of certain units in $^{-}\dfrac{hc}{\approx 4\pi(mr)}$

(while neglecting the sign).

$$\dfrac{hc}{\approx 4\pi(mr)} \Rightarrow \dfrac{(kg*m^2 * \cancel{s})}{(s)^2}\dfrac{(m)}{(\cancel{s})}\dfrac{(1)}{(kg*m)} \Rightarrow \dfrac{(m^3)}{(kg*s^2)}\dfrac{(kg)}{(m)} \Rightarrow \approx \dfrac{1}{2}G_T\dfrac{(kg)}{(m)}$$

FIG. 2A

In which case, (G_T) takes on the same numerical value as the conventional gravitational constant, i.e.,

$6.6\,x\,10^{-11}$, using Planck units as shown below:

$$G_{Planck} = \frac{(m)^3}{(kg)(s)^2} = \frac{(l_p)^3}{(m_P)(t_p)^2} = \frac{(1.6162\,x\,10^{-35})^3}{(2.1765\,x\,10^{-8})(5.3911\,x\,10^{-44})^2} = 6.6738\,x\,10^{-11}\,.$$

Similarly, the theoretical electromagnetic gradient of the unified field can be related to, for example, the conventional Coulombic potential. Wherein, an equivalent argument for the terms of the respective

theoretical electromagnetic potential can be made in which $\dfrac{^-h_q c}{\approx 4\pi(qr)} * e^{\left[\frac{\approx^- 0\pi(mcr)}{h}\right]} \approx ^-\dfrac{1}{2}c^2$ when $h_q=h=2\pi mcr$,

such that $e^{\left[\frac{\approx^- 0\pi(mcr)}{h}\right]} \approx 1$, in which case the exponential term can be dropped, and such that

$\dfrac{^-h_q c}{\approx 4\pi(qr)} = \dfrac{^-hc}{\approx 4\pi(mr)} = \dfrac{^-2\pi mc^2 r}{\approx 4\pi(mr)} \approx ^-\dfrac{1}{2}c^2$. Wherein, $\dfrac{^-h_q c}{\approx 4\pi(qr)} * e^{\left[\frac{\approx^- 0\pi(mcr)}{h}\right]}$ is considered the

theoretical electromagnetic potential counterpart to the theoretical gravitational potential shown before.

Moreover, similarly, figure (2B) shows the conversion of the units of theoretical electromagnetic potential

$\dfrac{^-h_q c}{\approx 4\pi(qr)}$ into the units of conventional Coulombic potential, including the units of the conventional

electrostatic constant, i.e., the units of $\dfrac{N*m^2}{C^2}$, for the production of a theoretical approximation of one half of

the conventional electrostatic potential, i.e., $\approx ^-\dfrac{1}{2}K_C * \dfrac{q}{r}$, after the cancellation of certain units while again

applying the following charge to mass ratio $\frac{(q_p)}{(m_p)}$ which has the units $\frac{(C)}{(kg)}$ (and also while neglecting the

sign):

$$\frac{hc\frac{(q_p)}{(m_p)}}{\approx 4\pi(mr)\frac{(q_p)}{(m_p)}\frac{(q_p)}{(m_p)}} \Rightarrow \frac{h_q c}{\approx 4\pi(qr)\frac{(q_p)}{(m_p)}} \Rightarrow \frac{\cancel{(kg)}\frac{(C)}{\cancel{(kg)}}(m)^2\cancel{(s)}\frac{(m)}{\cancel{(s)}}}{(s)^2\cancel{(kg)}\frac{(C)}{\cancel{(kg)}}\frac{(C)}{(kg)}(m)} \Rightarrow \frac{(N)*(m)^2}{(C)^2}\frac{(C)}{(m)} \Rightarrow \approx \frac{1}{2}K_C\frac{(C)}{(m)}$$

FIG. 2B

Now, substituting $\approx \frac{^-1}{2}K_T\frac{q}{r}$ for $\frac{^-h_q c}{\approx 4\pi(qr)}$ in equation (4D) provides for a different expression for

theoretical unified potential:

$$f = \frac{^-1}{\approx 2}K_T\frac{q}{r}*e^{\left[\frac{\approx^- 0\pi(mcr)}{h}\right]} \approx \frac{^-1}{2}c^2$$

which can be rewritten as Eq. (6)

$$f = \frac{^-1}{\approx 2}K_T(q)*\frac{e^{\left[\frac{\approx^- 0\pi(mcr)}{h}\right]}}{r} \approx \frac{^-1}{2}c^2.$$ Eq. (6)

Here, equation (6) is considered to be another expression which represents one half of the given portion of the theoretical unified potential. While, a whole portion of theoretical unified potential (when $n_1 \approx 2$ and $n_2 \approx 0$) is achieved by adding two equivalent portions of the function from equation (6) as shown in equation (7A) as follows:

$$V_{(\text{whole unified field potential portion})} = {}^{-}\frac{1}{\approx 2}K_T(q) * \frac{e^{\left[\frac{\approx^{-}0\pi(mcr)}{h}\right]}}{r} + {}^{-}\frac{1}{\approx 2}K_T(q) * \frac{e^{\left[\frac{\approx^{-}0\pi(mcr)}{h}\right]}}{r} \approx$$

$${}^{-}1K_T(q) * \frac{e^{\left[\frac{{}^{-}0\pi(mcr)}{h}\right]}}{r} \approx {}^{-}1c^2$$

Eq. (7A)

or

$$V_{(\text{whole unified field potential portion})} \approx {}^{-}K_T(\frac{q}{2}+\frac{q}{2}) * \frac{e^{\left[\frac{{}^{-}0\pi(mcr)}{h}\right]}}{r} \approx {}^{-}K_T(q) * \frac{e^{\left[\frac{{}^{-}0\pi(mcr)}{h}\right]}}{r} \approx {}^{-}1c^2 .$$

Then, after substituting ${}^{-}\dfrac{1}{\approx 2}G_T(m) * \dfrac{e^{\left[\frac{\approx^{-}0\pi(mcr)}{h}\right]}}{r}$ for ${}^{-}\dfrac{1}{\approx 2}K_T(q) * \dfrac{e^{\left[\frac{\approx^{-}0\pi(mcr)}{h}\right]}}{r}$ for one

portion (addend) in equation (7A), a different expression for a whole portion of theoretical unified potential is

formulated in equation (7B) by the addition of theoretical electromagnetic and gravitational potential functions as follows:

$$V_{\text{(whole unified field potential portion)}} = {}^{-}\frac{1}{\approx 2}K_T(q)*\frac{e^{\left[\frac{\approx^{-}0\pi(mcr)}{h}\right]}}{r} + {}^{-}\frac{1}{\approx 2}G_T(m)*\frac{e^{\left[\frac{\approx^{-}0\pi(mcr)}{h}\right]}}{r} \approx$$

$${}^{-}1K_T(q)*\frac{e^{\left[\frac{^{-}0\pi(mcr)}{h}\right]}}{r} \approx {}^{-}1c^2$$

Eq. (7B)

when $(n_1) \approx 2$ and $(n_2) \approx 0$.

While when $(n_1) \approx 1$ and $(n_2) \approx 1$, then:

$$V_{\text{(whole unified field potential portion)}} = {}^{-}\frac{1}{\approx 1}K_T(q)*\frac{e^{\left[\frac{\approx^{-}2\pi(mcr)}{h}\right]}}{r} + {}^{-}\frac{1}{\approx 1}G_T(m)*\frac{e^{\left[\frac{\approx^{-}2\pi(mcr)}{h}\right]}}{r} \approx$$

$${}^{-}2K_T(q)*\frac{e^{\left[\frac{^{-}2\pi(mcr)}{h}\right]}}{r}.$$

Eq. (7C)

Note that an equation for a whole portion of unified potential by the addition of electromagnetic and gravitational potential functions for when (n_1) and (n_2) are any of their other complementary values can also be achieved similarly.

Next, returning to gradients, upon substituting $\approx \dfrac{\bar{\,}1}{2} K_T \dfrac{q}{r^2}$ for $\dfrac{\bar{\,}h_q c}{\approx 4\pi(qr^2)}$ and $\approx \dfrac{\bar{\,}1}{2} G_T \dfrac{m}{r^2}$

for $\dfrac{\bar{\,}hc}{\approx 4\pi(mr^2)}$ in the components in equation (5A), and upon substituting $\approx \dfrac{\bar{\,}1}{2} K_T \dfrac{q}{r^2}$ for $\dfrac{\bar{\,}h_q c}{\approx 4\pi(qr^2)}$ in

the respective sum in equation (5A), another expression is provided in equation (8A) for the square of one half

of the total gradient of the given unified field portion for when $n_1 \approx 2$ and $n_2 \approx 0$:

$$\left(\bar{\,} \frac{1}{\approx 2\sqrt{2}} K_T(q) * \frac{e^{\left[\frac{\approx\bar{\,}0\pi(mcr)}{h}\right]}}{r^2} \right)^2 + \left(\bar{\,} \frac{1}{\approx 2\sqrt{2}} G_T(m) * \frac{e^{\left[\frac{\approx\bar{\,}0\pi(mcr)}{h}\right]}}{r^2} \right)^2 \approx \left(\bar{\,} \frac{1}{2} K_T(q) * \frac{e^{\left[\frac{\bar{\,}0\pi(mcr)}{h}\right]}}{r^2} \right)^2 .$$

Eq. (8A)

While the square of the whole unified field gradient of the given portion of the unified field in related terms is

considered to be formulated by adding two equivalent gradients in the addend squares of the gradient functions

from equation (8A) as follows:

$$\left(-\frac{1}{\approx 2\sqrt{2}} K_T(q) * \frac{e^{\left[\frac{\approx^{-}0\pi(mcr)}{h}\right]}}{r^2} + \frac{1}{\approx 2\sqrt{2}} K_T(q) * \frac{e^{\left[\frac{\approx^{-}0\pi(mcr)}{h}\right]}}{r^2} \right)^2 +$$

$$\left(-\frac{1}{\approx 2\sqrt{2}} G_T(m) * \frac{e^{\left[\frac{\approx^{-}0\pi(mcr)}{h}\right]}}{r^2} + \frac{1}{\approx 2\sqrt{2}} G_T(m) * \frac{e^{\left[\frac{\approx^{-}0\pi(mcr)}{h}\right]}}{r^2} \right)^2 \approx \left(^{-}1 K_T(q) * \frac{e^{\left[\frac{^{-}0\pi(mcr)}{h}\right]}}{r^2} \right)^2$$

such that

$$\left(-\frac{1}{\approx \sqrt{2}} K_T(q) * \frac{e^{\left[\frac{\approx^{-}0\pi(mcr)}{h}\right]}}{r^2} \right)^2 + \left(-\frac{1}{\approx \sqrt{2}} G_T(m) * \frac{e^{\left[\frac{\approx^{-}0\pi(mcr)}{h}\right]}}{r^2} \right)^2 \approx \left(^{-}1 K_T(q) * \frac{e^{\left[\frac{^{-}0\pi(mcr)}{h}\right]}}{r^2} \right)^2 ,$$

Eq. (8B)

and the negative of the whole gradient (i.e., the negative of the whole negative gradient) of the given portion of the unified field can be written as

$$\sqrt{\left(\approx\frac{-1}{\sqrt{2}}\bar{K}_T(q)*\frac{e^{\left[\frac{\approx^-0\pi(mcr)}{h}\right]}}{r^2}\right)^2 + \left(\approx\frac{-1}{\sqrt{2}}\bar{G}_T(m)*\frac{e^{\left[\frac{\approx^-0\pi(mcr)}{h}\right]}}{r^2}\right)^2} \approx {}^-1\bar{K}_T(q)*\frac{e^{\left[\frac{^-0\pi(mcr)}{h}\right]}}{r^2}.$$

Eq. (8C)

Here, the addition of two equivalent functions in equation (8B) involves the vector addition of two portions of the unified field which can be more clearly understood by referring to the geometry of the unified field described later as with respect to, in particular, figures 7A, 7B, 7C, 7D, and 7E. Furthermore, note that an equation for the square of the whole gradient of a given portion of the unified field for when (n_1) and (n_2) are any of their other complementary values can also be achieved similarly.

Nevertheless, the theoretical total potential of a static elementary particle can be considered to be arrived at by the following summation shown in equation (9A) (for eight octants):

$$V_{(\text{static particle total potential})} = 4*\sum V = 4*\left[\left(\frac{1}{n_1}{}^-\bar{K}_T(q)*\frac{e^{\left[\frac{n_2*^-2\pi(mcr)}{h}\right]}}{r}+\frac{1}{n_1}{}^-\bar{K}_T(q)*\frac{e^{\left[\frac{n_2*^-2\pi(mcr)}{h}\right]}}{r}\right)+\right.$$

$$\left.\left(\frac{1}{n_1}{}^-\bar{K}_T(q)*\frac{e^{\left[\frac{n_2*^-2\pi(mcr)}{h}\right]}}{r}+\frac{1}{n_1}{}^-\bar{K}_T(q)*\frac{e^{\left[\frac{n_2*^-2\pi(mcr)}{h}\right]}}{r}\right)+\ldots\right] \approx 1\frac{{}^-\bar{K}_T(q)}{r}$$

Eq. (9A)

wherein,

$$4\frac{\approx^{-}K_T(q)}{r}*\frac{1}{e^{\left[\frac{\approx 0\pi(mcr)}{h}\right]}}-8\frac{\approx^{-}K_T(q)}{r}*\frac{1}{e^{\left[\frac{\approx 2\pi(mcr)}{h}\right]}}\approx 1\frac{^{-}K_T(q)}{r}$$

or

$$4\frac{\approx^{-}K_T(q)}{r}-3\frac{\approx^{-}K_T(q)}{r}\approx 1\frac{^{-}K_T(q)}{r} \qquad\qquad \text{Eq. (9B)}$$

In the summation hereinbefore, (V) is potential, and (n_1) and (n_2) are the same complementary pair for a pair of terms inside parentheses, while (n_1) goes from ≈ 2 to ≈ 1 as (n_2) goes from ≈ 0 to ≈ 1 sequentially from one parenthetical term to the next in the summation.

While furthermore, the theoretical total potential of a system (e.g., a system of bonded nucleons) can be considered to be arrived at by the following summation shown in equation (9C):

$$V_{(\text{system total potential})}=\sum 4*V=4*\left[\left(\frac{1}{n_1}{}^{-}K_T(q)*\frac{e^{\left[\frac{n_2*^{-}2\pi(mcr)}{h}\right]}}{r}+\frac{1}{n_1}{}^{-}K_T(q)*\frac{e^{\left[\frac{n_2*^{-}2\pi(mcr)}{h}\right]}}{r}\right)+\ldots\right]+$$

$$4*\left[\left(\frac{1}{n_1}{}^{-}K_T(q)*\frac{e^{\left[\frac{n_2*^{-}2\pi(mcr)}{h}\right]}}{r}+\frac{1}{n_1}{}^{-}K_T(q)*\frac{e^{\left[\frac{n_2*^{-}2\pi(mcr)}{h}\right]}}{r}\right)+\ldots\right]+\ldots$$

Eq. (9C)

Wherein, in the summation shown in equation (9C), (n_1) and (n_2) are the same complementary pair for a pair of terms inside parentheses, and (n_1) goes from ≈ 2 to ≈ 1 as (n_2) goes from ≈ 0 to ≈ 1 sequentially from one parenthetical term to the next in the bracketed terms (one quarter particle potentials). In which case, here, the term 1/N is excluded since it is considered to cancel in the summation of whole particles.

Moreover, the negative of the negative gradient extending out from an elementary particle or a system of particles can be written as:

$$ {}^{-}\nabla \varphi_{(systeml)} = {}^{-}\left(\frac{\partial \varphi}{\partial x}\hat{i} + \frac{\partial \varphi}{\partial y}\hat{j} + \frac{\partial \varphi}{\partial z}\hat{k} \right) \qquad \text{Eq. (10A)} $$

and the respective Laplacian can be written as:

$$ \nabla^2 \varphi = \left(\frac{\partial^2}{\partial x^2} + \frac{\partial^2}{\partial y^2} + \frac{\partial^2}{\partial z^2} \right)\varphi \qquad \text{Eq. (10B)} $$

In which case, ∇ is gradient and ∇^2 is the Laplacian such that in both cases

$$ \varphi = {}^{-}8\frac{1}{n_1}\sum K_T(q) * \frac{e^{\left[\frac{n_2 * {}^{-}2\pi(mcr)}{h}\right]}}{r} $$, in which case $1 < n_1 < 2$, and, correspondingly, $1 > n_2 > 0$; or, relativistically,

$$ \varphi = {}^{-}8\frac{1}{n_1}\sum \gamma_T{}^2 K_T(q) * \frac{e^{\left[\frac{1}{\gamma_T{}^2}\frac{n_2 * {}^{-}2\pi(mcr)}{h}\right]}}{r} $$, in which case $1 < n_1 < 2$, and, correspondingly, $1 > n_2 > 0$ (wherein the

relativistic version of the function will be derived later as pertains to equation 14A).

Note that when using charge in a gradient or a Laplacian related equation herein, one must use "charge" in the following form:

$$q_T = \frac{m_p \dfrac{(q_p)}{(m_p)}}{\dfrac{(q_p)}{(m_p)}}$$

Wherein, $\bar{G}_T(Q_T * q_T) \equiv \bar{K}_C(Q_C * q_C)$ when using the form of charge shown above (such that $Q_T = \Sigma q_T$). This form of charge is needed because $(1/q)$ and the charge to mass ratio in the denominator of K_T in the potential (φ) is not squared upon taking the gradient or the Laplacian (which, for example, is unlike the process involved in the formulation of equation 12 shown later).

Also, note that the manner in which force is obtained from the negative of the gradient in equation (10A) is different from the manner in which forces are obtained from equations (11B), (12), and (13) in that the mass (or charge) and the exponential term are squared (in the denominator) in the formation of force for equations (11B), (12), and (13) unlike in equation (10A). Thus, the negative of the gradient of equation (10A) and the Laplacian of equation (10B) need to be multiplied by not only a mass (or a charge) term, but also multiplied by an exponential term in order to achieve their respective results as, for example, shown (in relativistic form) for a force derived from a gradient below (in contrast to the squaring process by which force is derived for equation 13):

$$\approx^- 4 * \frac{1}{4} G_T(m) * \frac{e^{\left[\frac{0^* \approx^- 0\pi(mcr)}{h}\right]}}{r^2} * \left(M * e^{\left[\frac{0^* \approx^- 0\pi(mcr)}{h}\right]}\right) \approx^- G_T(m*M) * \frac{e^{\left[2 * \left(\frac{0^* \approx^- 0\pi(mcr)}{h}\right)\right]}}{r^2} \approx$$

$$\approx^- \frac{G_T(m*M)}{r^2} = g_F.$$

Note that the relativistic (¼) factor, and the relativistic zero factors in the exponents, are described later

following figure 6D. Also, refer to equations (15E), (15F), and (15G) for the derivation of the forgoing force

equation and its respective functions.

Now, here, note how the form of the terms of a time independent particle in quantum mechanics

support the form of the potential of the unified field presented herein:

$$\psi(x) = Ae^{-ikx} = Ae^{\frac{-i2\pi ncx}{h}} = Ae^{\frac{-i2\pi mcr}{h}} \quad \text{(when k=2πmc/h and x=r)}$$

Wherein, (A) can be a scalar amplitude, such that, for example, $A = \frac{1}{2}kx^2 \equiv mgh$ which pertains to $\approx^- G_T m/r$

(when the other mass of potential energy is positioned at infinity) which, herein, is equivalent to $\approx^- K_T q/r$; or

(A) can be a vector amplitude, e.g., E (electric field vector), i.e., $^- K_C q/r^2$, which is the negative of the gradient

of the potential $^- K_C q/r$ which herein relates to $\approx^- K_T q/r$ which again, herein, is equivalent to $\approx^- G_T m/r$.

Next, a general theoretical unified force equation (11B) pertaining to a portion of the unified field,

which can be related to the conventional strong force (including the conventional residual nuclear force), the

conventional weak force, and the conventional electromagnetic and gravitational forces, can be achieved by

taking the derivative of the resulting potential of equation (4C) as follows upon substituting $\dfrac{1}{N}\dfrac{1}{n_1}\overline{K}_T\dfrac{q}{r}$ for

$\dfrac{1}{N}\dfrac{\overline{h}_q c}{n_1 * 2\pi(qr)}$ in equation (4C) (wherein the derivative is denoted here as taking the second regular

derivative of a first regular derivative):

$$f' = \frac{1}{N}\frac{1}{n_1}\overline{K}_T(q) * \frac{e^{\left[\frac{1}{N}\frac{n_2 *\overline{} 2\pi(mcr)}{h}\right]}}{r} \qquad \text{Eq. (4C)}$$

$$D_u f' = \frac{1}{N}\frac{1}{n_1}K_r * D_u \overline{} \frac{1}{\left(\dfrac{1}{q}\dfrac{(q_p)}{(m_p)} * r * e^{\left[\frac{1}{N}\frac{n_2 * 2\pi(mcr)}{h}\right]}\right)}$$

wherein K_r is the remainder of K_T without the charge to mass ratio $\dfrac{(q_p)}{(m_p)}$, such that

$$f'' = \frac{1}{N}\frac{1}{n_1}K_r * \overline{} \frac{1}{\left(\dfrac{1}{q}\dfrac{(q_p)}{(m_p)} * r * e^{\left[\frac{1}{N}\frac{n_2 * 2\pi(mcr)}{h}\right]}\right)^2} . \qquad \text{Eq. (11A)}$$

Here, (q) in the numerator is rewritten and placed in the denominator as $\left(\dfrac{1}{q}\right)$ along with $(r), \dfrac{(q_p)}{(m_p)}$

(the charge to mass ratio), and $e^{\left[\frac{1}{N}\frac{n_2*2\pi(mcr)}{h}\right]}$, such that $\left(\frac{1}{q}\frac{(q_p)}{(m_p)}*r*e^{\left[\frac{1}{N}\frac{n_2*2\pi(mcr)}{h}\right]}\right)=u$ in the function

$f = \frac{1}{N}\frac{1}{n_1}K_r\frac{^-1}{u}$. In which case, for the derivation of equation (11A),

$D_u\frac{1}{N}\frac{1}{n_1}K_r\frac{^-1}{u} = \frac{1}{N}\frac{1}{n_1}K_r\frac{1}{u^2} = \frac{1}{N}\frac{1}{n_1}K_r\frac{1}{\left(\frac{1}{q}\frac{(q_p)}{(m_p)}*r*e^{\left[\frac{1}{N}\frac{n_2*2\pi(mcr)}{h}\right]}\right)^2}$,

such that

$$f'' = \frac{^-1}{N}\frac{1}{n_1}K_C\frac{q^2}{r^2}*e^{\left[2*\left(\frac{1}{N}\frac{n_2*^-2\pi(mcr)}{h}\right)\right]}$$

or

$$f'' = \frac{^-1}{N}\frac{1}{n_1}K_C(q^2)*\frac{e^{\left[2*\left(\frac{1}{N}\frac{n_2*^-2\pi(mcr)}{h}\right)\right]}}{r^2}$$
Eq. (11B)

Wherein, the negative of the resulting derivative was taken for convention, and the resulting force is in newtons

when h=2πmcr, such that the units of $\left[2*\left(\frac{1}{N}\frac{n_2*^-2\pi(mcr)}{h}\right)\right]$ in the exponent cancel.

Then, with respect to the sum in equation (7B), $f'' \approx {}^{-}\dfrac{1}{N} 1 K_C (q^2) * \dfrac{e^{\left[2 * \left(\frac{1}{N} \frac{{}^{-}0\pi(mcr)}{h}\right)\right]}}{r^2}$ when $(n_1) \approx 2$ and

$(n_2) \approx 0$; and, with respect to the sum in equation (7C), $f'' \approx {}^{-}\dfrac{1}{N} 2 K_C (q^2) * \dfrac{e^{\left[2 * \left(\frac{1}{N} \frac{{}^{-}2\pi(mcr)}{h}\right)\right]}}{r^2}$ when

$(n_1) \approx 1$ and $(n_2) \approx 1$.

A theoretical electromagnetic force equation (12) for the unified field (i.e., a force equation which can

be related to, in particular, the conventional electromagnetic force, e.g., at weak field and low velocity), and a

theoretical gravitational force equation (13) for the unified field (i.e., a force equation which can be related to,

in particular, the conventional Newtonian gravitational force, e.g., at weak field and low velocity), can both be

produced from equation (11B), or can both be produced by applying a similar second derivative process to each

of the two halves of potential which produce the sum of equation (7B) as shown below (while 1/N is considered

equal to one):

$$V_{(\text{whole unified field potential portion})} = {}^{-}\dfrac{1}{\approx 2} K_T(q) * \dfrac{e^{\left[\frac{\approx {}^{-}0\pi(mcr)}{h}\right]}}{r} + {}^{-}\dfrac{1}{\approx 2} G_T(m) * \dfrac{e^{\left[\frac{\approx {}^{-}0\pi(mcr)}{h}\right]}}{r} \approx$$

$${}^{-}1 K_T(q) * \dfrac{e^{\left[\frac{{}^{-}0\pi(mcr)}{h}\right]}}{r} \approx {}^{-}1c^2.$$

Eq. (7B)

In which case, electromagnetic force equation (12) is produced upon taking the second derivative of the charge

portion

$$D_u \frac{1}{\approx 2} K_r \overset{-1}{\underset{u}{}} = \frac{1}{\approx 2} K_r \frac{1}{u^2} = \frac{1}{\approx 2} K_r \frac{1}{\left(\dfrac{1}{q} \dfrac{(q_p)}{(m_p)} * r * e^{\left[\frac{\approx 0\pi(mcr)}{h} \right]} \right)^2} ,$$

such that

$$f'' \approx \overset{-1}{\underset{2}{}} K_C(q^2) * \frac{e^{\left[2 * \left(\frac{-0\pi(mcr)}{h} \right) \right]}}{r^2} = em_F , \qquad\qquad \text{Eq. (12)}$$

and gravitational force equation (13) is produced upon taking the second derivative of the mass portion

$$D_u \frac{1}{\approx 2} G_T \overset{-1}{\underset{u}{}} = \frac{1}{\approx 2} G_T \frac{1}{u^2} = \frac{1}{\approx 2} G_T \frac{1}{\left(\dfrac{1}{m} * r * e^{\left[\frac{\approx 0\pi(mcr)}{h} \right]} \right)^2} ,$$

such that

$$f'' \approx \overset{-1}{\underset{2}{}} G_T(m^2) * \frac{e^{\left[2 * \left(\frac{-0\pi(mcr)}{h} \right) \right]}}{r^2} = g_F . \qquad\qquad \text{Eq. (13)}$$

Wherein, $1/n_1$, i.e., $\approx\frac{1}{2}$, is treated as a constant in these cases, and, here also, the negatives of the resulting

derivatives were taken for convention.

$$K_r \frac{1}{\left(\dfrac{1}{q}\dfrac{(q_p)}{(m_p)}*r*e^{\left[\frac{\approx 0\pi(mcr)}{h}\right]}\right)^2} = G_T \frac{1}{\left(\dfrac{1}{m}*r*e^{\left[\frac{\approx 0\pi(mcr)}{h}\right]}\right)^2}$$ in the forgoing

derivatives since $\dfrac{1}{q}\dfrac{(q_p)}{(m_p)} = \dfrac{1}{m}$ when $(q) = (q_p)$ and $(m) = (m_p)$. Also, note that the additional charge to

mass ratio applied in the denominator in (K_C) in figure (2B) is also derived in the forgoing second derivative

which pertains to equation (12) along with the other charge to mass ratio in the numerator (which was brought

down into the denominator with 1/q) , such that only a value of one is effectively applied, which, accordingly,

does not affect the respective function (as the first set of charge to mass ratios applied in figure 1A).

Furthermore, note that the squaring of the potential functions in the process of taking the second derivatives in

order to obtain the electromagnetic and gravitational force functions are considered to pertain to the symmetry

of the internal structure, and the self interaction of virtual particles (described later) at Planck scale in the

unified field. Moreover, notice that each of two equivalent unified field potential portions (i.e., the

electromagnetic and gravitational potential portions) provides potential for one half of the force needed to create

a whole respective force of interaction, as implied by the gravitational potentials in the gravitational lensing

effect described later.

Nevertheless, consider the following equivalence of the electromagnetic and gravitational forces from

the sum of two half portions of each force at Planck scale from equations (12) and (13) when $(n_1) \approx 2$ and

$(n_2) \approx 0$, wherein the exponential terms for the electromagnetic and gravitational force functions are each

approximately one, and thus dropped in this case:

$$\approx {}^-K_C \frac{q^2}{r^2} \approx {}^- 8.98x10^9 * \frac{(1.87x10^{-18})^2}{(1.61x10^{-35})^2} \approx {}^- 1.21x10^{44} \approx F_P$$

$$\approx {}^-G_T \frac{m^2}{r^2} \approx {}^- 6.67x10^{-11} * \frac{(2.17x10^{-8})^2}{(1.61x10^{-35})^2} \approx {}^- 1.21x10^{44} \approx F_P$$

when $(q) = (q_p)$, $(m) = (m_p)$, and $(r) = (l_p)$

Now, consider the relative force strengths shown below with respect to the following approximate equivalences

of $\hbar c$ in Planck units taken from the "fundamental" forces established above:

$$\approx K_C q^2 \approx 8.98x10^9 * (1.87x10^{-18})^2 \approx 3.14x10^{-26} \approx \hbar c$$

$$\approx G_T m^2 \approx 6.67x10^{-11} * (2.17x10^{-8})^2 \approx 3.14x10^{-26} \approx \hbar c$$

when $(q) = (q_p)$ and $(m) = (m_p)$

For conventional gravitational force strength:

$$\frac{G_C (\text{proton mass})^2}{\approx K_C (q_P)^2} \approx \frac{6.67x10^{-11} * (1.67x10^{-27})^2}{8.98x10^{+9} * (1.87x10^{-18})^2} \approx 5.92x10^{-39}$$

For conventional electromagnetic force strength:

$$\frac{K_C (\text{electron charge})^2}{\approx K_C (q_P)^2} \approx \frac{8.98x10^{+9} * (1.60x10^{-19})^2}{8.98x10^{+9} * (1.87x10^{-18})^2} \approx 7.32x10^{-3}$$

For conventional weak force strength:

$$\frac{(\text{electron charge})^2}{\approx K_C(q_P)^2} \approx \frac{(1.60x10^{-19})^2}{8.98x10^{+9} * (1.87x10^{-18})^2} \approx 8.15x10^{-13}$$

For conventional strong force strength:

$$\frac{K_C(q_P)^2}{\approx K_C(q_P)^2} \approx \frac{8.98x10^{+9} * (1.87x10^{-18})^2}{8.98x10^{+9} * (1.87x10^{-18})^2} \approx 1.$$

Here, the agreement of these relative force strengths with convention with respect to the terms taken from the

fundamental forces at Planck scale established above, which are approximately equal to $\hbar c$, support the values

and forms of the functions of the present theory of unification. While, the problem pertaining to gravitational

interactions at Planck "length scale" is considered to be addressed by the microscopic applicability of the

unified field function at Planck scale, the quantum mechanical equivalence of the form of the function with the

time independent wave function (and the time dependent wave function as mentioned later), and the

macroscopic applicability of the unified functions as, for example, applied later.

CONSTRUCTION OF THE UNIFIED FIELD:

Now, "virtual particles" (with momentum) are considered to follow the gradient functions previously

presented, and are considered to provide substance to the structure and function of the unified field.

Accordingly, the unified field theory herein applies a four dimensional gradient vector system which provides

for an understanding of the internal structure of the unified field, elementary particles, etc. This greater depth of

information proposes to allow for a more detailed understanding of events in physics (e.g., for predictability).

The virtual particles which follow a gradient function in the families of functions described previously are considered to transition through values of potential while having complementary values of (n_1) and (n_2), and while having one constant value of 1/N. Wherein, when 1/N is equal to one amongst member functions, the unified field is considered to be in an "elementary" state, while when 1/N is an integer number greater than one amongst member functions, the unified field is considered to experience a macroscopic form of quantization.

The potential of a virtual particle is considered to change as it follows a gradient function due to changes in the values of its parameters as it rotates in its trajectory (i.e., screws) during oscillation along its respective virtual particle path (gradient function) as shown in figures (3A) and (3B).
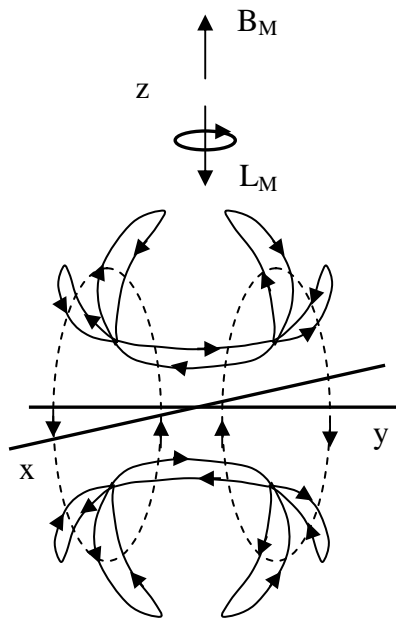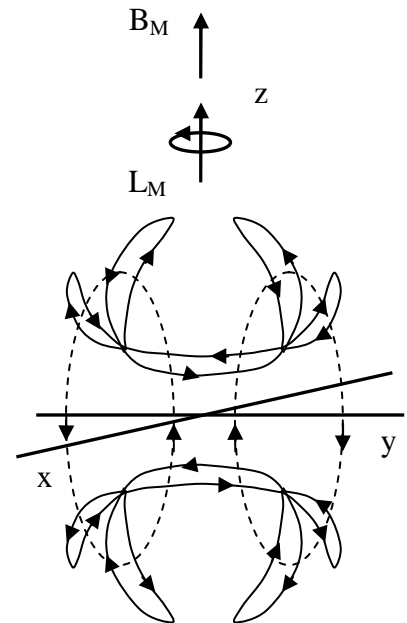
Side view of a
negative unified field

FIG. 3A

Side view of a
positive unified field

FIG. 3B

Figures (3A) and (3B) show a select few virtual particle paths, which include "more bent" and "less bent" virtual particle paths, in simplified drawings of elementary negative and positive unified fields. Wherein, each virtual particle path is comprised in a respective "band" of virtual particle paths, and each band of virtual particle paths comprises a multitude of virtual particle paths which each comprise respective curvatures, dimensions, and alignments; complementary values of (n_1) and (n_2); and a constant value of $1/N$. (Note that the significance of "more bent" and "less bent" virtual particle paths will be explained more so later, as, for example, with respect to in figures 26A and 26B. Also, note that references to the front and back sides in figures 3A and 3B are relative references.)

Virtual particles are considered to account for parameters of a unified field including the respective

flow of virtual particle "electric" charge (q) as shown directed along the arrows on solid lines in figures (3A) and (3B). In which case, the virtual particle paths form "currents" which produce the unified field of, for example, an elementary electrically charged particle comprising an intrinsic angular momentum (L_M) (i.e., intrinsic spin), and a "macroscopic" magnetic field (B_M), for the electrically charged particle as a whole along a respective (z) axis (also shown in figures 3A and 3B).

While, later it will be understood how the magnetic moment of a static electrically charged particle increases as the bending of its virtual particle paths increase in direct proportion to its respective decrease in mass (wherein this agrees with convention in which the magnetic moment of a static proton is less than the magnetic moment of a static electron of lesser mass). (Note that the opposite electrically charged unified fields are symmetrical reflections, and are considered to comprise the same density so as to represent matter and antimatter unified fields. However, certain portions of the unified field are not "mirror" symmetrical reflections when spin is added to the unified field, e.g., in terms of angular momentum as shown, and in terms of microscopic spins which are described later.)

The basic "static" geometry of the internal structure of the unified field is considered to be representative of the basic geometry of the internal structure of a static elementary electrically charged particle, and pertinent to the operational terms of black holes ranging from a theoretical Planck particle (i.e., a theoretical miniature black hole) to a supermassive black hole. Wherein, the internal structure of the unified field provides parameters for describing certain characteristics of a black hole including the event horizon, accretion disc, jets, etc. (Note that drawings of unified fields such as those shown in figures 3A and 3B, and other drawings which pertain to them, are only intended to be drawn as rough approximations or also exaggerations of what they represent for viewing purposes.)

Nevertheless, each of the virtual particle paths in the top band of virtual particle paths of a negative

electrically charged particle are considered to comprise a right hand screw, and each of the virtual particle paths in the bottom band of virtual particle paths of a negative electrically charged particle are considered to comprise a left hand screw. While, each of the virtual particle paths in the top band of virtual particle paths of a positive electrically charged particle are considered to comprise a left hand screw, and each of the virtual particle paths in the bottom band of virtual particle paths of a positive electrically charged particle are considered to comprise a right hand screw.

In more detail, the unified field is considered to be constructed with a simple set of orthogonal vectors which provide for the predicable structure and function of the unified field. Accordingly, each virtual particle path is considered to have orthogonal "microscopic spins" comprising microscopic charge (q), mass (m), and magnetic (B_m) spin vectors.

In terms of static negative and positive electrically charged particles, figures (4A) and (4B) show the left hand and right hand electric (q), mass (m), and magnetic (B_m) microscopic spin vectors of the example virtual particle paths on the top and bottom sides of the negative and positive unified fields shown in figures (3A) and (3B), respectively. (Note that, other than vectors which relate to the Pythagorean theorem and the summation of vectors, the length of a drawn vector is not presently a matter of concern throughout the theory.)
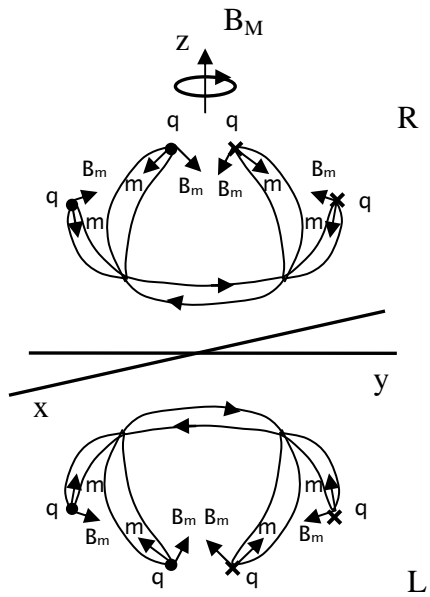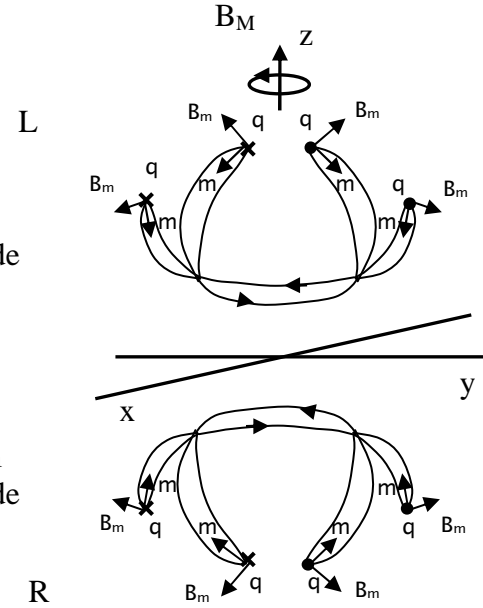
Side view of a negative
electrically charged particle

FIG. 4A

Side view of a positive
electrically charged particle

FIG. 4B

Figures (5A) and (5B) show how the three spin vectors change alignments during portions of oscillation in the nuclear and extranuclear regions in a negative and positive unified field, respectively. Wherein, importantly, the microscopic magnetic spin vectors basically have a relatively inverted alignment in the nuclear region compared to the extranuclear region.
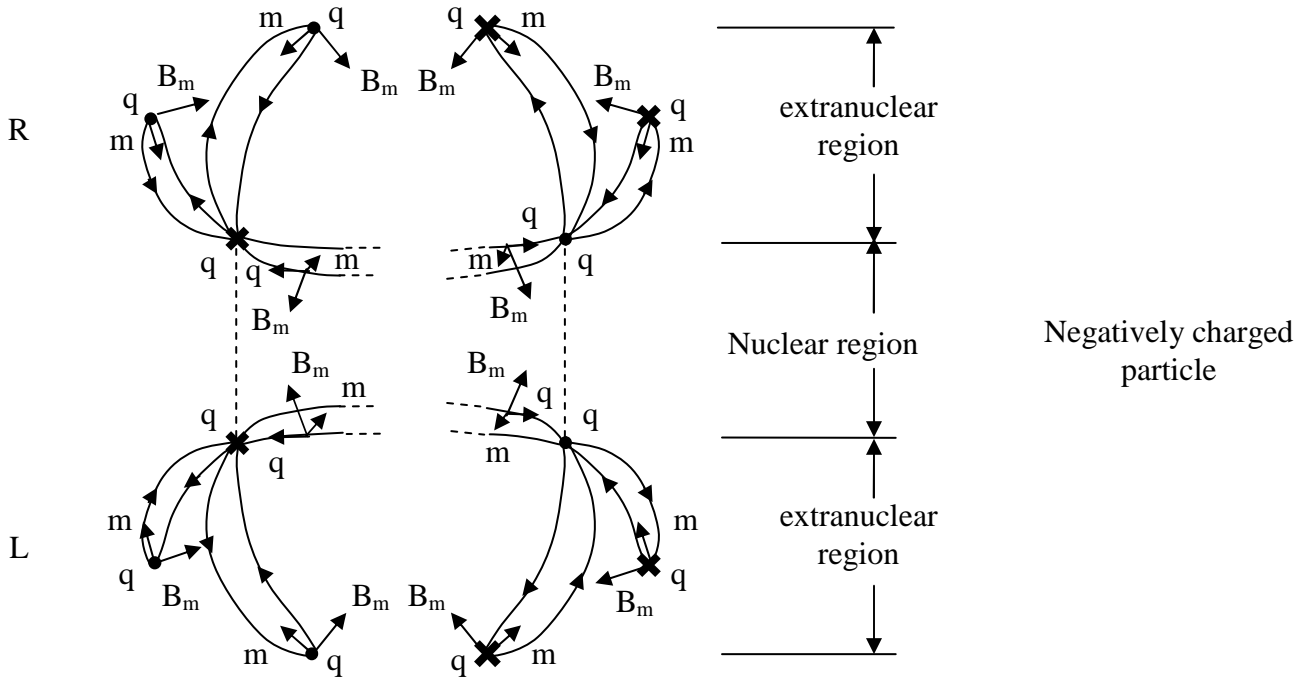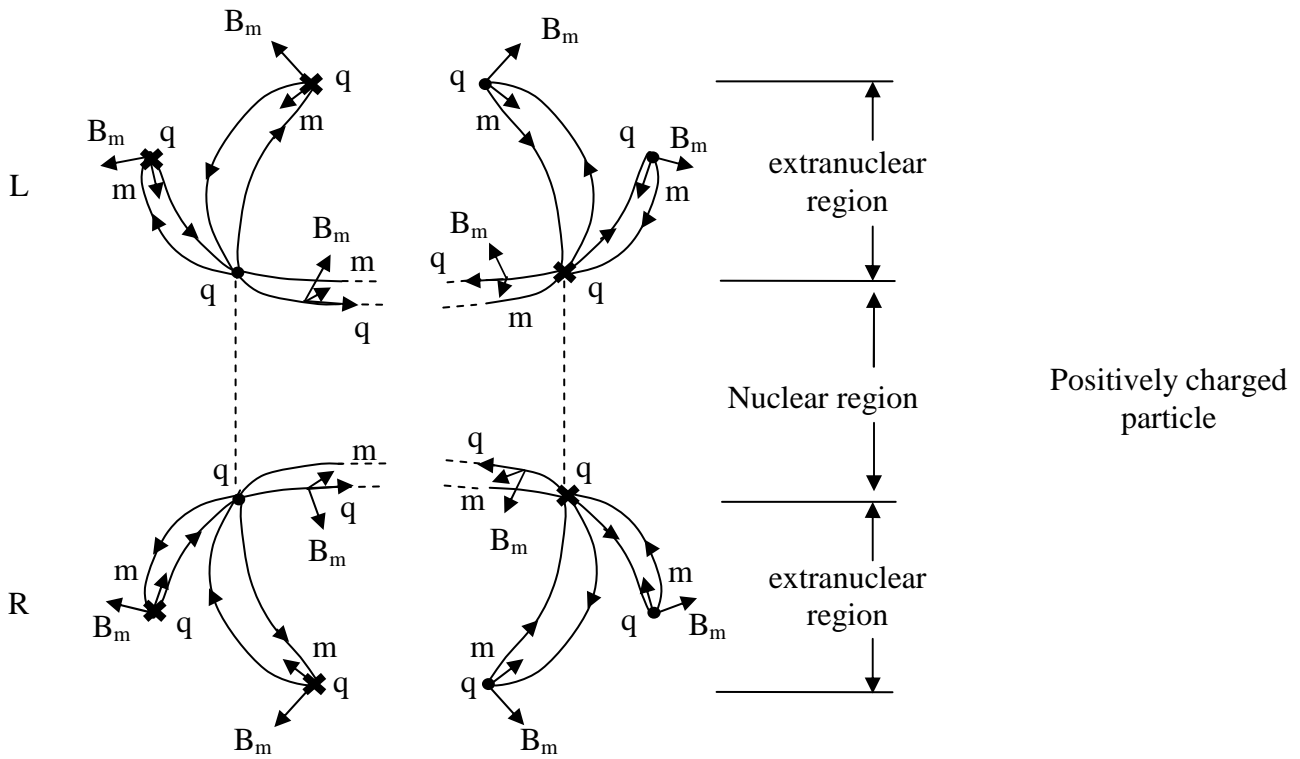
FIG. 5A

FIG. 5B

Note that the nuclear virtual particle paths are shown in figures 3A-5B as merged in the nuclear region such that the theoretical separations of virtual particle paths are not shown. Also, note that virtual particle paths may not be shown with bending hereinafter (for simplification), except, for example, where curvature is emphasized, e.g., in magnetic interactions.

Figure (6A) shows a vector component in the (x-y) plane of a tangent at the leading edge of a select portion of a virtual particle path of a negative electrically charged particle when $(n_1) \approx +2$ $(n_2) \approx +0$. Wherein, the (x) and (y) axes of the vector component in the (x-y) plane relate to the constants (n_1) and (n_2) of the components $(^-1/n_1*K_T q/r^2)$ and $(1/e^{[n_2(2\pi mcr)/h]})$, respectively, of the gradient function $^-1/n_1*K_T q/r^2 *1/e^{[n_2(2\pi mcr)/h]}$. In which case, the (x) and (y) axes, and the respective values of (n_1) and $(n_2,)$, are considered to relate to the energy, geometry, etc., of the given virtual particle path. (Note that the arrow on the virtual particle path corresponds to respective microscopic electric spin vector (q) direction along the gradient function.)
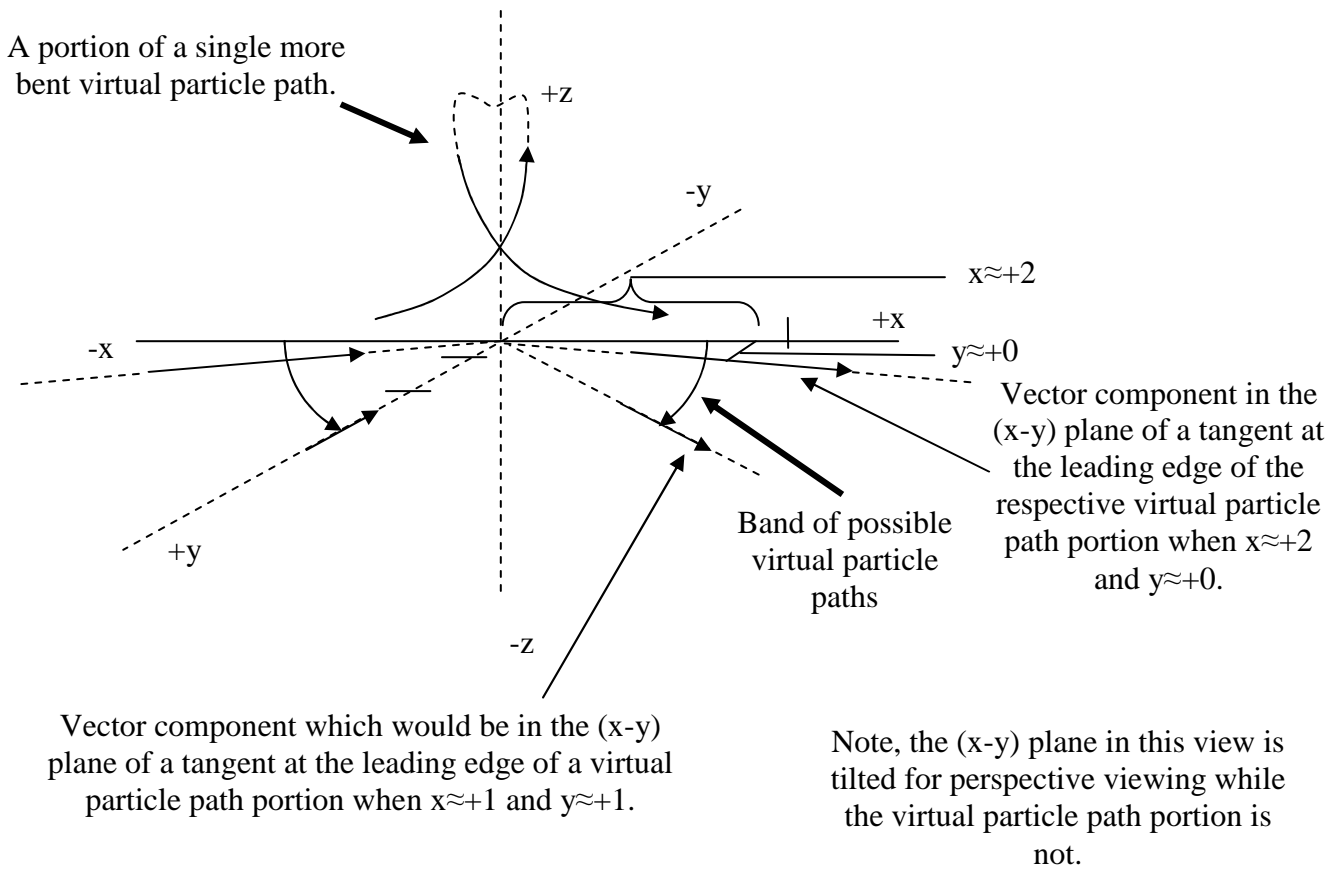
A portion of a single more bent virtual particle path.

+z

-y

x≈+2

+x

-x

y≈+0

Vector component in the (x-y) plane of a tangent at the leading edge of the respective virtual particle path portion when x≈+2 and y≈+0.

+y

Band of possible virtual particle paths

-z

Vector component which would be in the (x-y) plane of a tangent at the leading edge of a virtual particle path portion when x≈+1 and y≈+1.

Note, the (x-y) plane in this view is tilted for perspective viewing while the virtual particle path portion is not.

FIG. 6A

Note that when x≈+2 and y≈+0, then the gradient of the virtual particle path is

$\approx {}^{-}\frac{1}{2}K_T q/r^2 * 1/e^{[0(2\pi mcr)/h]}$ for the given one half portion of the theoretical unified gradient function (top side); is

$\approx {}^{-}1K_T q/r^2 * 1/e^{[0(2\pi mcr)/h]}$ for the whole gradient portion of the unified field (the sum of the top and bottom side

portions as described more so later); and is $\approx {}^{-}4K_T q/r^2 * 1/e^{[0(2\pi mcr)/h]}$ for the unified field gradient portion of the

particle as a whole (for eight octants). While, when x≈+1 and y≈+1, then the gradient of the virtual particle

path is $\approx {}^{-}1K_T q/r^2 * 1/e^{[1(2\pi mcr)/h]}$ for the given one half portion of the theoretical unified gradient function (top

side); is $\approx {}^{-}2K_T q/r^2 * 1/e^{[1(2\pi mcr)/h]}$ for the whole gradient portion of the unified field (the sum of the top and

bottom side portions as also described more so later); and is $\approx {}^{-}8K_T q/r^2 * 1/e^{[1(2\pi mcr)/h]}$ for the unified field

gradient portion of the particle as a whole (for eight octants).

Figures (6B) and (6C) describe how certain parameters of the virtual particle paths vary as their angles of trajectory vary. Wherein, figures (6B) and (6C) relate to the (x) and (y) axes of the vector component in the (x-y) plane of the tangent to the given virtual particle path portion, and, correspondingly, (n_1) and (n_2) values of the respective gradient function shown in figure (6A).
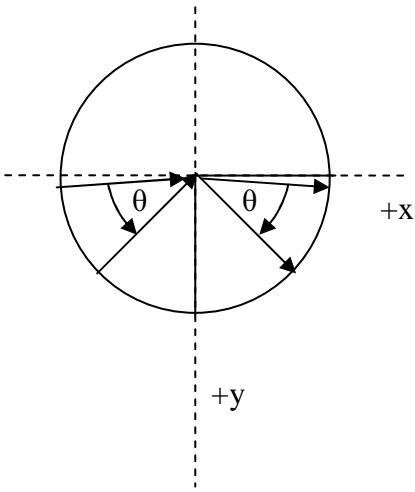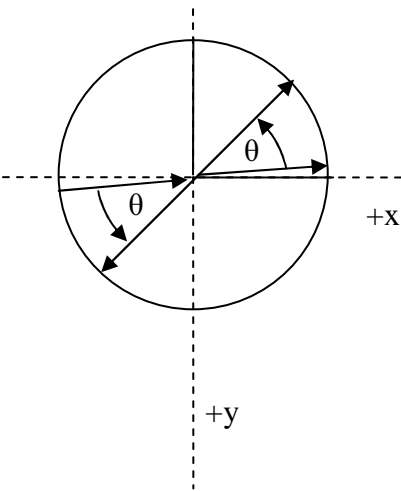
Top view

FIG. 6B

Consider the following conditions to be present for virtual particle paths in a band of virtual particle paths as theta increases for a static particle as shown in figure (6B) (moving from one virtual particle path to another):

1) Spin vector alignments rotate according to the change in potential;
2) Path length and radius decrease for each virtual particle path. In which case, the virtual particles in a virtual particle path propagate with an increased average frequency and a decreased average radius, such that the virtual particle paths can propagate (statically here) in unison as a wave packet;
3) Complementary (n_1) and (n_2) values change, and the elliptically helical geometry of the virtual particle paths approach a circularly helical geometry (eccentricity decreases);
4) Densities of the virtual particle paths increase; and
5) Virtual particles propagate at the same velocity, i.e., virtual particles propagate at the same velocity on all virtual particle paths (refer to the description under the heading "VIRTUAL PARTICLES, SELF INTERACTION, AND SUPERLUMINAL VELOCITY").

When diagram (6B) is applied to an electron in an atomic orbital the following would occur as theta increases along the direction shown:

1) Kinetic energy increases;
2) Negative potential energy increases; and
3) Positional potential energy decreases.

Top view

FIG. 6C

While the conditions of the virtual particle paths for figure (6B) are basically equivalent for the virtual particle paths of a propagating particle as a whole, nevertheless, further consider the following conditions to be the case when figure (6B) is modified for forward propagation as in figure (6C), such that theta changes in opposite directions in diagonally positioned quadrants for the leading and trailing edge (for one portion, e.g., the front portion) of a propagating particle as a whole:

1) When this diagram is applied to an accelerated propagating electrically charged particle, "relativistic mass" increases for the particle as a whole (and individual virtual particle paths) as theta increases along the direction shown for the band of virtual particle paths.

2) When this diagram is applied to a quantum of electromagnetic radiation, virtual particle paths on both the top and bottom sides are comprised in a narrow band with constants (n_1) ≈1 and (n_2) ≈1, wherein the narrow band of virtual particle paths for quanta of higher energies have virtual particles with higher average frequencies and smaller average radii on virtual particle paths with correspondingly shorter path lengths and smaller radii.

3) When this diagram is applied to relativity, length contraction and time dilation increase along the (x) axis as theta increases along the direction shown (as explained more so later).

Upon acceleration of an electrically charged particle, the spin vectors of the virtual particles in each of the virtual particle paths are considered to rotate (as relates, for example, to figures 6B-6D, and as more specifically depicted later in figures 14A and 14B). Wherein, the rotations of the spin vectors of the virtual particles are considered to affect the parameters of, in particular, a forward propagating particle including the radius, amplitude, wavelength, frequency, relativistic mass, energy, etc. (in agreement with the self interactions of the respective virtual particles as analogized with the interactions of propagating electrically charged particles described later).

Accordingly, upon acceleration and rotation of the spin vectors as for the example virtual particle path shown in figure (6D) for forward propagation, theta (as applied therein) correspondingly increases, and each virtual particle path changes its trajectory and projects forward. In which case, the eccentricity of each of the virtual particle paths decreases so as to approach a respective circularly helical geometry to a directly proportional extent, and, correspondingly, the forward translational velocity of the particle as a whole is considered to increase. (Note that the virtual particle paths propagate in particular agreement with certain conventional spacetime interval diagrams, e.g., the example virtual particle path shown in figure 6D propagates in particular agreement with the "light clock" interval diagram applied in relativity.)
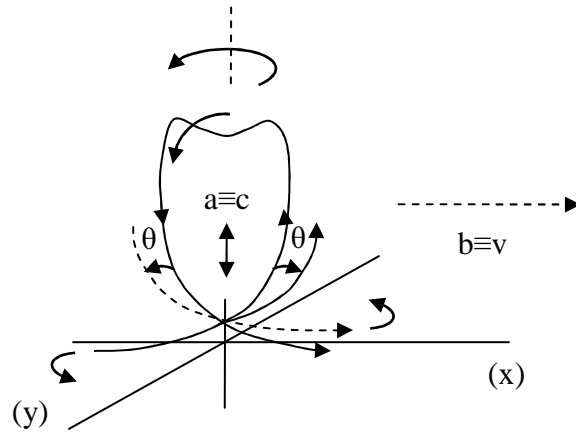
Changes in the trajectory of a virtual
particle path in an accelerating
propagating particle are shown
(excluding size change) as theta
increases upon rotations of the virtual
particle paths, and corresponding upon
changes in (n_1) and (n_2) values.

FIG. 6D

With respect to relativity, figures (6A-6D) (with particular consideration for figure 6D), and when

working with ellipses, assume $\dfrac{1}{\gamma} \equiv e$, wherein $\left(\dfrac{1}{\gamma}\right)$ is the reciprocal Lorentz factor and (e) is eccentricity, such

that $\dfrac{1}{\gamma} \equiv e = \sqrt{1-\left(\dfrac{b}{a}\right)^2}$. In which case, assuming that b≡v and a≡c, then $\dfrac{1}{\gamma} = \sqrt{1-\left(\dfrac{v}{c}\right)^2}$. Wherein, for a

propagating electrically charged particle as a whole, when v=0, then $\left(\dfrac{1}{\gamma}\right)$ is equal to one, and each virtual

particle path has its respective maximum eccentricity, such that each virtual particle path has a respective

minimum Lorentz contraction, minimum time dilation, and minimum relativistic mass. While, when v=c, then

$\left(\dfrac{1}{\gamma}\right)$ is equal to zero, and each virtual particle path approximates a respective circularly helical geometry

comprising a respective minimum eccentricity, and the virtual particle paths each have a respective maximum

Lorentz contraction, maximum time dilation, and maximum relativistic mass.

It is considered that each virtual particle path in a band is related to its own Lorentz factors due to their

differences in potentials, i.e., the basic multiplicative components of a potential are related to, or (n_1) and (n_2)

can be correlated with, their own Lorentz factors, such that corresponding Lorentz factors vary amongst virtual

particle paths in a band (affecting scale), and such that such Lorentz factors change in a virtual particle path as

the potential changes (e.g., as with respect to changes in the parameters of charge or mass, and radius, or the

equivalents) for virtual particles in a virtual particle path as they oscillate, and the virtual particles converge and

then diverge. Wherein, consequentially, the curvature of a virtual particle path changes as it oscillates due to

changes in the directions of the spin vectors, length contractions, etc. as the potential changes.

Thus, consider that the function

$$f = \pm e^{\left[\frac{1}{N}n_1 \frac{\pm 2\pi(qcr)}{h_q} + \frac{1}{N}n_2 \frac{\pm 2\pi(mcr)}{h}\right]} \qquad \text{Eq. (3A)}$$

can be written relativistically as

$f = \pm e^{\left[\frac{1}{\gamma_T^2} * \frac{1}{N}n_1 \frac{\pm 2\pi(qcr)}{h_q} + \frac{1}{\gamma_T^2} * \frac{1}{N}n_2 \frac{\pm 2\pi(mcr)}{h}\right]}$. Then, upon reflection of the function and taking the partial

derivative, the forgoing function becomes:

$$f_x(x, y) = {}^{\pm}\gamma_T{}^2 \frac{1}{N} \frac{h_q c}{n_1 * 2\pi(qr)} * {}^{\pm}e^{\left[\frac{1}{\gamma_T{}^2}\frac{1}{N}\frac{n_2{}^{*\pm}2\pi(mcr)}{h}\right]},$$

or when rewritten becomes

$$f_x(x, y) = {}^{\pm}\gamma_T{}^2 \frac{1}{N} \frac{1}{n_1} K(q) * \frac{{}^{\pm}e^{\left[\frac{1}{\gamma_T{}^2}\frac{1}{N}\frac{n_2{}^{*\pm}2\pi(mcr)}{h}\right]}}{r} . \qquad \text{Eq. (14A)}$$

Equation (14A) is considered a relativistic version of the unified field function shown in equation (4A), such

that the square of the Lorentz factor, i.e., $\gamma_T{}^2$, in the unified field function accounts for the two indices of the

Lorentz factor in general relativity which conventionally relates to energy and volume (or energy density).

Note, refer to the example below and equations (16A-16D) shown later as relates to certain forms of the

theoretical squares of the reciprocal Lorentz factor applicable in the present theory.

For example, as relates to the figure (6D) and the square of the Lorentz factor for a interval portion of

the charge component of the unified potential (along the x-axis), consider $\gamma_T{}^2 = \dfrac{1}{\left(\dfrac{\Delta n_1}{1}\right)^2}$ such that when

$(\Delta n_1)=2$, then, $\gamma_T{}^2=\frac{1}{4}$, i.e., $1/(2-0)^2/(1)=\frac{1}{4}$ (expressed here, and in similar cases elsewhere, in terms of a fraction

of the relevant interval such that, now, $1 \leq n_1 \leq 2$ and $1 \geq n_2 \geq 0$). Then, also, as relates to the figure (6D) and the

square of the Lorentz factor for the related interval portion of the mass component of the unified potential

(along the y-axis), consider $\dfrac{1}{\gamma_T{}^2} = \left(\dfrac{\Delta n_2}{1}\right)^2$ such that when $(\Delta n_2)=0$, then, $1/\gamma_T{}^2=0$, i.e., $(1-1)^2/(1)=0$.

Wherein:

$$\left(\gamma_T{}^2\right)*4*2*\underset{\approx 2}{\dfrac{^-1}{}}\dfrac{K_T(q)}{r}*\dfrac{1}{e^{\left[\frac{1}{\gamma_T{}^2}\frac{\approx 0\pi(mcr)}{h}\right]}} \approx \left(\dfrac{1}{4}\right)*4*2*\dfrac{^-1}{2}\dfrac{K_T(q)}{r}*\dfrac{1}{e^{\left[0*\frac{0\pi(mcr)}{h}\right]}} \approx 1\dfrac{^-K_T(q)}{r}$$

Eq. (14B)

In which case, (14B) is considered to be the extreme relativistic unified field potential function of the most

eccentric virtual particle path for a static electrically charged particle, i.e., when $(n_1) \approx 2$ and $(n_2) \approx 0$.

Then, when $(n_1) \approx 1$ and $(n_2) \approx 1$ for what is considered to be the extreme relativistic unified field

potential function of the least eccentric virtual particle path for a static electrically charged particle or a

quantum of electromagnetic radiation, when $(\Delta n_1)=1$, then, $\gamma_T{}^2=1$, i.e., $1/(2-1)^2/(1)=1$; and when $(\Delta n_2)=1$, then,

$1/\gamma_T{}^2=1$, i.e., $(1-0)^2/(1)=1$ such that:

$$\left(\gamma_T{}^2\right)*4*2\dfrac{\approx {}^-K_T(q)}{r}*\dfrac{1}{e^{\left[\frac{1}{\gamma_T{}^2}\frac{\approx 2\pi(mcr)}{h}\right]}} \approx (1)*4*2\dfrac{^-K_T(q)}{r}*\dfrac{1}{e^{\left[1*\frac{2\pi(mcr)}{h}\right]}} \approx 8\dfrac{^-K_T(q)}{r}*\dfrac{1}{e^{\left[\frac{2\pi(mcr)}{h}\right]}}.$$

Eq. (14C)

Accordingly, while

$$4\frac{\approx^-K_T(q)}{r} - 3\frac{\approx^-K_T(q)}{r} \approx 1\frac{^-K_T(q)}{r}$$ (as stated before for an elementary particle in equation 9B),

nevertheless, "relativistically,"

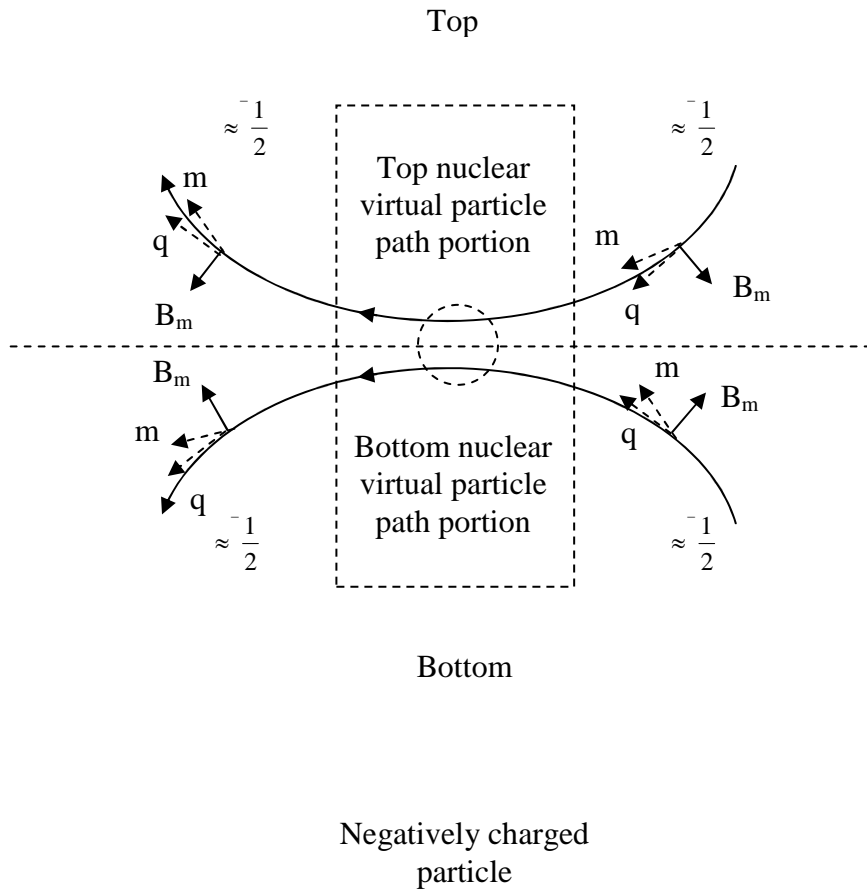$$8\frac{\approx^-K_T(q)}{r} * \frac{1}{e^{\left[\frac{\approx 2\pi(mcr)}{h}\right]}} - 1\frac{\approx^-K_T(q)}{r} \approx 2\frac{^-K_T(q)}{r}$$

or

$$3\frac{\approx^-K_T(q)}{r} - 1\frac{\approx^-K_T(q)}{r} \approx 2\frac{^-K_T(q)}{r} \qquad \text{Eq. (14D)}$$

(That is, in essence, approximately $^-3 - ^-1 = ^-2$. Here, consider how the difference of equation 14D derived from subtraction can be related to the trace of the Minkowski metric derived from the sum of its diagonal elements.)
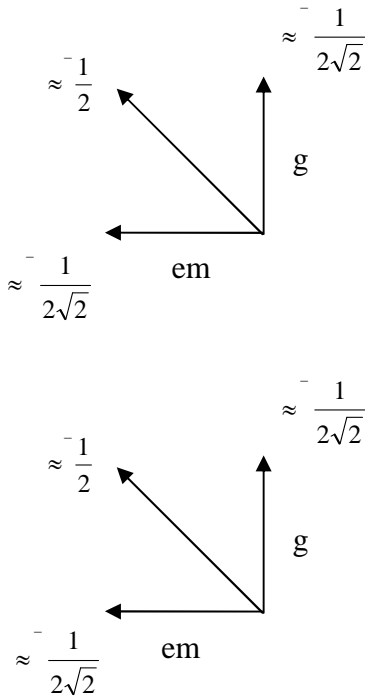
In theory, the difference in potential in equation (14D) can be expressed as $\approx ^-1K_Tq/r + \approx ^-1G_Tm/r \approx ^-2K_Tq/r$. Also, note that a theoretical version of the Schwarzschild radius can be derived from the difference in potential in equation (14D), such that $r_T \approx 2G_TM/c^2$ when G_TM is substituted for ^-K_Tq. Moreover, note that the terms in equation (14B-14D), and elsewhere throughout the theory, approximate their expected values upon adjusting the values of the terms (n_1) and (n_2) taken from their respective intervals $1 < n_1 < 2$ and $1 > n_2 > 0$ by a small percentage, e.g., $\approx 1\%$, thus accounting for the significance of the approximation symbol ($\approx$) used throughout the theory.

Next, the vector sums of the gradient components of the unified field with respect to equations (5A), (5B), (8A), (8B), and (8C) can be related to the geometry of the unified field as depicted in figures (7A), (7B), and (7C). In this case, only the basic multiplicative factors of the vector summation process are shown (note that a positively charged particle can be presented similarly).

Top

Top nuclear
virtual particle
path portion

$\approx \frac{^-1}{2}$ $\approx \frac{^-1}{2}$

m   m B_m

q   q

B_m

B_m m B_m

m   q

q

Bottom nuclear
virtual particle
path portion

$\approx \frac{^-1}{2}$ $\approx \frac{^-1}{2}$
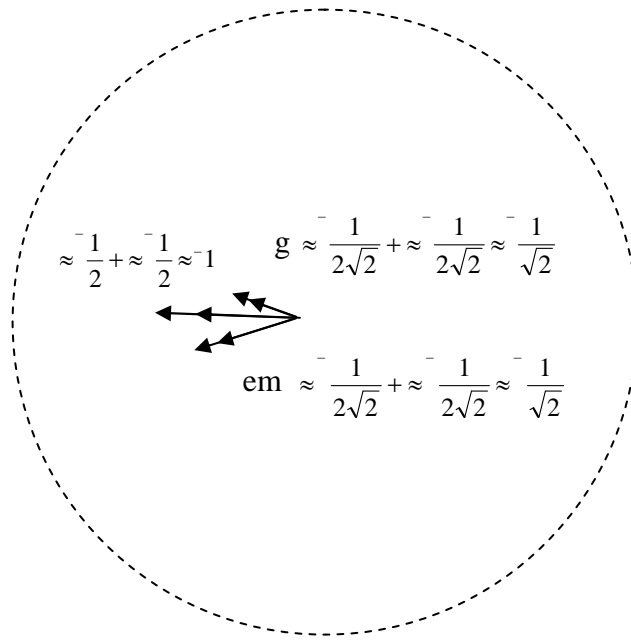
Bottom

Negatively charged
particle

Here, the vector resultant gradients of the top and bottom virtual particle paths when $(n_1) \approx 2$ and $(n_2) \approx 0$ can propagate into the nuclear region and add as $\approx {^-1/2} + \approx {^-1/2} \approx {^-1}$. Alternatively, vector components can propagate into the nuclear region and add as follows so as to produce the resultant gradient ${^-\sqrt{(\approx {^-1/2}\sqrt{2} + \approx {^-1/2}\sqrt{2})^2 + (\approx {^-1/2}\sqrt{2} + \approx {^-1/2}\sqrt{2})^2}} \approx {^-1}$.

FIG. 7A

$\approx \dfrac{^{-}1}{2\sqrt{2}}$

$\approx \dfrac{^{-}1}{2}$

$\approx \dfrac{^{-}1}{2\sqrt{2}}$

g

em

$\approx \dfrac{^{-}1}{2\sqrt{2}}$

$\approx \dfrac{^{-}1}{2}$

$\approx \dfrac{^{-}1}{2\sqrt{2}}$

g

em

$\approx \dfrac{^{-}1}{2} + \approx \dfrac{^{-}1}{2} \approx {}^{-}1$

$g \approx \dfrac{^{-}1}{2\sqrt{2}} + \approx \dfrac{^{-}1}{2\sqrt{2}} \approx \dfrac{^{-}1}{\sqrt{2}}$

$em \approx \dfrac{^{-}1}{2\sqrt{2}} + \approx \dfrac{^{-}1}{2\sqrt{2}} \approx \dfrac{^{-}1}{\sqrt{2}}$

Basic geometry of the (em) and (g) gradient vector components of the top and bottom virtual particle paths when $(n_1) \approx 2$ and $(n_2) \approx 0$ (in a Cartesian coordinate system).
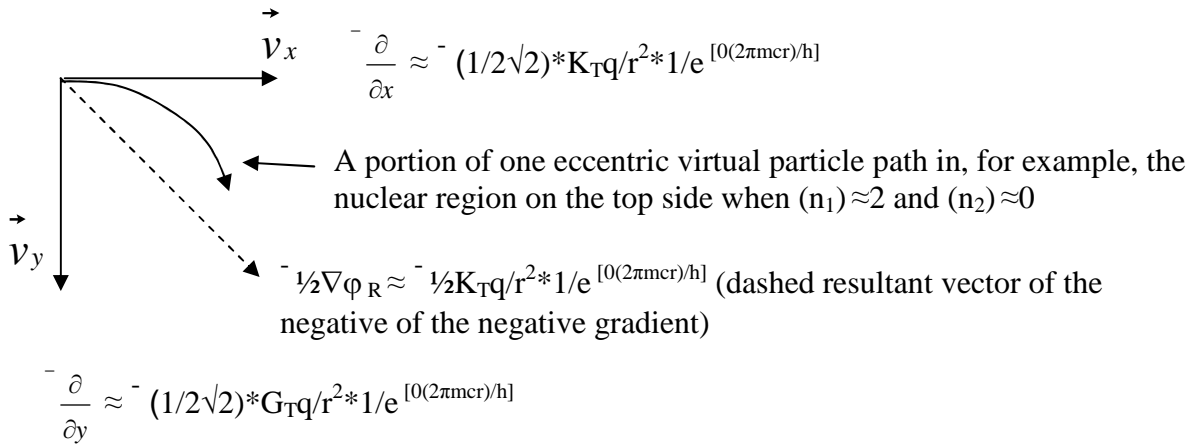
An enlarged perspective view of what is occurring in the dashed circle in figure (7A) which shows the basic geometry of the respective addition of vector components of (em) and (g) of the top and bottom virtual particle paths in the nuclear region when $(n_1) \approx 2$ and $(n_2) \approx 0$.

FIG. 7B

FIG. 7C

Then, figure (7D) shows the symmetrical vector components of a portion of one example virtual particle path in terms of its respective electromagnetic and gravitational gradient components, and respective unified field gradient resultant.
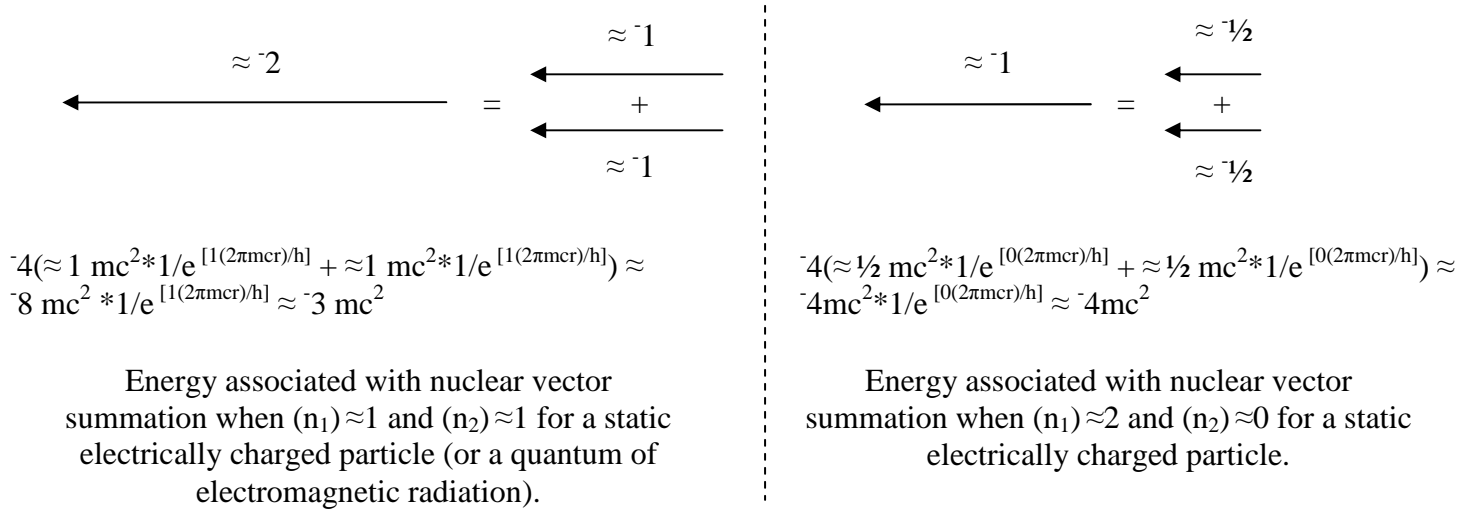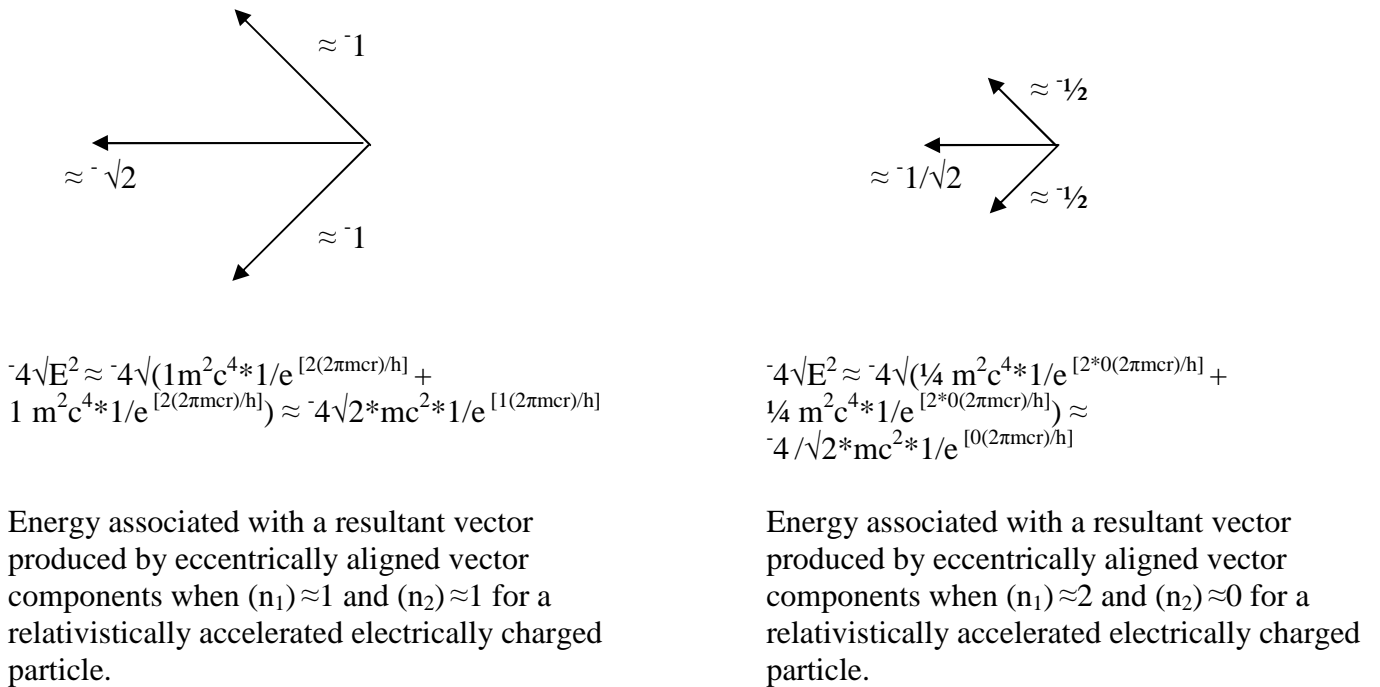
$$\vec{v}_x \qquad {}^-\frac{\partial}{\partial x} \approx {}^- (1/2\sqrt{2})*K_Tq/r^2*1/e^{[0(2\pi mcr)/h]}$$

A portion of one eccentric virtual particle path in, for example, the nuclear region on the top side when $(n_1) \approx 2$ and $(n_2) \approx 0$

$$\vec{v}_y \qquad {}^-\tfrac{1}{2}\nabla\varphi_R \approx {}^- \tfrac{1}{2}K_Tq/r^2*1/e^{[0(2\pi mcr)/h]} \text{ (dashed resultant vector of the negative of the negative gradient)}$$

$${}^-\frac{\partial}{\partial y} \approx {}^- (1/2\sqrt{2})*G_Tq/r^2*1/e^{[0(2\pi mcr)/h]}$$

Top view

Here, the vector components ($\vec{v}_x$ and $\vec{v}_y$) of the negatives of the electromagnetic and gravitational negative gradient components along the ($^+$x) and ($^+$y) axes of the negative of the theoretical unified field negative gradient resultant ${}^-\tfrac{1}{2}\nabla\varphi_R \approx {}^- \tfrac{1}{2}K_Tq/r^2 *1/e^{[0(2\pi mcr)/h]}$ are shown in the nuclear region, such that ${}^-\sqrt{[(\approx {}^-1/2\sqrt{2})*K_Tq/r^2*1/e^{[\approx 0(2\pi mcr)/h]}]^2 + [(\approx {}^-1/2\sqrt{2})*G_Tm/r^2*1/e^{[\approx 0(2\pi mcr)/h]}]^2} \approx {}^- \tfrac{1}{2}K_Tq/r^2*1/e^{[0(2\pi mcr)/h]}$ (dashed line).

FIG. 7D

While, in terms of mc^2, figure (7E) shows how the resultant vectors are produced with respect to vector summation and the Pythagorean theorem as the eccentricity of the virtual particle paths change due to relativistic acceleration and the respective vector rotations. Note that the terms in figure (7E) (and the terms elsewhere throughout the theory, as said before in this regard) approximate their expected values upon adjusting the values of the terms (n_1) and (n_2) taken from their respective intervals $1 < n_1 < 2$ and $1 > n_2 > 0$ by a small percentage, e.g., $\approx 1\%$, thus accounting for the significance of the approximation symbol ($\approx$) used in figure (7E) (and throughout the theory).

≈ ⁻2

≈ ⁻1
+
≈ ⁻1

=

≈ ⁻1

≈ ⁻½
+
≈ ⁻½

=

$^-4(\approx 1\ mc^2*1/e^{[1(2\pi mcr)/h]} + \approx 1\ mc^2*1/e^{[1(2\pi mcr)/h]}) \approx$
$^-8\ mc^2 *1/e^{[1(2\pi mcr)/h]} \approx\ ^-3\ mc^2$

Energy associated with nuclear vector summation when $(n_1)\approx 1$ and $(n_2)\approx 1$ for a static electrically charged particle (or a quantum of electromagnetic radiation).

$^-4(\approx ½\ mc^2*1/e^{[0(2\pi mcr)/h]} + \approx ½\ mc^2*1/e^{[0(2\pi mcr)/h]}) \approx$
$^-4mc^2*1/e^{[0(2\pi mcr)/h]} \approx\ ^-4mc^2$

Energy associated with nuclear vector summation when $(n_1)\approx 2$ and $(n_2)\approx 0$ for a static electrically charged particle.

Wherein: $(^-4mc^2) - (^-3\ mc^2) \approx\ ^-1\ mc^2$, and relativistically $\approx\ ^-2\ mc^2$ (refer to equation 14D).

≈ ⁻1

≈ ⁻√2

≈ ⁻1

≈ ⁻½

≈ ⁻1/√2

≈ ⁻½

$^-4\sqrt{E^2} \approx\ ^-4\sqrt{(1m^2c^4*1/e^{[2(2\pi mcr)/h]}} +$
$1\ m^2c^4*1/e^{[2(2\pi mcr)/h]}) \approx\ ^-4\sqrt{2}*mc^2*1/e^{[1(2\pi mcr)/h]}$

Energy associated with a resultant vector produced by eccentrically aligned vector components when $(n_1)\approx 1$ and $(n_2)\approx 1$ for a relativistically accelerated electrically charged particle.

$^-4\sqrt{E^2} \approx\ ^-4\sqrt{(¼\ m^2c^4*1/e^{[2*0(2\pi mcr)/h]}} +$
$¼\ m^2c^4*1/e^{[2*0(2\pi mcr)/h]}) \approx$
$^-4/\sqrt{2}*mc^2*1/e^{[0(2\pi mcr)/h]}$

Energy associated with a resultant vector produced by eccentrically aligned vector components when $(n_1)\approx 2$ and $(n_2)\approx 0$ for a relativistically accelerated electrically charged particle.

Wherein: $(\approx\ ^-4/\sqrt{2}*mc^2*1/e^{[0(2\pi mcr)/h]}) - (\approx\ ^-4\sqrt{2}*mc^2 *1/e^{[1(2\pi mcr)/h]}) \approx\ ^-\sqrt{2}/2*mc^2$, and relativistically $\approx\ ^-\sqrt{2}*mc^2$.

Here, figure (7E) shows, in terms of mc^2, how the resultant vectors are produced with respect to vector summation and the Pythagorean theorem as the eccentricity of the virtual particle paths change due to relativistic acceleration and respective vector rotations.

FIG. 7E

CHARGED PARTICLE INTERACTION:

It has been a longstanding contentious issue as to how electrically charged particles interact. Wherein, while Newtonian physics suggests that gravitational interactions are based on instantaneous action-at-a-distance, relativity proposes that gravitational interactions are based on the action of the curvature of spacetime on mass over velocity (c).

Herein, electrically charged particles are considered to interact over relatively long distances ("locally") by the "extranuclear" virtual particle paths of a particle extending outward to, and interacting with, another particle (or other particles) over a superluminal velocity. In which case, long range interaction of one particle with another can cause attractive or repulsive effects which included particle acceleration, the formation of molecules, etc. (refer to the description under the heading "VIRTUAL PARTICLES, SELF INTERACTION, AND SUPERLUMINAL VELOCITY" for the mathematical derivation of the respective superluminal velocity).

For example, figure (8) shows a top view of two possible general directions of the four possible varieties of virtual particle paths of the extended extranuclear field of a given irregular distribution of static positive electrically charged particles which can interact with a negatively charged particle. (Note that the dashed lines in figure 8 represent virtual particle paths hidden from view.)

Negative particle

$$^-em_F + {^-g_F}$$

Irregular distribution
of positive particles
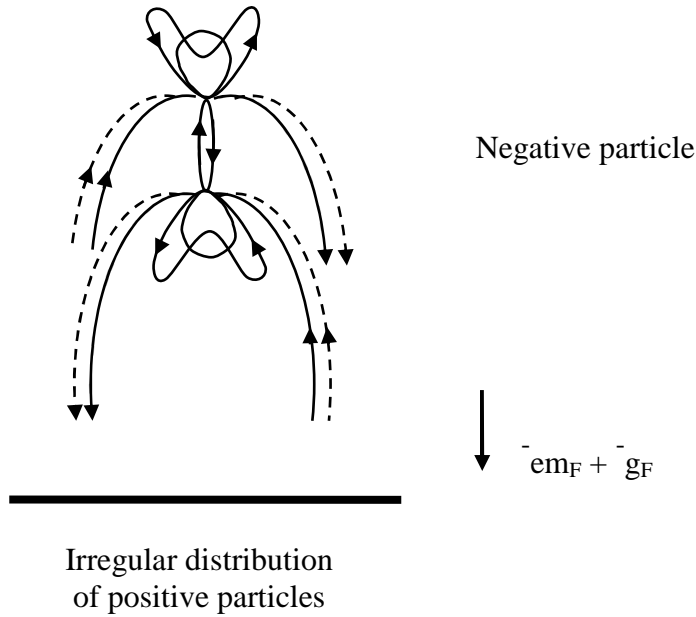
Electromagnetic and gravitational attraction

FIG. 8

In this case, the virtual particle paths of the extended extranuclear fields of the irregular distribution of

positively charged particles enter, and subsequently exit, on respective sides of the negative particle along the

portions of the nuclear region where the virtual particle paths converge and then diverge. (Note that the top side

where virtual particle paths enter and exit represents the front side of the negative particle with respect to figure

4A, and the bottom side where virtual particle paths enter and exit represents the back side of the negative

particle with respect to figure 4A. Also, note that the four possible virtual particle paths of the irregular

distribution of positively charged particles can be visualized as: a) comprising an irregular distribution of the

two varieties of virtual particle paths which extend out going in opposite directions from the top side of each

upright positive electrically charged particle (with respect to figure 4B); and, in addition, b) comprising an

irregular distribution of the two varieties of virtual particle paths which extend out going in opposite directions

from the bottom side of each inverted positive particle (with respect to figure 4B).

Figure (9) shows a perspective view of certain portions of the interacting particles shown in figure (8).

Electromagnetic and
gravitational attraction
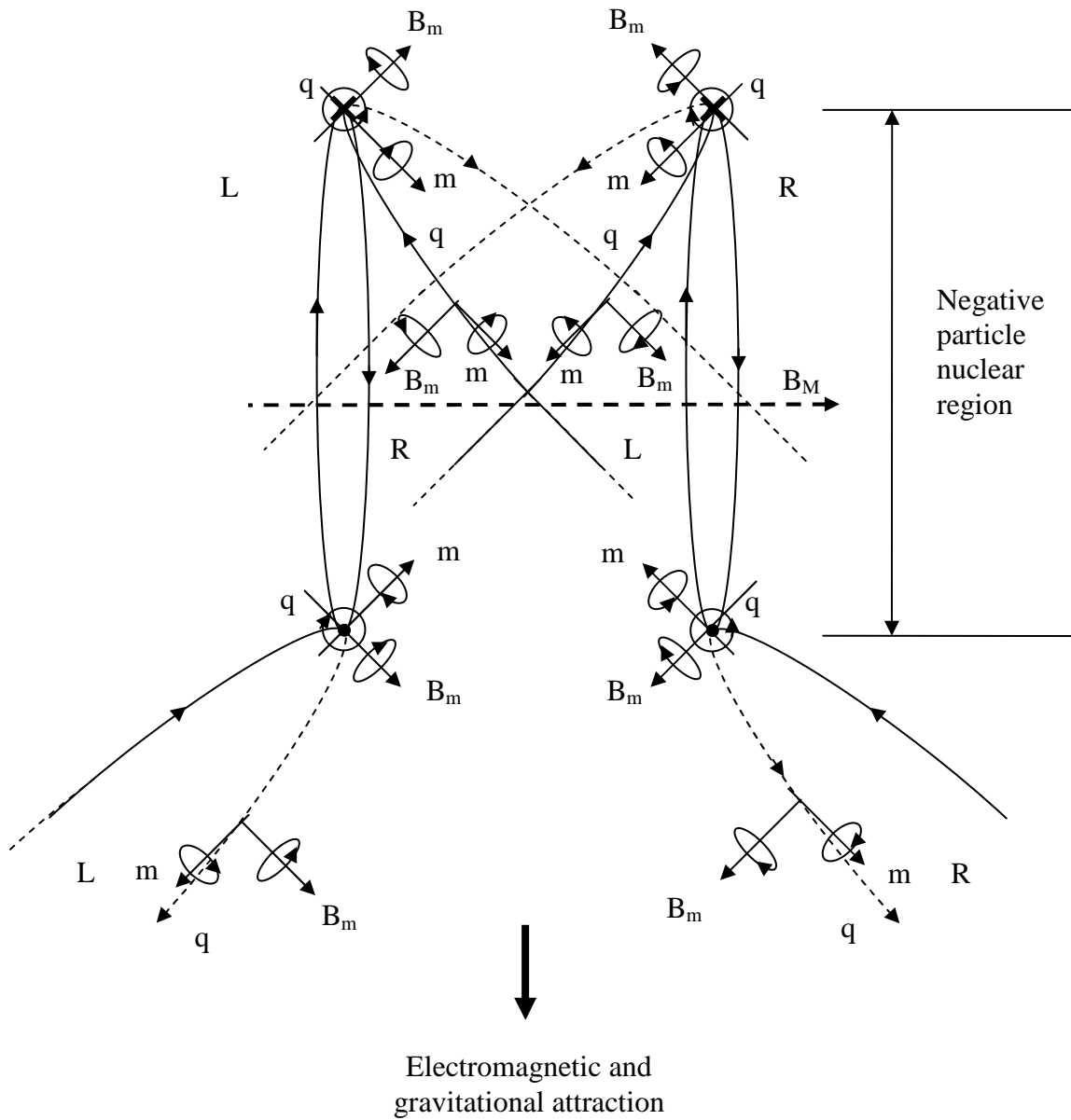
Side view

FIG. 9

In figure (9), the four possible varieties of effective virtual particle paths of the extranuclear fields of the irregular distribution of positive particles which can interact with the negative particle are shown along with their respective microscopic spins. Also, figure (9) shows the example virtual particle paths of the nuclear region of the negative particle which is interacted upon, their respective microscopic spins, and the macroscopic magnetic field alignment of the negative particle as a whole through the nuclear region.

In this case, the effective virtual particle paths from the irregular distribution of positive particles entering the nuclear region on the top section of the negative particle have microscopic charge (q) and mass (m) spins which are parallel with the microscopic charge (q) and mass (m) spins comprised by the virtual particle paths in the nuclear region of the negatively charged particle so as to attract. While, the effective virtual particle paths from the irregular distribution of positive particles entering the nuclear region on the top section of the negative particle also have microscopic magnetic spins (B_m) which are antiparallel with the microscopic magnetic spins (B_m) comprised by the virtual particle paths of the top section of the nuclear region of the negatively charged particle so as to also produce attraction. In effect, the virtual particle paths interacting on the top section of the negative particle are considered to attract such that the top section of the unified field of the negative particle shown in figure (9) increases in mass and accelerates to an extent. Note that the "interacting" spins are separated for viewing purposes in figures (9) and (18). Thus, one must conceptually reposition the orthogonal sets of virtual particle path spins from the irregular distribution of positive particles while keeping them aligned as they are so that the origin of each orthogonal set of extranuclear spins from the irregular distribution of positive particles is almost abutting the origin of the respective orthogonal set of nuclear spins of the charged particle interacted upon for proper alignments.

Similarly, in figure (9), the microscopic charge spins (q) of the effective virtual particle paths from the irregular distribution of positive particles which enter the nuclear region on the bottom section of the negative particle are parallel to the microscopic charge spins (q) of the virtual particle paths of the bottom section of the

nuclear region of the negative particle so as to attract. Yet, the microscopic magnetic spins (B_m) of the effective virtual particle paths from the irregular distribution of positive particles which enter the nuclear region on the bottom section of the negative particle are parallel to the microscopic magnetic spins (B_m) of the virtual particle paths of the bottom section of the nuclear region of the negative particle so as to repel. While, the microscopic mass spins (m) of the effective virtual particle paths from the irregular distribution of positive particles which enter the nuclear region on the bottom section of the negative particle are antiparallel to the microscopic mass spins (m) of the virtual particle paths of the bottom section of the nuclear region of the negative particle so as to also repel, and, in effect, produce a form of "mass repulsion."

In this case, the virtual particle paths which are interacting on the bottom section of the negative particle are considered to relatively repel due to the repulsion of respective microscopic magnetic and mass spins. Wherein, the bottom section of the unified field of the negative particle shown in figure (9) is considered to decrease in mass and decelerate to an extent.

Consequently, the top section of the negative particle as shown in figures (9) and (10) (starting in the nuclear region where the virtual particle paths begin to converge on the front side of the negative particle) is considered to project forward and downward, and, in effect, establish the leading edge of the particle as indicated in the perspective view of the nuclear region of the negatively charged particle shown in figure (10).

Edge formation of an accelerated
negative particle
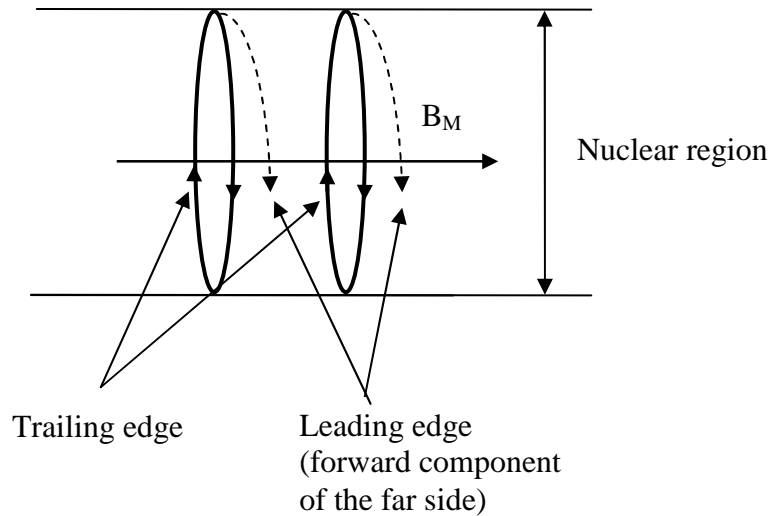
FIG. 10

Correspondingly, the bottom section of the negative particle (in figures 9 and 10) is considered to rotate around

with a changed geometrical path (difference not shown) and follow the leading edge, such that, in effect, this

portion of the unified field of the particle establishes the trailing edge of the particle.

The attractive, repulsive, or neutral condition of coupling microscopic charge and mass spins is

considered to occur according to the alignment of the respectively coupled charge and mass spin vectors.

Figures (11A) and (11B) show how two right hand and two left hand charge and mass microscopic spin vectors

can have a totally attractive, a totally repulsive, or a "neutral" alignment (wherein partial attraction would be

situated between neutral and total attraction, and partial repulsion would be situated between neutral and total

repulsion). Note that parallel electric spin (q) alignment is a special requirement for "coupling" of (q) spin

vectors (or respective components) in interactions where the entrance of an interacting virtual particle path from

one particle into the nuclear region of another particle is pertinent.

Microscopic charge and mass spin vector attraction, repulsion, and
neutral alignment

| Total attraction | Neutral | Total repulsion |

FIG. 11A

| Total attraction | Neutral | Total repulsion |
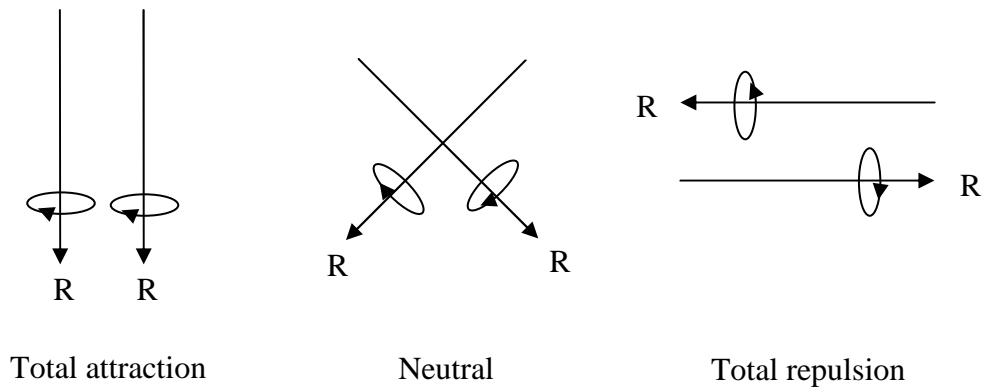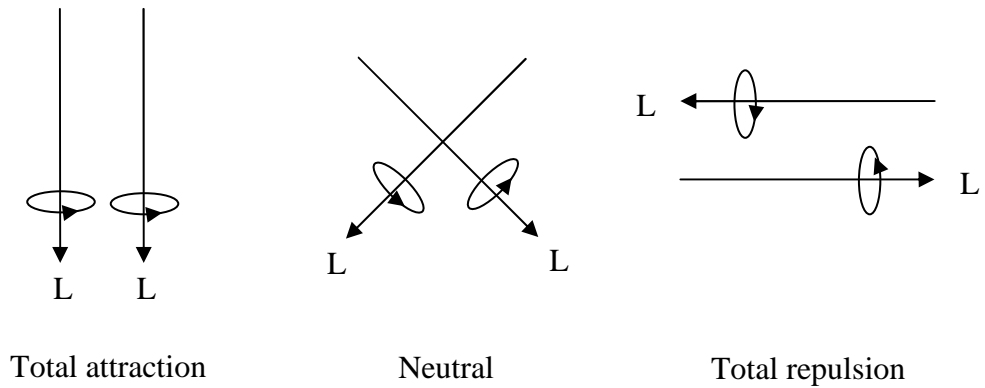
FIG. 11B

However, the attractive, repulsive, or "neutral" condition of coupling microscopic magnetic spins is

considered to occur according to the alignment of the respectively coupled microscopic magnetic spin vectors in

an effectively different manner. Figures (12A) and (12B) show how two right hand and two left hand

microscopic magnetic spin vectors can have a totally attractive, a totally repulsive, or a "neutral" alignment (wherein, similarly, partial attraction would be situated between neutral and total attraction, and partial repulsion would be situated between neutral and total repulsion).

Microscopic magnetic spin vector attraction, repulsion, and
neutral alignment

Total attraction   Neutral   Total repulsion

FIG. 12A

Total attraction   Neutral   Total repulsion
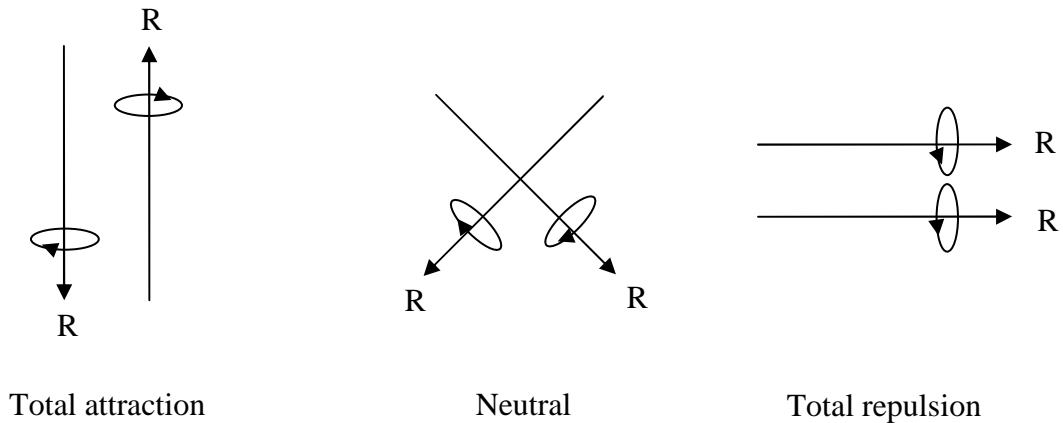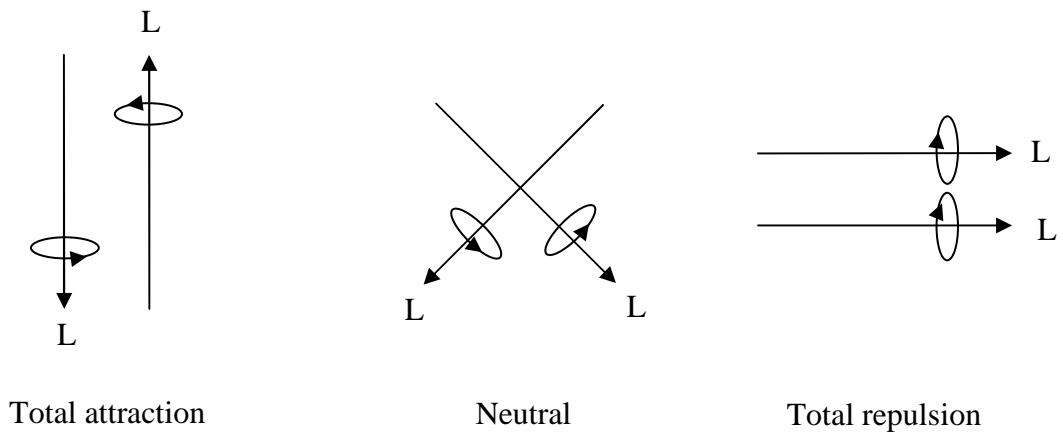
FIG. 12B

Nevertheless, continuing with the interaction of the irregular distribution of positive particles with the negative particle, as the negative particle rotates around and realigns itself in the interacting extranuclear field

extended by the irregular distribution of positive particles, the relatively decelerated trailing edge of the negative particle aligns itself with the field like the leading edge, and establishes the accelerated conditions equivalent to those of the leading edge. Wherein, the negative particle propagates towards the irregular distribution of positive particles as the attractive spin vectors of the extranuclear virtual particle paths of the positive particles continue to accelerate the negative particle, such that the electromagnetic and gravitational attraction of the negative particle by the positive particles results.

Then, the extended extranuclear fields of the positive particles continue to interact with the transformed geometry of the unified field of the propagating negative particle, such that the propagating negatively charged particle moves forward towards the irregular distribution of positive particles according to spin vector interactions, and accelerates according to the increase in the angular rotation of the orthogonal spin vectors of the extranuclear virtual particle paths from the positive particles in conjunction with the increase in the density of the extranuclear virtual particle paths from the positive particles as the negative particle approaches the positive particles. While, the virtual particle paths of the top and bottom sides of the accelerated negative particle propagate side-by-side with respective elliptical helicities and relative orientations.

Figures (13A) and (13B) each show how the leading edge of example top and bottom virtual particle paths of accelerated negative and positive electrically charged particles effectively rotate around certain lines (including lines which are aligned along the vertical dashed lines shown, and the horizontal dashed line which is in the plane of symmetry separating the top and bottom sides), and project forward in order to establish the respectively combined right and left hand elliptically helical virtual particle paths of the top and bottom sides of the respectively propagating electrically charged particle.
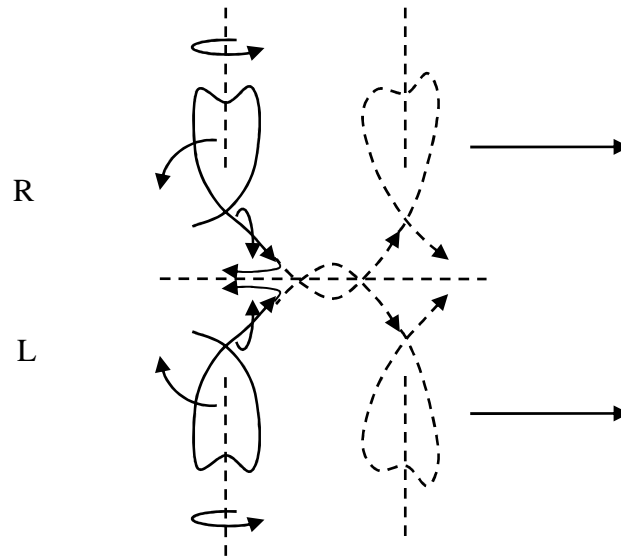
Rotations of an accelerated negative
particle

FIG. 13A

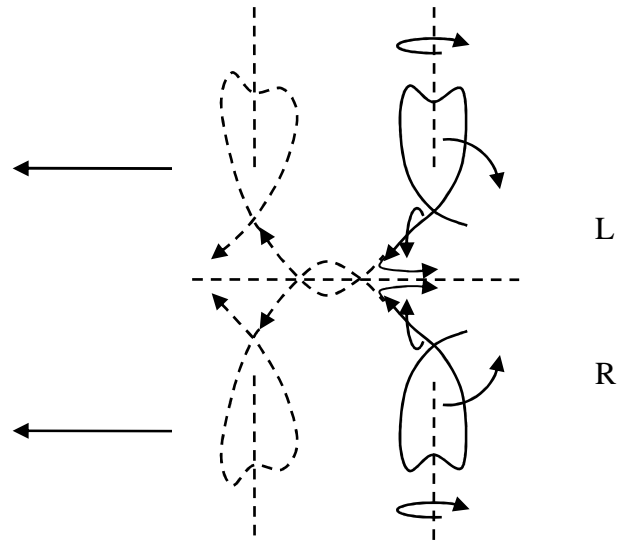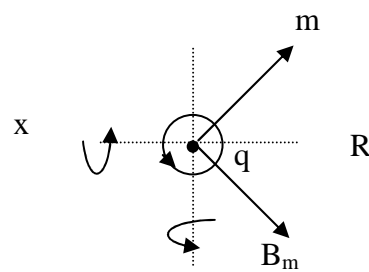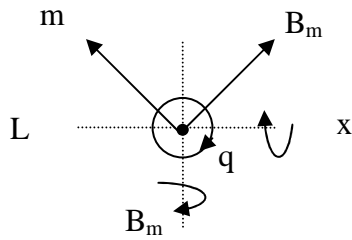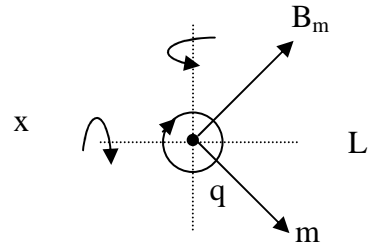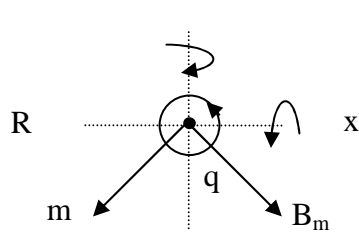Rotations of an accelerated positive
particle

L

R

FIG. 13B

Figures (14A) and (14B) show a front view (with respect to the direction of propagation) of the rotations of the

microscopic spin vectors (at the leading edge) of some example nuclear virtual particle paths of a negatively

and a positively charged particle, respectively, which are each accelerated out of the page. It is considered that

the spin vectors rotate around orthogonal rotational axes using the intersecting point of the spin vectors at a

tangent point along a respective virtual particle path as a pivot point.

Rotations of nuclear virtual particle paths (at the leading edge) of the front side of a negatively charged particle due to acceleration.

Rotations of nuclear virtual particle paths (at the leading edge) of the front side of a positively charged particle due to acceleration.

Note that the direction of rotation of a spin reverses as the spin inverts.

FIG. 14A   FIG. 14B

Note that the directions of the rotations in figures (14A) and (14B) are considered equivalent to the directions of

the rotations experienced by virtual particles while oscillating in electrically charged particles as pertains to, for

example, figures 3A-5B; and are considered equivalent to the directions of the rotations experienced by the

virtual particles of accelerated electrically charged particles as pertains to, for example, figure 6D, and figures

13A and 13B.

Figures (15A) and (15B) show front views of example top and bottom more bent and less bent virtual particle paths of the front portions of propagating negative and positive electrically charged particles.

R

L

L

R
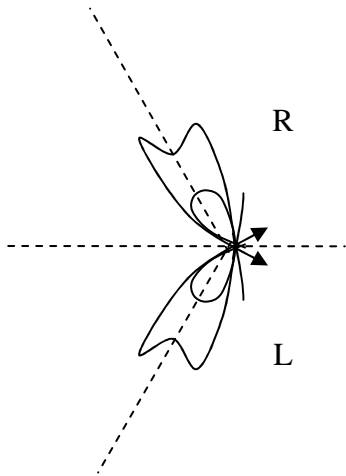
Front view of more and less bent
virtual particle paths of a negatively
electrically charged particle
propagating out of the page
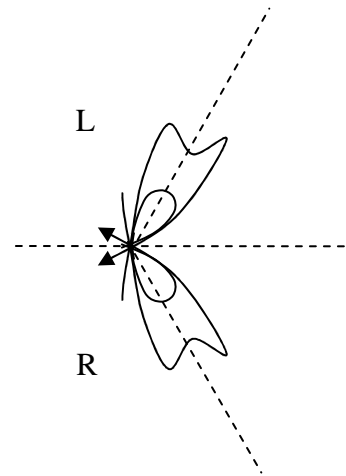
Front view of more and less bent
virtual particle paths of a positively
electrically charged particle
propagating out of the page

FIG. 15A

FIG. 15B

As shown in figures (15A) and (15B), it is considered that the virtual particle paths of an electrically charged particle only partially rotate around the horizontal dashed line in the plane of symmetry which separates the top and bottom sides while propagating in an elliptically helical manner around respective axes and one common central axis, such that the top and bottom virtual particle paths of an electrically charged particle do not completely come together. Respectively, it is considered that the virtual particle paths in a band of virtual particle paths comprised in an electrically charged particle have relatively different angular alignments (in a

graduated way), and are rotated to respectively different extents upon acceleration. Accordingly, each virtual particle path in a particle has a respectively different energy attributable to it before and during propagation. While, as the degrees of rotation around the respective rotational axes change for all of the virtual particle paths in the respective bands of virtual particle paths in an accelerated particle, the energy (including "relativistic mass") for an accelerated particle as a whole changes.

Consider here how the form of the function for a time dependent particle in quantum mechanics corresponds to the unified field function presented herein (as with a time independent particle in quantum mechanics):

$$\psi(x) = Ae^{-ikx-\omega t} = Ae^{\frac{-i2\pi mcr}{h} - (kc)t} = Ae^{\frac{-i2\pi mcr}{h} - \frac{2\pi mc^2 t}{h}} = Ae^{\frac{-i2\pi mcr}{h} - \frac{2\pi mcr}{h}}$$

(when k=2πmc/h and x=r)

Wherein, quantum mechanically, (A) can be a scalar amplitude, such that, for example, $A=\frac{1}{2}kx^2 \equiv mgh$ which pertains to $\approx {}^{-}G_T m/r$ (when the other mass of potential energy is positioned at infinity) which, herein, is equivalent to $\approx {}^{-}K_T q/r$; or (A) can be a vector amplitude, e.g., E (electric field vector), i.e., ${}^{-}K_C q/r^2$, which is the negative of the gradient of the potential ${}^{-}K_C q/r$ which herein relates to $\approx {}^{-}K_T q/r$ which again, herein, is equivalent to $\approx {}^{-}G_T m/r$.

Inertia has been a curious issue over the centuries particularly since Galileo. Respectively, the virtual particle paths in a band of virtual particle paths in an electrically charged particle are considered to interact (in the form of self interaction) and resist acceleration while having "inertia" (i.e., requiring potential or force to change their respective alignments), and, additionally, virtual particle paths from an electrically charged particle

are considered to interact with the virtual particle paths of an interacting particle during, for example, long range electromagnetic and gravitational interactions, thus accounting for the source of the equivalence of inertial and gravitational mass.
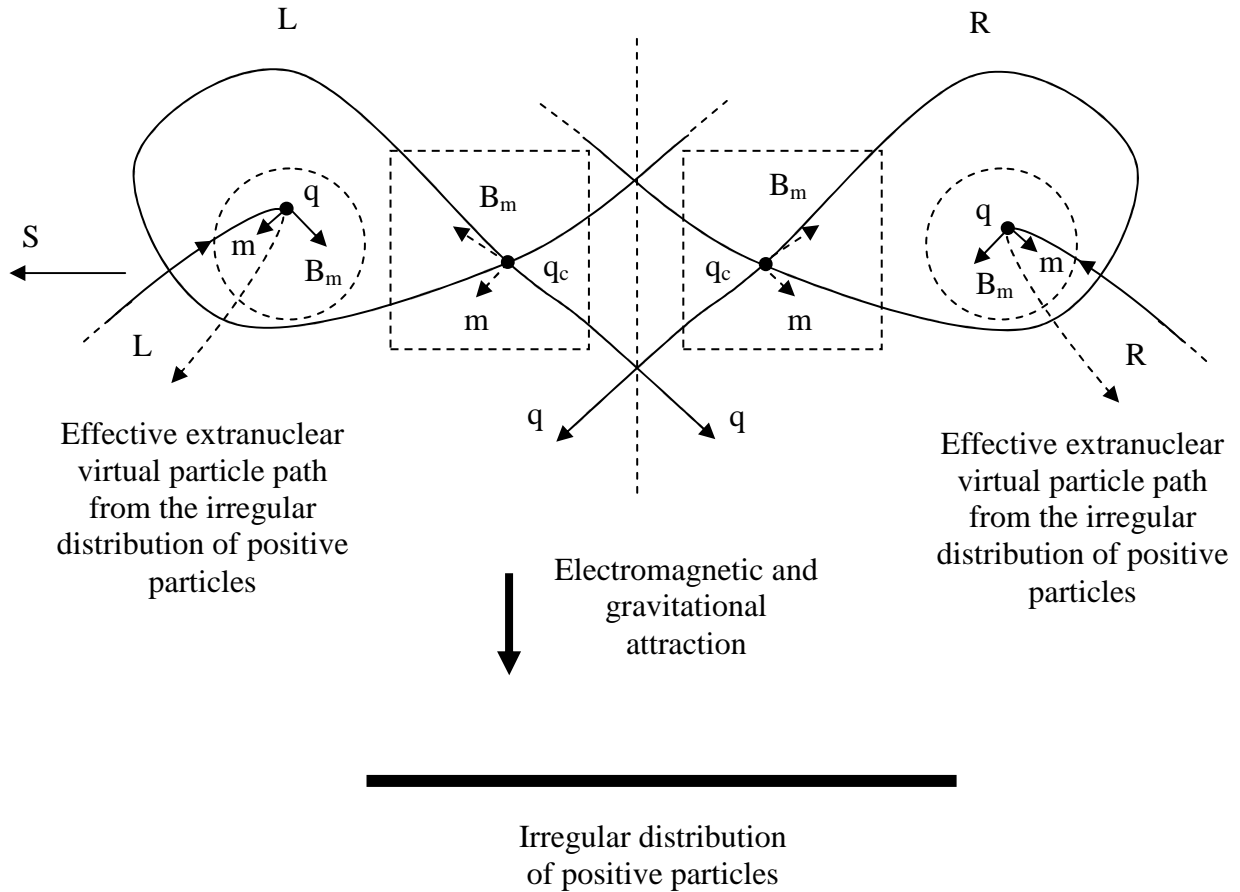
However, the bands of virtual particle paths in a quantum of electromagnetic radiation (which is described more so later) are considered to be relatively converged due to the absence of a significant extent of their eccentricities, such that the each band of virtual particle paths in the quantum of electromagnetic radiation is relatively narrow compared to a band of virtual particle paths in a propagating electrically charged particle. In which case, the virtual particles on the top side and the virtual particles on the bottom side of the quantum propagate in a more aligned manner while also having inertia (i.e., while also requiring potential or force to change their respective alignments), but while also having only an infinitesimal small amount of "gravitational mass."

Conventionally, an electron has arguably been considered to be a point particle with no internal structure. However, the structure and function of the present unified field has shown how the virtual particle paths of an electrically charged particle can statically oscillate, and then open upon acceleration, such that the internal structure of the static unified field transitions into the propagating unified field of an electrically charged particle such as a propagating electron or proton. While, virtual particle paths of the resulting propagating electrically charged particle can be considered to constitute a wave packet, which, in furtherance of the equations provided, can be described in terms of families of complex exponential functions representing helically propagating virtual particle paths.

Continuing with the interaction described with respect to figures (8), (9), and (10), next, figure (16) shows a side view of the two possible varieties of effective virtual particle paths of the irregular distribution of positively charged particles which interact with the virtual particle paths of the propagating negatively charged

particle as it propagates down the page. In which case, it is consider that interaction occurs as if a "dense nuclear region" of sorts has been preserved on the top and bottom sides of the propagating electrically charged particle. Accordingly, as shown in figure (16), the respective microscopic charge (q) and mass (m) spin vectors are aligned parallel, and the respective microscopic magnetic (B_m) spin vectors are aligned antiparallel, such that the propagating negatively charged particle is accelerated downward towards the positively charged particles.

Negative particle propagating down the
page interacting with two effective
varieties of virtual particle paths from an
irregular distribution of positive particles

L   R

S

Effective extranuclear
virtual particle path
from the irregular
distribution of positive
particles

Effective extranuclear
virtual particle path
from the irregular
distribution of positive
particles

Electromagnetic and
gravitational
attraction

Irregular distribution
of positive particles

Effective extranuclear virtual particle paths (with spins in dashed circles)
extend out from the irregular distribution of positively charged particles
(thick solid line), and interact with the "nuclear region" of the propagating
negatively charged particle (with spins in dashed squares), such that the
microscopic charge (q) and mass (m) spins of respectively interacting right
and left hand screw sides are parallel and respectively attract, and such that
the microscopic magnetic spins (B_m) of respectively interacting right and left
hand screw sides are antiparallel and respectively attract. Note that the top
and bottom sides of the propagating negatively charged particle tilt out of
the page, and (q_c) is the component of the respective microscopic electric
charge spin vector aligned out of the page.

FIG. 16

Note that for figures (16), (20), and (21), only the front portion of the negatively charged particle is shown, and note that the spin vectors in the dashed squares are aligned in a somewhat tilted manner in and out of the page. Moreover, note that for figures (16), (20), and (21), the "interacting" spins are separated for viewing purposes. Thus, one must conceptually reposition each orthogonal set of extranuclear spins shown in a dashed circle (along with the respective virtual particle path) while keeping it aligned as it is so that the origin of each orthogonal set of extranuclear spins is almost abutting the origin of the orthogonal set of nuclear spins shown in a corresponding dashed square for proper alignments.

Now, if the irregular distribution of particles creating the extended extranuclear fields and the static particle located a distance away have the same charge, then electromagnetic repulsion will be produced along with respective gravitational attraction as shown in figures (17), (18), and (19) for an irregular distribution of positively charged particles interacting with a positively charged particle. Wherein, in this case, electromagnetic repulsion would dominate over gravitational attraction.
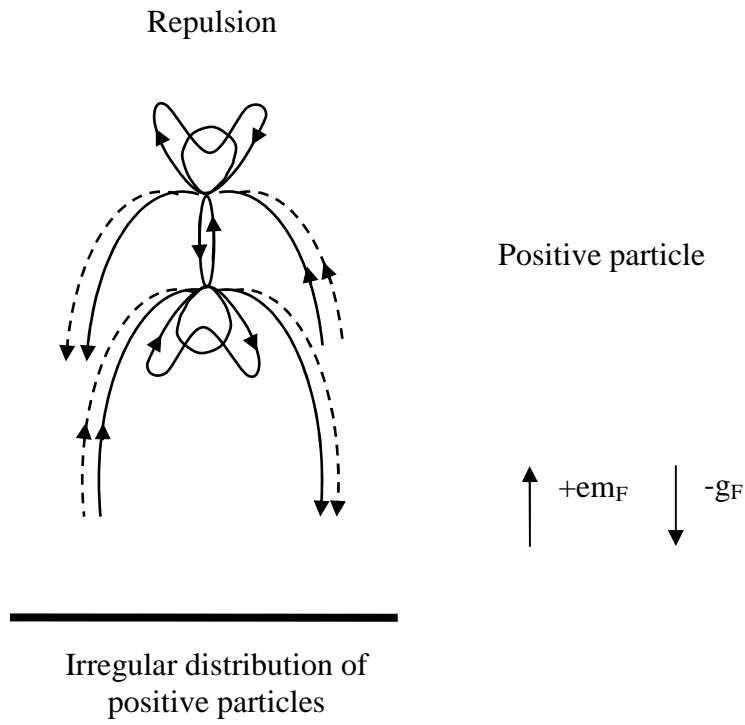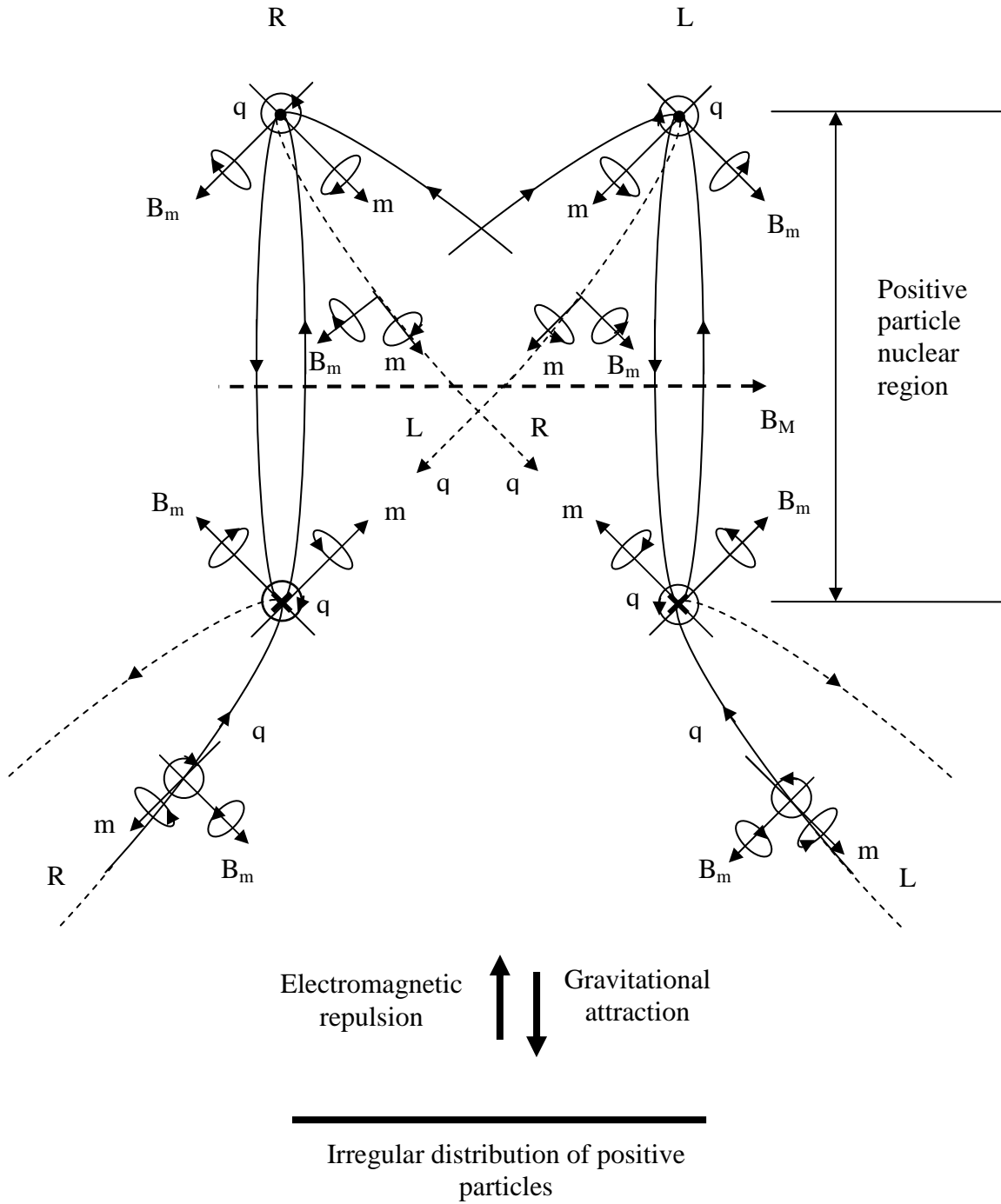
Repulsion

Positive particle

$+em_F$ $-g_F$

Irregular distribution of
positive particles

FIG. 17

FIG. 18

Edge formation of an accelerated
positive particle

Leading edge (forward
component of the far
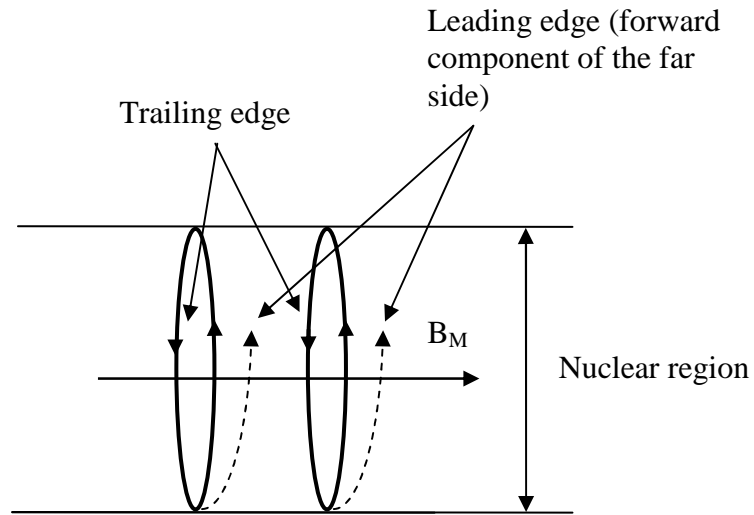side)

Trailing edge

B_M

Nuclear region

FIG. 19

While, figure (20) shows the two possible varieties of effective virtual particle paths of the irregular

distribution of positively charged particles which would interact with the virtual particle paths of a positively

charged particle if it were initially propagating down the page, such that the positively charged particle would

be decelerated as it approaches the positively charged particles.

Positive particle propagating down the
page interacting with two effective
varieties of virtual particle paths from an
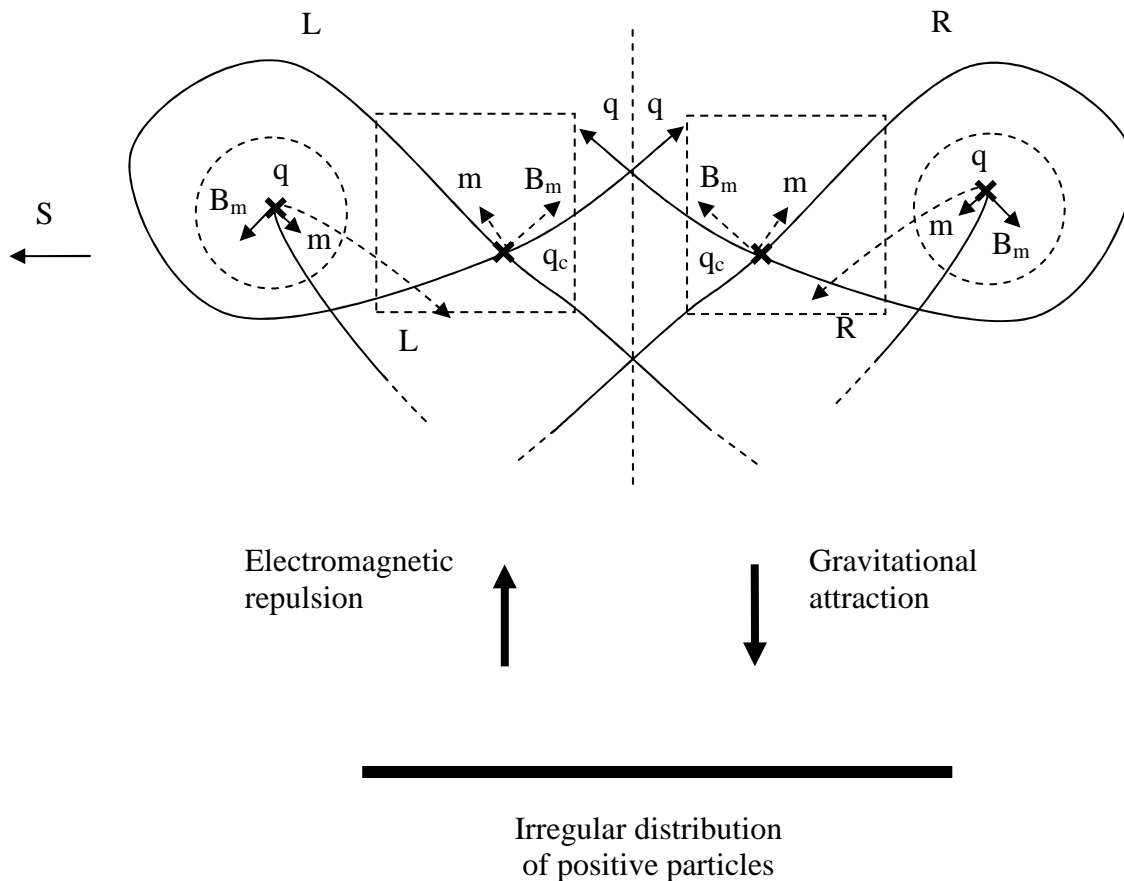irregular distribution of positive particles
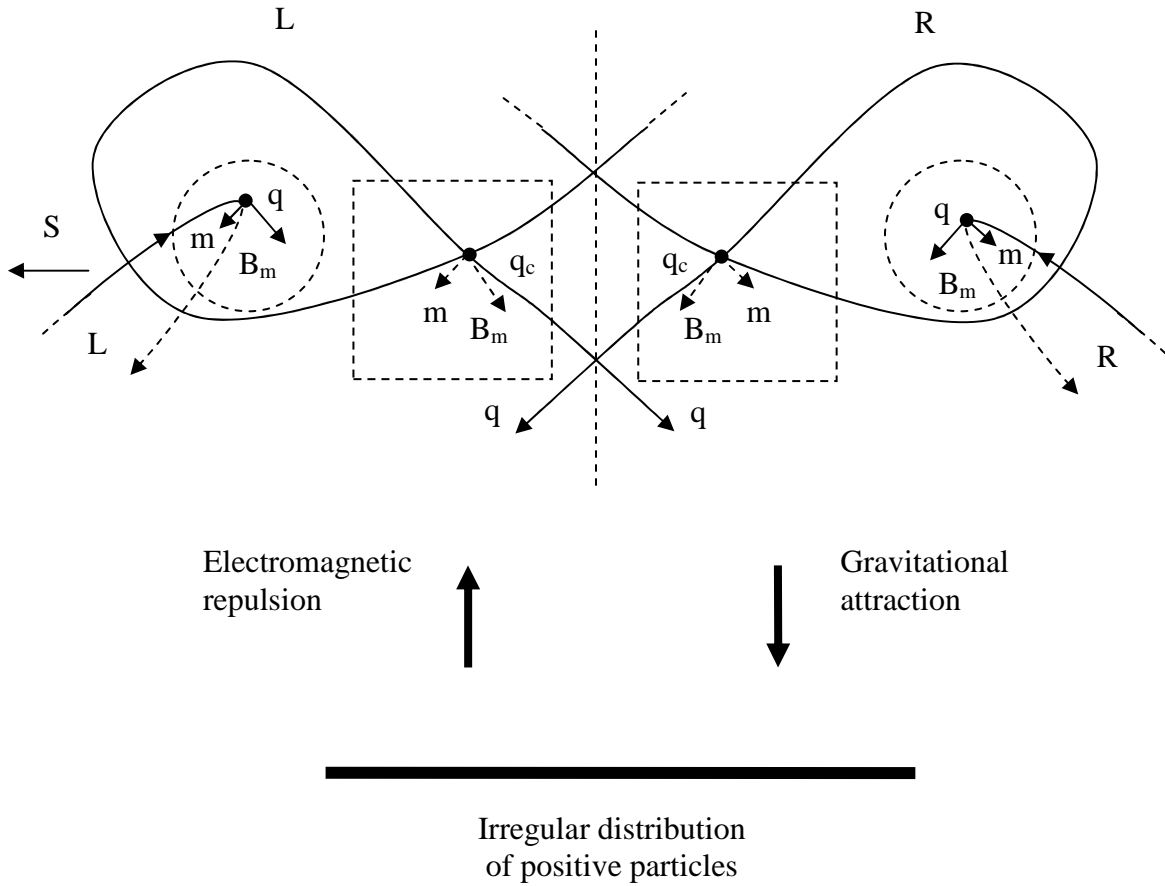
Effective extranuclear virtual particle paths (with spins in dashed circles)
extend out from the irregular distribution positively charged particles (thick
solid line), and interact with the "nuclear region" of the propagating positively
charged particle (with spins in dashed squares), such that the microscopic
charge (q) and mass (m) spins of respectively interacting right and left hand
screw sides are parallel and respectively attract, and such that the microscopic
magnetic spins (B_m) of respectively interacting right and left hand screw sides
are parallel and repel. Note that the top and bottom sides of the propagating
positively charged particle tilt out of the page, and (q_c) is the component of
the respective microscopic electric charge spin vector aligned out of the page.

FIG. 20

Here, the virtual particle paths of the irregular distribution of positively charged particles would, in effect, electromagnetically repel the virtual particle paths of the propagating positive particle, and cause the virtual particle paths of the propagating positive particle to change geometry such that the positive particle would decelerate and turn away from the positively charged particles. In this case, the positive particle would turn away from the irregular distribution of positively charged particles against the affect of the gravitational attraction of the virtual particle paths of the same irregular distribution of positively charged particles. Wherein, the gravitational attraction would cancel an extent of the electromagnetic repulsion while attempting to cause (to a respective extent) the opposite turning effect on the positive particle in effort to cause the positive particle to "accelerate" toward the positively charged particles (or cause the positive particle to "decelerate" in terms of its propagation away from the positively charged particles). In effect, the positive particle would be accelerated in the opposite direction away from the irregular distribution of positive particles by electromagnetic repulsion, which in this example, as said, would dominate over gravitational attraction.

Figure (21) shows the two possible varieties of effective virtual particle paths of the irregular distribution of positively charged particles which interact with the virtual particle paths of the propagating positively charged particle which is turned around and accelerated up the page away from the same irregular distribution of positively charged particles. Here, while the microscopic electric charge spins (q) are parallel, the mass spins (m) of respectively interacting right and left hand screw sides are now antiparallel and repel in attempt to turn the positive particle around, such that, in effect, the mass spin vectors are producing gravitational attraction as the positive particle is repelled away from the irregular distribution of positive particles by electromagnetic repulsion due to the attraction caused by the antiparallel microscopic magnetic spins (B_m) of respectively interacting right and left hand screw virtual particle paths of the irregular distribution of positively charged particles and the positively charged propagating particle.

Positive particle propagating up the page
interacting with two varieties of effective
virtual particle paths from an irregular
distribution of positive particles

Electromagnetic
repulsion

Gravitational
attraction

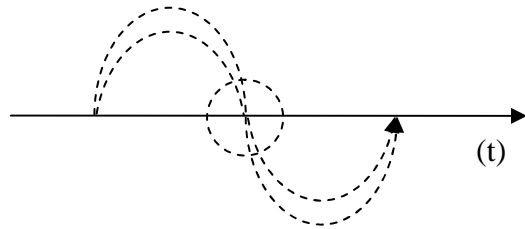Irregular distribution
of positive particles

Effective extranuclear virtual particle paths (with spins in dashed circles) extend out from the irregular distribution of positively charged particles (thick solid line), and interact with the "nuclear region" of the propagating positively charged particle (with spins in dashed squares), such that the microscopic charge spins (q) of respectively interacting right and left hand screw sides are parallel and respectively attract, and such that the microscopic mass spins (m) of respectively interacting right and left hand screw sides are antiparallel and repel (attempting to turn the positively charged propagating particle around), and, furthermore, such that the microscopic magnetic spins (B_m) of respectively interacting right and left hand screw sides are antiparallel and attract (thus repelling the positive particle away from the irregular distribution of positive particles). Note that the top and bottom sides of the propagating positive particle are now tilted into the page, and (q_c) is the component of the respective microscopic electric charge spin vector aligned into the page.

FIG. 21

It is considered that the virtual particle paths of oppositely electrically charged particles can produce electrically neutral effects. Wherein, if a uniform irregular distribution of both positive and negative electrically charged particles (with respective mass) interact with an electrically charged particle, then the microscopic magnetic spins of the four effective varieties of extranuclear virtual particle paths (from eight possible virtual particle paths altogether) from the given irregular distribution positive and negative electrically charged particles would "symmetrically" neutralize so as to neutralize the electromagnetic effects, while the same mass spins would continue to be affective and maintain gravitational attraction. (Note that gravitational attraction occurs with both electromagnetic attraction and electromagnetic repulsion, e.g., as shown in figures 16, 20, and, effectively, in figure 21, and thus gravity is perceived as only causing acceleration towards a massive particle.)

As further examples of the symmetric electrically neutral affects of virtual particle paths, it is considered that a neutron comprises the virtual particle paths of a positive electrically charged proton and a negative electrically charged electron (as elaborated upon later) which can effectively interact together in a symmetrical manner so as to produce an electrically neutral effect. While, a quantum of electromagnetic radiation is considered to comprise top and bottom sides which propagate side-by-side, and interact electromagnetically in an "electrically neutral" manner upon being "symmetrically" absorbed into a particle (such as an electron) along the nuclear region. While other than this sort of interaction, it is considered that a quantum of electromagnetic radiation can not be significantly electrically interacted upon by electrically charged particles due to the particular alignment of the microscopic spin vectors of the virtual particle paths on the top and bottom sides in its internal structure.
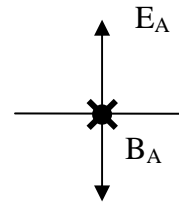
Figure (22A) shows a rotated view of the top and bottom virtual particle paths of a matter quantum with respect to an interacting irregular distribution of positive and negative electrically charged particles (e.g., an irregular distribution of positive and negative electrically charged particles comprised by a star of significant mass).

Matter quantum

Irregular distribution of positive
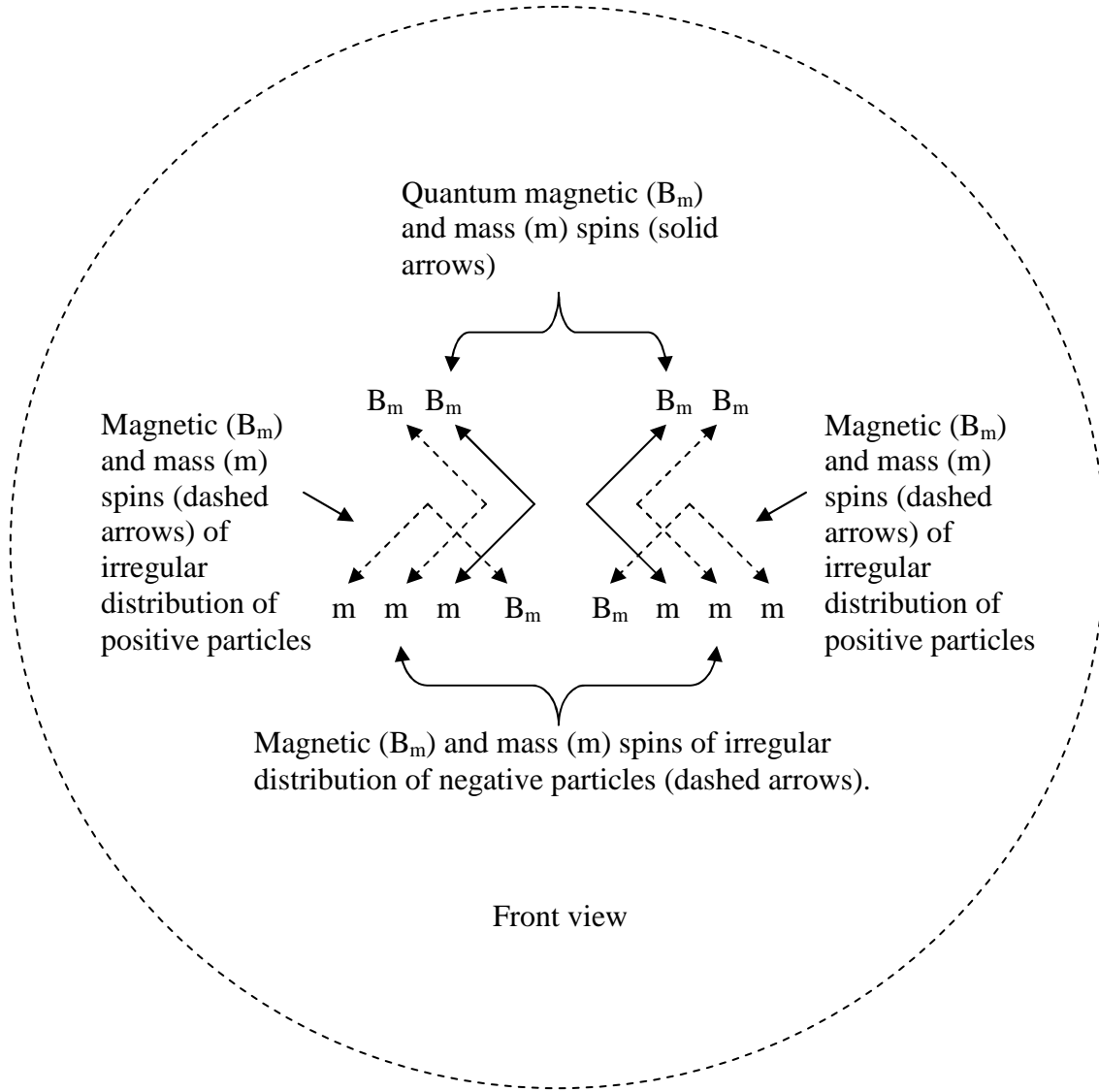and negative electrically
charged particles

E_A

B_A

Matter quantum
(B_A) is in and out
of the page

Arrangement of a propagating matter quantum of
electromagnetic radiation with respect to an interacting
irregular distribution of positive and negative electrically
charged particles (thick solid line).

FIG. 22A

Figure (22B) is an enlarged view of what is occurring with the spin vectors in the dashed sphere in figure (22A)
as would be seen from the front by rotating the (t) axis 90 degrees.

Quantum magnetic (B_m) and mass (m) spins (solid arrows)

B_m B_m B_m B_m

Magnetic (B_m) and mass (m) spins (dashed arrows) of irregular distribution of positive particles

Magnetic (B_m) and mass (m) spins (dashed arrows) of irregular distribution of positive particles

m m m B_m B_m m m m

Magnetic (B_m) and mass (m) spins of irregular distribution of negative particles (dashed arrows).

Front view

Here, figure (22B) is an enlarged view of what is occurring in the dashed sphere in figure (22A) as would be seen from the front view of the quantum by rotating the (t) axis 90 degrees. Wherein, in figure (22B), the mass spins (m) from the irregular distribution of positive and negative particles are aligned parallel with the matter quantum mass spins (m), and thus all attract so as to produce gravitational attraction. While, the magnetic spins (B_m) of the irregular distribution positive particles are all aligned antiparallel and thus attract, and the magnetic spins (B_m) of the irregular distribution of negative particles are all aligned parallel and thus repel, such that antiparallel and parallel magnetic spins cancel and effectively produce charge neutralization. Note that the quantum top and bottom (B_m) and (m) spin vectors are rotated into the plane of the page, but actually are approximately in the portions of the dashed planes aligned perpendicularly shown in figure (22C).

FIG. 22B
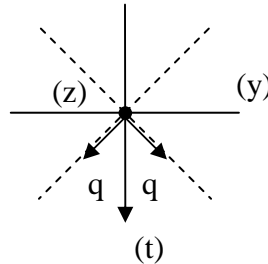
When figure (22B) is viewed from the top, the quantum top and bottom (B_m) and (m) microscopic spin vectors are aligned approximately in the dashed planes aligned perpendicularly. While, the (q) spin vectors are aligned perpendicular to their respective (B_m) and (m) spin vectors, and the quantum as a whole would be propagating along the (t) axis.

FIG. 22C

Note that gravitational "attraction" would be represented by the attempt to turn the virtual particles around on the apposite side of the quantum (with respect to figure 22B) where the mass spins of the quantum would invert alignment and be antiparallel with the mass spins of the extranuclear virtual particle paths of the large mass (as in figure 21 during electromagnetic interaction where the repelled electrically charged particle is propagating away from the repulsive source).

Equation (15A) shows the theoretical reasoning for the apparent doubling of the gravitational potential in the gravitational lensing effect upon the interaction of a massive irregular distribution of positively and

negatively charged particles with a quantum of electromagnetic radiation at weak field (the result of which is similar to that of general relativity):

$$V_{(\text{large mass total gravitational potential})} = 1*4*2*\sum V_g =$$

$$1*4*2*\left[\left(^{-}\frac{1}{\approx 4}G_T\frac{m}{r}*e^{[1*\,\approx\,^{-}0\pi(mcr)/h]} + {}^{-}\frac{1}{\approx 4}G_T\frac{m}{r}*e^{[1*\,\approx\,^{-}0\pi(mcr)/h]}\right) + \ldots\right] =$$

$$1*4*2*\left[\left(^{-}\frac{1}{\approx 2}G_T\frac{m}{r}*e^{[1*\,\approx\,^{-}0\pi(mcr)/h]}\right) + \ldots\right] = 4*\left[\left(\approx^{-}1G_T\frac{m}{r}*e^{[1*\,\approx\,^{-}0\pi(mcr)/h]}\right) + \ldots\right] \approx$$

$$^{-}4G_T\frac{M}{r}*e^{[^{-}0\pi(mcr)/h]} \approx {}^{-}4G_T\frac{M}{r}.$$

Eq. (15A)

Here, $e^{[\,1*\,\approx\,-0\pi(mcr)/h]}$ is considered equal to one.

Wherein with respect to equation (15A), the net charge of the interacting large mass is equal to zero so that only the gravitationally associated virtual particle path portions of potential which are associated with the interacting particles are considered. In which case, more specifically, the gravitationally associated potentials of the constituent particles, i.e., $\approx {}^{-}\frac{1}{4}G_Tm/r*1/e^{[1*\,\approx 0(2\pi mcr)/h]}$ each, from the large mass enter the "nuclear region" of the quantum of electromagnetic radiation by way of their respective gradient virtual particle paths, and interact by summating with the gravitationally associated potentials of the quantum. While, the Lorentz factors of the quantum are transferred to the gravitationally related potentials of the large mass. (Note that the Lorentz factors of the large mass are considered to be effectively transferred to the gravitationally associated potentials

of the quantum as well.) Nevertheless, the effective gravitational potential of the large mass would thus be $\approx^-$

$4G_TM/r$ as formulated in equation (15A).

It is considered that the two interacting sources exchange their respective Lorentz factors such that, for

the example in which a quantum of electromagnetic radiation is involved, the effective gravitational potential of

the quantum which is interacted upon would be $\approx^- 2G_Tm/r$ as shown in equation (15B) below:

$$V_{\text{(photon gravitational potential)}} = \frac{1}{4}*4*2*\sum V_g =$$

$$\frac{1}{4}*4*2*\left[\left(\frac{^-1}{\approx 2}G_T\frac{m}{r}*e^{[0*\ (\approx^- 2\pi mcr)/h]}+\frac{^-1}{\approx 2}G_T\frac{m}{r}*e^{[0*\ (\approx^- 2\pi mcr)/h]}\right)\right]=$$

$$\frac{1}{4}*4*2*\left[\left(\frac{^-1}{\approx 1}G_T\frac{m}{r}*e^{[0*\ (\approx^- 2\pi mcr)/h]}\right)\right]\approx^- 2G_T\frac{m}{r}*e^{(^-0\pi mcr/h)}\approx^- 2G_T\frac{m}{r}.$$

Eq. (15B)

Note that the result of equation (15B) is in agreement with the photon gravitational potential implied

conventionally by the Schwarzschild radius, i.e., $c^2=2G_CM/r_S$.

Then, the respective force between the large mass and the quantum would be:

$$\approx^- 4G_T(M)*\frac{e^{\left[\frac{1*\ \approx^- 0\pi(mcr)}{h}\right]}}{r^2}*\left(2m*e^{\left[\frac{0*\approx^- 0\pi(mcr)}{h}\right]}\right)\approx \frac{^-8G_T(M*m)}{r^2}=g_F.$$

While, for example, if a relativistically accelerated electrically charged particle were applied instead of a quantum, the internal spin vectors of the electron would rotate (and the constants would move along their respective intervals) so that the potential of the large mass would be multiplied times a factor of (½) which corresponds to the square of the respective Lorentz factor, i.e., $(\Delta n_1)=\sqrt{2}$ such that $1/(\sqrt{2})^2/1=½$, such that the effective potential of the large mass in this case would be $\approx {}^-2G_TM/r$ as shown below:

$$V_{\text{(large mass total gravitational potential)}} = \frac{1}{2}*4*2*\sum V_g =$$

$$\frac{1}{2}*4*2*\left[\left({}^-\frac{1}{\approx 4}G_T\frac{m}{r}*e^{[.171*\ \approx\ {}^-0\pi(mcr)/h]}+{}^-\frac{1}{\approx 4}G_T\frac{m}{r}*e^{[.171*\ \approx\ {}^-0\pi(mcr)/h]}\right)+...\right]=$$

$$\frac{1}{2}*4*2*\left[\left({}^-\frac{1}{\approx 2}G_T\frac{m}{r}*e^{[.171*\ \approx\ {}^-0\pi(mcr)/h]}\right)+...\right]=4*\left[\left({}^-\frac{1}{\approx 2}*G_T\frac{m}{r}*e^{[.171*\ \approx\ {}^-0\pi(mcr)/h]}\right)+...\right]\approx$$

$$^-2G_T\frac{M}{r}*e^{[\ ^-0\pi(mcr)/h]}\approx{}^-2G_T\frac{M}{r}.$$

Eq. (15C)

While, upon exchanging Lorentz factors, the effective gravitational potential for the relativistically accelerated electrically charged particle which is interacted upon would be $\approx {}^-\sqrt{2}*G_Tm/r$ as shown below:

$$V_{\text{relativistically accelerared particle gravitational potential}} = \frac{1}{4} * 4 * 2 * \sum V_g =$$

$$\frac{1}{4} * 4 * 2 * \left[\left(^{-}\frac{1}{\approx 2\sqrt{2}} G_T \frac{m}{r} * e^{[0*(.414*\approx^{-}2\pi mcr)/h]} + {}^{-}\frac{1}{\approx 2\sqrt{2}} G_T \frac{m}{r} * e^{[0*(.414*\approx^{-}2\pi mcr)/h]} \right) \right] =$$

$$\frac{1}{4} * 4 * 2 * \left[\left(^{-}\frac{1}{\approx \sqrt{2}} G_T \frac{m}{r} * e^{[0*(.414*\approx^{-}2\pi mcr)/h]} \right) \right] = 2 * \left[\left(^{-}\frac{\sqrt{2}}{\approx 2} G_T \frac{m}{r} * e^{[0*(.414*\approx^{-}2\pi mcr)/h]} \right) \right] \approx$$

$$^{-}\sqrt{2} G_T \frac{m}{r} * e^{(^{-}0\pi mcr/h)} \approx {}^{-}\sqrt{2} G_T \frac{m}{r}.$$

Eq. (15D)

Consequentially, the respective force between the large mass and the relativistically accelerated electrically charged particle would be:

$$\approx {}^{-}2G_T(M) * \frac{e^{\left[\frac{.171* \approx {}^{-}0\pi(mcr)}{h} \right]}}{r^2} * \left(\sqrt{2}m * e^{\left[\frac{0* \approx .414* {}^{-}2\pi(mcr)}{h} \right]} \right) \approx \frac{^{-}2\sqrt{2}G_T(M*m)}{r^2} = g_F.$$

Still, if a static electrically charged particle were applied, then the large mass would be multiplied times yet another factor of (½) according to the square of the respective Lorentz factor, i.e., $(\Delta n_1)=2$ such that $1/(2)^2/1=\frac{1}{4}$, wherein, the gravitational potential of the large mass would then be $\approx {}^{-}G_T M/r$ (approximately reducing to Newton's law of gravitation) as shown below:

$$V_{(\text{large mass total gravitational potential})} = \frac{1}{4} * 4 * 2 * \sum V_g =$$

$$\frac{1}{4} * 4 * 2 * \left[\left({}^{-}\frac{1}{\approx 4}G_T \frac{m}{r} * e^{[0* \approx {}^{-}0\pi(mcr)/h]} + {}^{-}\frac{1}{\approx 4}G_T \frac{m}{r} * e^{[0* \approx {}^{-}0\pi(mcr)/h]}\right) + \cdots\right] =$$

$$2 * \left[\left({}^{-}\frac{1}{\approx 2}G_T \frac{m}{r} * e^{[0* \approx {}^{-}0\pi(mcr)/h]}\right) + \cdots\right] \approx$$

$${}^{-}1G_T \frac{M}{r} * e^{[{}^{-}0\pi(mcr)/h]} \approx {}^{-}G_T \frac{M}{r}.$$

Eq. (15E)

While the effective gravitational potential for the static electrically charged particle which is interacted upon would be $\approx {}^{-}G_T m/r$ as shown below:

.

$$V_{(\text{photon gravitational potential})} = \frac{1}{4} * 4 * 2 * \sum V_g =$$

$$\frac{1}{4} * 4 * 2 * \left[\left({}^{-}\frac{1}{\approx 4}G_T \frac{m}{r} * e^{[0* (\approx {}^{-}2\pi mcr)/h]} + {}^{-}\frac{1}{\approx 4}G_T \frac{m}{r} * e^{[0* (\approx {}^{-}2\pi mcr)/h]}\right)\right] =$$

$$2 * \left[\left({}^{-}\frac{1}{\approx 2}G_T \frac{m}{r} * e^{[0* (\approx {}^{-}2\pi mcr)/h]}\right)\right] = \left[\left(\approx {}^{-}1G_T \frac{m}{r} * e^{[0* (\approx {}^{-}2\pi mcr)/h]}\right)\right] \approx$$

$${}^{-}1G_T \frac{m}{r} * e^{({}^{-}0\pi mcr/h)} \approx {}^{-}G_T \frac{m}{r}.$$

Eq. (15F)

Wherein, the respective force between the large mass and the static electrically charged particle would be:

$$\frac{1}{4} * \approx^- 4G_T(M) * \frac{e^{\left[\frac{0* \approx^- 0\pi(mcr)}{h}\right]}}{r^2} * \left(m * e^{\left[\frac{0* \approx^- 0\pi(mcr)}{h}\right]}\right) \approx^- 1G_T(M * m) * \frac{e^{\left[2 * \left(\frac{^- 0\pi(mcr)}{h}\right)\right]}}{r^2} \approx$$

$$\frac{^- G_T(M * m)}{r^2} = g_F.$$

Eq. (15G)

Nevertheless, here, also note that according to the present unified field theory, and contrary to convention, it is considered that a quantum can be electrically interacted upon by an electrically charged particle to an infinitesimally small extent, such that, in particular, a large collection of electrically charged particles comprising the same electrical charge could electrically interact in a observable way with a quantum of electromagnetic radiation according to the spins of the charged particles in the collection of particles and the spins of the quantum.

Now, it is considered that the virtual particle paths which extend out from a particle interact by their respective potentials summating (i.e., adding and subtracting) with the potentials of the virtual particle paths of another particle in agreement with their respective spins, so as to effectively attract or repel, and consequently cause a respective extent of electromagnetic attraction or repulsion, and gravitational attraction. Wherein, in order to unify "spacetime" (as considered with respect to the unified field herein) with the mass-energy of the unified field, the Lorentz factor is related to the geometry of the propagation of the mass-energy of the unified field (or of a particle), as with respect to figure 6D and the reasoning which follows immediately thereafter, and, aside from the relevant conventional Lorentz factor, i.e., γ(v), under certain circumstance, the square of the

reciprocal Lorentz factor (or the square of the Lorentz factor) is redefined and applicable herein according to a change in potential as shown in equations (16A-16D) below, for example, in terms of squared theoretical reciprocal Lorentz factors:

$$\frac{1}{\gamma_T^{\,2}} = 1 - \frac{4 *^{\approx} K_T(q) * \dfrac{e^{\left[\dfrac{\approx^- 0\pi(mcr)}{h}\right]}}{r} - 8 * \dfrac{1}{n_1} K_T(q) * \dfrac{e^{\left[\dfrac{n_2{}^- 2\pi(mcr)}{h}\right]}}{r}}{1 * K_T \dfrac{q}{r}}.$$

Eq. (16A)

Here, the relevant interval is equal to $1K_Tq/r$, i.e., the absolute value of the relative whole maximum possible difference between the potentials in the numerator in equation (16A) (as relates to the absolute value of equation 9B). The reciprocal Lorentz factor in equation (16A) can be used in a manner which is similar to the manner in which the conventional reciprocal Lorentz factor is used. Respectively, the square of the conventional Lorentz factor can be written as:

$$\frac{1}{\gamma^2} = 1 - \frac{v^2}{c^2} = \frac{c^2}{c^2} - \frac{v^2}{c^2} = \frac{c^2 - v^2}{c^2}$$, which allows for the following squared reciprocal Lorentz factor in the theory herein:

$$\frac{1}{\gamma_T^{\,2}} = 1 - \frac{\Delta V}{V_{interval}}.$$

For example, consider the following reciprocal Lorentz factor which applies $\approx 4K_T q/r$ for the dependent variable in the numerator of equation (16A):

$$\frac{1}{\gamma_T^{\,2}} = 1 - \frac{\approx 4K_T \dfrac{q}{r} - \approx 4K_T \dfrac{q}{r}}{1K_T \dfrac{q}{r}} = 1 \, .$$

Here, for example, the Lorentz factor would represent a minimum spatial contraction (i.e., zero spatial contraction) of the given virtual particle path with a potential of $\approx 4K_T q/r$ (the dependent variable) with respect to the given reference virtual particle path with a potential of $\approx 4K_T q/r$.

While also in regard to equation (16A), consider the following reciprocal Lorentz factor which applies $\approx 3K_T q/r$ for the dependent variable in the numerator of equation (16A):

$$\frac{1}{\gamma_T^{\,2}} = 1 - \frac{\approx 4K_T \dfrac{q}{r} - \approx 3K_T \dfrac{q}{r}}{1K_T \dfrac{q}{r}} \approx 0$$

Here, for example, the Lorentz factor would represent a maximum spatial contraction of the given virtual particle path with a potential of $\approx 3K_T q/r$ (the dependent variable) with respect to the given reference virtual particle path with a potential of $\approx 4K_T q/r$. Note that, in this case, when $(\Delta n_1)=1.99$ and $(\Delta n_2)=.01$, then the term $\approx 4K_T q/r$ approximately equals $3.9800998*K_T q/r$, and when $(\Delta n_1)=1.99$ and $(\Delta n_2)=.99$, then the term $\approx 3K_T q/r$ approximately equals $2.9875513*K_T q/r$, such that:

$$\frac{1}{\gamma_T^{\,2}} \approx 1 - \frac{3.9800998 - 2.9875513}{1} \approx .00745144 \, ,$$ which is considered to be a respective fine structure

constant such that $\dfrac{1}{134.20216} \approx .00745144$.

Now, another reciprocal Lorentz factor is applicable in the present theory:

$$\frac{1}{\gamma_T^2} = 1 - \frac{4 *^{\approx} K_T(q) * \dfrac{e^{\left[\frac{\approx^- 0\pi(mcr)}{h}\right]}}{r} - 8 * \dfrac{1}{n_1} K_T(q) * \dfrac{e^{\left[\frac{n_2^- 2\pi(mcr)}{h}\right]}}{r}}{4 *^{\approx} K_T \dfrac{q}{r}} \ .$$

Eq. (16B)

Here, the relevant interval is approximately $4K_Tq/r$. The reciprocal Lorentz factor in equation (16B) can be used to transform one virtual particle path with a given potential to that of another virtual particle path with a different potential (as relates to the absolute values of potentials).

For example, consider the following reciprocal Lorentz factor which applies $\approx 4K_Tq/r$ for the dependent variable in the numerator of equation (16B):

$$\frac{1}{\gamma_T^2} = 1 - \frac{\approx 4K_T \dfrac{q}{r} - \approx 4K_T \dfrac{q}{r}}{\approx 4K_T \dfrac{q}{r}} = 1$$

Here, the Lorentz factor would leave a virtual particle path with a potential of $\approx 4K_Tq/r$ unchanged with respect to the given reference virtual particle path with a potential of $\approx 4K_Tq/r$.

However, also consider the following reciprocal Lorentz factor with respect to equation (16B) which applies

≈ 3K$_T$q/r for the dependent variable in the numerator of equation (16B):

$$\frac{1}{\gamma_T{}^2} = 1 - \frac{\approx 4K_T\dfrac{q}{r} - \approx 3K_T\dfrac{q}{r}}{\approx 4K_T\dfrac{q}{r}} \approx \frac{3}{4}$$

Here, the Lorentz factor would transform a virtual particle path with a potential of ≈ 4K$_T$q/r to a virtual particle

path with a potential of ≈ 3K$_T$q/r with respect to the given reference virtual particle path with a potential of

≈ 4G$_T$M/r (i.e., without the absolutes, ≈ 3/4 * $^{≈ -}$4K$_T$q/r ≈ $^-$3K$_T$q/r).

While, another reciprocal Lorentz factor is applicable in the present theory in relativistic terms as

follows:

$$\frac{1}{\gamma_T{}^2} = 1 - \frac{8*^{\approx}K_T(q)*\dfrac{e^{\left[\dfrac{\approx^- 2\pi(mcr)}{h}\right]}}{r} - \gamma_T{}^2 8 * \dfrac{1}{n_1}K_T(q)*\dfrac{e^{\left[\dfrac{1}{\gamma_T{}^2}\dfrac{n_2{}^-2\pi(mcr)}{h}\right]}}{r}}{2*K_T\dfrac{q}{r}}.$$

Eq. (16C)

Here, the relevant interval is 2K$_T$q/r, i.e., the absolute value of the relative whole maximum possible difference

between the relativistic potentials in the numerator in equation (16C) (as relates to the absolute value of

equation 14D). The reciprocal Lorentz factor in equation (16C) can also be used in a manner which is similar to

the manner in which the conventional reciprocal Lorentz factor is used.

For example, consider the following reciprocal Lorentz factor which applies ≈ 3K$_T$q/r for the dependent variable

in the numerator of equation (16C):

$$\frac{1}{\gamma_T{}^2} = 1 - \frac{\approx 3K_T\dfrac{q}{r} - \approx 3K_T\dfrac{q}{r}}{2K_T\dfrac{q}{r}} = 1$$

Here, for example, the Lorentz factor would represent a minimum spatial contraction (i.e., zero spatial contraction) of a relativistic virtual particle path with a potential of $\approx 3K_Tq/r$ with respect to a given reference relativistic virtual particle path with a potential of $\approx 3K_Tq/r$.

While also in the regard to equation (16C), consider the following reciprocal Lorentz factor which applies $\approx 1K_Tq/r$ for the dependent variable in the numerator of equation (16C):

$$\frac{1}{\gamma_T{}^2} = 1 - \frac{\approx 3K_T\dfrac{q}{r} - \approx 1K_T\dfrac{q}{r}}{2K_T\dfrac{q}{r}} \approx 0$$

Here, for example, the Lorentz factor would represent a maximum spatial contraction of a relativistic virtual particle path with a potential of $\approx 3K_Tq/r$ with respect to a given reference relativistic virtual particle path with a potential of $\approx 3G_TM/r$. In this case, the relativistic version is formulated by applying the Lorentz factors which relate to equation 14B, such that the potential of $\approx 4K_Tq/r * 1/e^{[0* 0(2\pi mcr)/h]} * \frac{1}{4}$ is observed as a potential of $\approx 1K_Tq/r$.

Moreover, still, another relativistic reciprocal Lorentz factor is applicable in the present theory:

$$\frac{1}{\gamma_T{}^2} = 1 - \frac{8 *^{\approx} K_T(q) * \dfrac{e^{\left[\frac{\approx^{-} 2\pi(mcr)}{h}\right]}}{r} - \gamma_T{}^2 8 * \dfrac{1}{n_1} K_T(q) * \dfrac{e^{\left[\frac{1}{\gamma_T{}^2} n_2{}^{-} \frac{2\pi(mcr)}{h}\right]}}{r}}{3 *^{\approx} K_T \dfrac{q}{r}}.$$

Eq. (16D)

Here, the relevant interval is equal to approximately $3K_T q/r$. The reciprocal Lorentz factor in equation (16D) can be used to transform one relativistic virtual particle path with a given potential to that of another relativistic virtual particle path with a different potential (as also relates to the absolute values of potentials).

For example, consider the following reciprocal Lorentz factor which applies $\approx 3K_T q/r$ for the dependent variable in the numerator of equation (16D):

$$\frac{1}{\gamma_T{}^2} = 1 - \frac{\approx 3K_T \dfrac{q}{r} - \approx 3K_T \dfrac{q}{r}}{\approx 3K_T \dfrac{q}{r}} = 1$$

Here, the Lorentz factor would leave a relativistic virtual particle path with a potential of $\approx 3K_T q/r$ unchanged with respect to the reference relativistic virtual particle path potential of $\approx 3G_T M/r$.

While also in the regard to equation (16D), consider the following reciprocal Lorentz factor which applies $\approx 1K_T q/r$ for the dependent variable in the numerator of equation (16D):

$$\frac{1}{\gamma_T{}^2} = 1 - \frac{\approx 3K_T \dfrac{q}{r} - \approx 1K_T \dfrac{q}{r}}{\approx 3K_T \dfrac{q}{r}} \approx \frac{1}{3}$$

Here, the Lorentz factor would transform a relativistic virtual particle path with a potential of $\approx 3K_Tq/r$ to a relativistic virtual particle path with a potential of $\approx 1K_Tq/r$ with respect to the given reference relativistic virtual particle path with a potential of $\approx 3K_Tq/r$ (i.e., without the absolute values, $\approx 1/3 * {}^{\approx -}3K_Tq/r \approx {}^-1K_Tq/r$). In this case too, the relativistic version is formulated by applying the Lorentz factors which relate to equation 14B, such that the potential of $\approx 4K_Tq/r * 1/e^{[0* \, 0(2\pi mcr)/h]} * \frac{1}{4}$ is observed as a potential of $\approx 1K_Tq/r$.

It is considered that the Lorentz factor is "carried" by the virtual particle paths (mass-energy) and the respective volume subtended by the virtual particles (virtual particle paths) of the unified field, such that the parameters of Lorentz transformations are inherent in the unified field (providing background independence). Thus, the gradient of a single virtual particle path (or a four dimensional array of virtual particle paths) provides the gravitational (and electromagnetic) energy of interaction, and effectively supplies the Lorentz factor (i.e., the Lorentz factor and its respective reciprocal). While, the path along which a respective body interacted upon travels is effectively produced by the respectively interacting virtual particle paths of the bodies of interaction according to such terms which include the gradients of the virtual particle paths of the interacting fields of the bodies before, and as a consequence of, interaction.

In result, the mass-energy and the "spacetime" of "gravity" are both comprised by the virtual particle paths of the unified field, and are applied together in a more direct manner then in general relativity. Yet, the unified field described herein unifies "spacetime" with not only mass, but also electric charge. Wherein, a virtual particle path of the unified field, which carries the Lorentz factor of "spacetime" for mass and electric charge, comprises both a gravitational component which accounts for conventional gravitational interaction, and

an electromagnetic component which accounts for conventional electromagnetic interaction, while both account for "nuclear interaction." In which case, for example, in proton-proton nuclear interaction, the electromagnetic component includes attractive spins, while the gravitational component includes repulsive spins as will be described later (wherein gravity is considered negligible in the nuclear region in conventional terms).

In view of what has been presented thus far, the theory herein does not support the existence of gravitons, and therefore neither supports gravitons as mediators of the gravitational interaction nor gravitational waves as existing independent of electromagnetic waves. Similarly, the theory herein does not support photons as the gauge boson mediators of the electromagnetic interaction. Wherein, overall, the present unified field theory neither supports "gauge bosons" as the force carriers of interactions nor the Standard Model for the most part. In response, the unification herein proposes that the gravitational and electromagnetic components of the unified field together mediate gravitational and electromagnetic interactions (etc.) in a unified manner by way of virtual particles as described before, and more so later.

CHARGED PARTICLE PROPAGATION AND INTERACTION:

Now, consider that a propagating electrically charged particle has an intrinsic spin (S) which is aligned through the elliptical virtual particle paths which only partially rotate around the axis in the plane of symmetry which separates the top and bottom sides as shown for a propagating negatively charged particle in figures (23A), (23B), and (23C), and for a positively charged propagating particle in figures (24A), (24B) and (24C). (Note that only the front portion of each propagating particle is shown.)
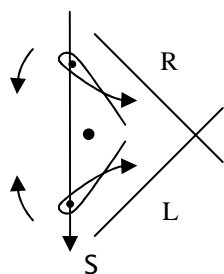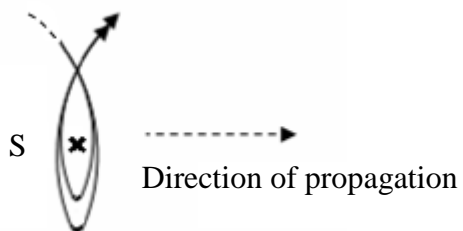
Front view

FIG. 23A
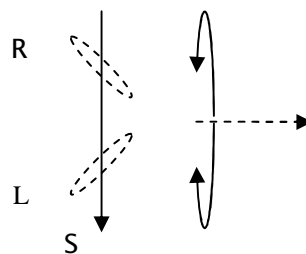
Side view

FIG. 23B

Direction of propagation

Top view

Intrinsic spin for a propagating
negatively charged particle. Note that (S)
is into the page using the right hand rule
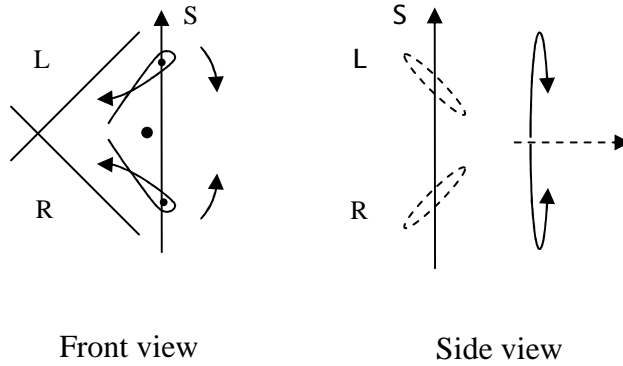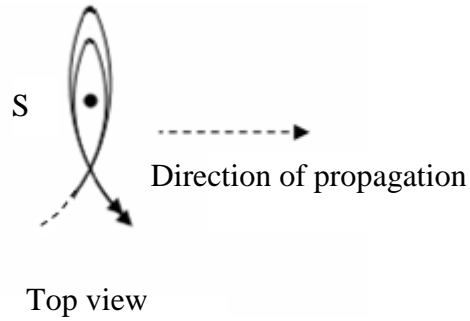with respect to the top view.

FIG. 23C

Front view

Side view

FIG. 24A

FIG. 24B

S

Direction of propagation

Top view

Intrinsic spin for a propagating
positively charged particle. Note that (S)
is out of the page using the right hand
rule with respect to the top view.

FIG. 24C

It is considered that propagating negatively charged particles prefer to be relatively upright during interaction while propagating in parallel or antiparallel, and similarly for propagating positively charged particles. Figure (25A) shows the preferred relative upright alignment for juxtaposed parallel propagating negatively charged particles, and separately shows the preferred relative upright alignment for juxtaposed parallel propagating positively charged particles. While similarly, figure (25C) shows the preferred relative upright alignment for vertically aligned parallel propagating negatively charged particles, and shows the preferred relative upright alignment for vertically aligned parallel propagating positively charged particles.

On the other hand, it is considered that propagating positively and negatively charged particles prefer to be relatively inverted during interaction while propagating in parallel or antiparallel as shown in figure (25B) for juxtaposed parallel propagating positively and negatively charged particles, and as shown in figure (25D) for vertically aligned parallel propagating positively and negatively charged particles. Nevertheless, in each of the cases in figures (25A-25D), the intrinsic spins are aligned parallel.
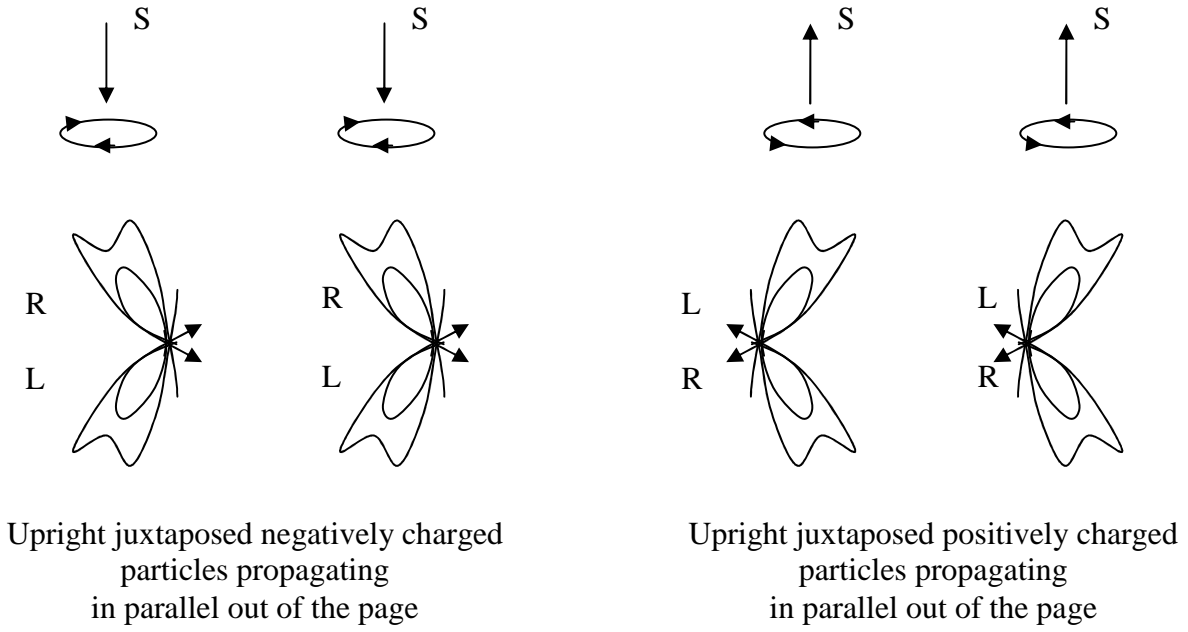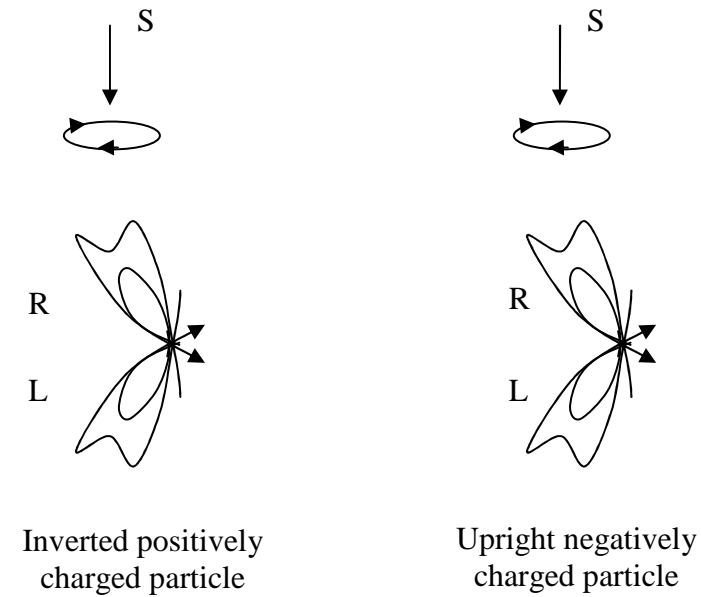
S
S
S
S

R
L

R
L

L
R

L
R

Upright juxtaposed negatively charged
particles propagating
in parallel out of the page

Upright juxtaposed positively charged
particles propagating
in parallel out of the page

FIG. 25A

S
S

R
L

R
L

Inverted positively
charged particle

Upright negatively
charged particle

Juxtaposed positively and negatively charged particles
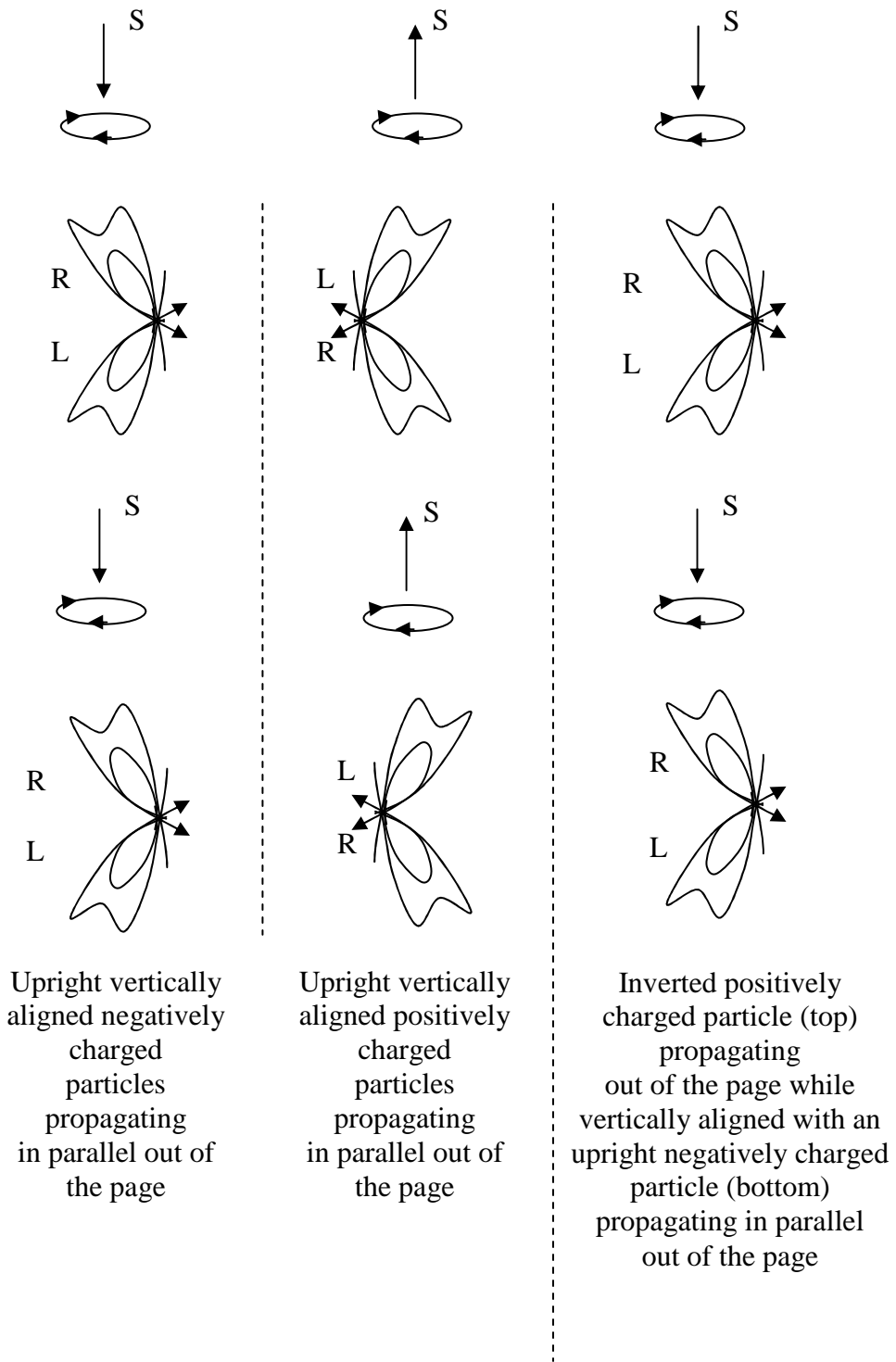propagating in parallel out of the page

FIG. 25B

Upright vertically
aligned negatively
charged
particles
propagating
in parallel out of
the page

Upright vertically
aligned positively
charged
particles
propagating
in parallel out of
the page

Inverted positively
charged particle (top)
propagating
out of the page while
vertically aligned with an
upright negatively charged
particle (bottom)
propagating in parallel
out of the page

FIG. 25C

FIG. 25D

For certain interactions, it is consider especially important that the microscopic spin vectors of extended more bent virtual particle paths are relatively inverted due to "bending" compared to less bent virtual particle paths, such that, for example, the microscopic electric spin vector (q) rotation around the respective (z) axis is reversed, and, importantly, the magnetic (B_m) and mass (m) spin vectors are inverted as shown in figures (26A) and (26B), for example, for the extranuclear region on the front top right hand screw side of a negatively charged particle. Wherein, this inversion characteristic, or the lack thereof, affects the alignment and rotational directions of the spin vectors of interacting virtual particle paths, and thus consequentially affects the respective attraction or repulsion which results from affected spin vectors during interactions.

R   R

z   z

B~m~

q   q
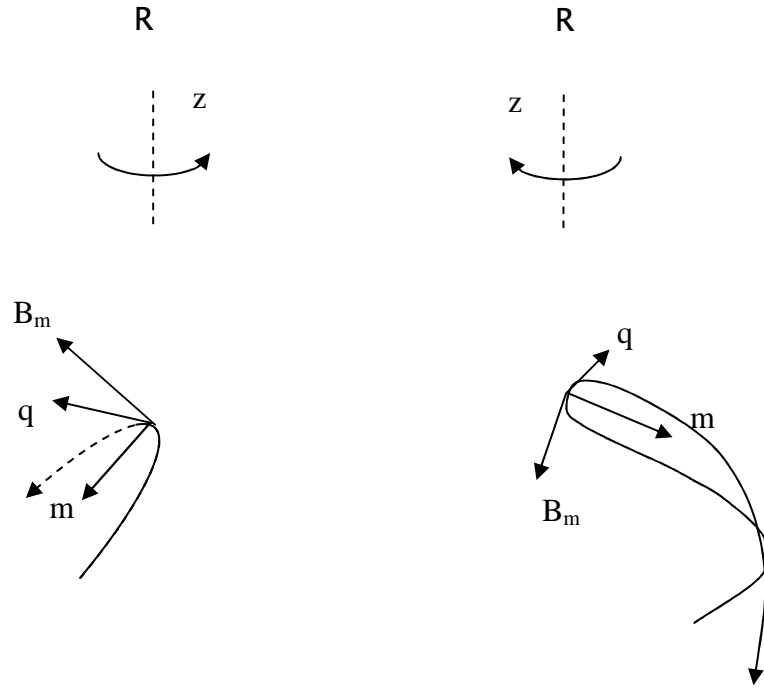
m   m

B~m~

FIG. 26A   FIG. 26B

Spin rotation reversal around the (z) axis depicted for electric spin vector (q) such that the direction of the rotation is relatively reverse in the less bent virtual particle path shown in figure (26A) compared to the electric spin vector (q) in the more bent virtual particle path shown in figure (26B) in the extranuclear region on the front top right hand screw side of a negatively charged particle. While importantly, the microscopic magnetic and mass spin vectors are also inverted along respective axes accordingly.

Interactions in which this inversion characteristic is especially important include certain interactions which are described in more detail later including the self interaction of virtual particles paths, and interactions of electrically charged particles which are in a orderly aligned distribution as in the case of the interactions of spin aligned propagating electrically charged particles, the interactions of magnets, and molecular interactions.

Also, consider important for interaction during propagation, that the acceleration of the unified field causes relatively opposite rotations in different portions of a virtual particle path. In figure (27A), the rotations shown by the dashed curved arrows for an increase in mass cause relatively opposite microscopic mass spin

vector (m) rotations for different portions of the virtual particle path. Then, when considered together as shown

by the dashed curved arrows in figure (27B), the bent condition of a more bent virtual particle path is

maintained while the different portions of the virtual particle path continue to effectively rotate in relatively

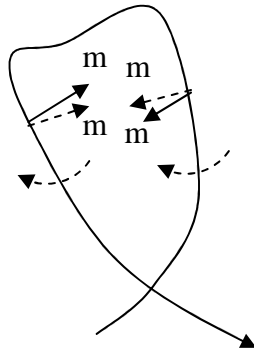opposite directions, and while the relativistic mass of the electrically charged particle as a whole increases.
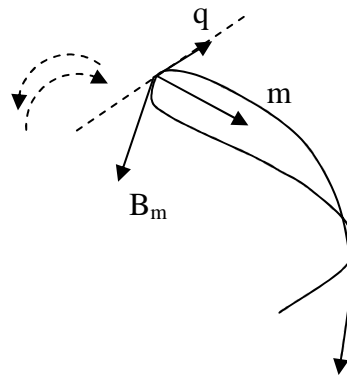

FIG. 27A   FIG. 27B

Here, as different portions of the example virtual particle
path effectively rotate in relatively opposite directions as
shown in figure (27A), nevertheless, the bent condition of a
more bent virtual particle path is maintained where such
rotations cancel each other out as shown by the curved
arrows in figure (27B).

Now, figure (28) shows how the microscopic magnetic spin vector component (B_{mc}) of a more bent

virtual particle path (dashed oval) of the right hand screw side of an upright negatively charged particle

propagating on the bottom is aligned antiparallel (in a horizontal plane) to the microscopic magnetic spin vector

component (B_{mc}) of the coupling virtual particle path of the right hand screw side in the "nuclear region"

(dashed rectangle) of an upright negatively charged particle which is propagating in parallel on the top, thus

causing magnetic attraction.

Note, the particles in figures (28-31) are shown separated. Thus, one must conceptually reposition each orthogonal set of extranuclear spins shown in a dashed oval (along with the respective particle) while keeping it aligned as it is so that the origin of the orthogonal set of extranuclear spin vectors in each oval is almost abutting the origin of the orthogonal set of nuclear spins shown in a corresponding dashed rectangle of the other relevant electrically charged particle for proper alignments. Also, note that the vertical component of (q) is effective in both parallel and antiparallel propagating cases. Furthermore, note that the following examples of propagating electrically charged particle interaction also include attraction or repulsion according to the interaction of microscopic charge, mass, and magnetic spin vectors of the respectively less bent virtual particle paths of the extranuclear field of a propagating electrically charged particle with the nuclear region of the opposing propagating electrically charged particle, i.e., in particular, during juxtaposed propagating charged particle interaction, so as to account for respective electric and gravitational interaction accordingly. Wherein in figures (28-31), the less bent virtual particle paths are shown separated from, and adjacent to, their respective more bent virtual particle paths, and thus would also need to be conceptually repositioned accordingly. Moreover, note that, with respect to figures (28-29), two equivalently arranged positively charged propagating particles are considered to interact similarly.
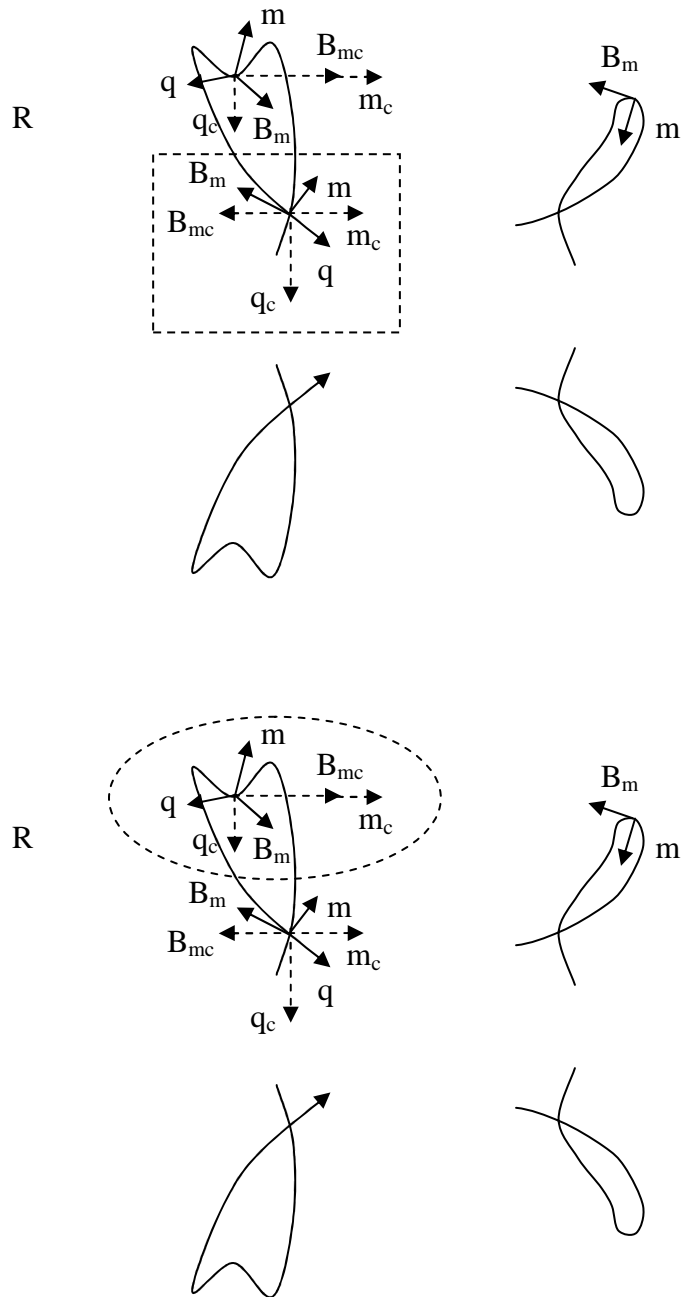
Here, the microscopic magnetic spin vector component (B_{mc}) of the more bent virtual particle path (dashed oval) of an upright negatively charged particle propagating out of the page on the bottom is aligned antiparallel in the horizontal plane to the microscopic magnetic spin vector component (B_{mc}) of the "nuclear region" (dashed rectangle) of an upright negatively charged particle propagating in parallel out of the page on the top, thus causing magnetic attraction.
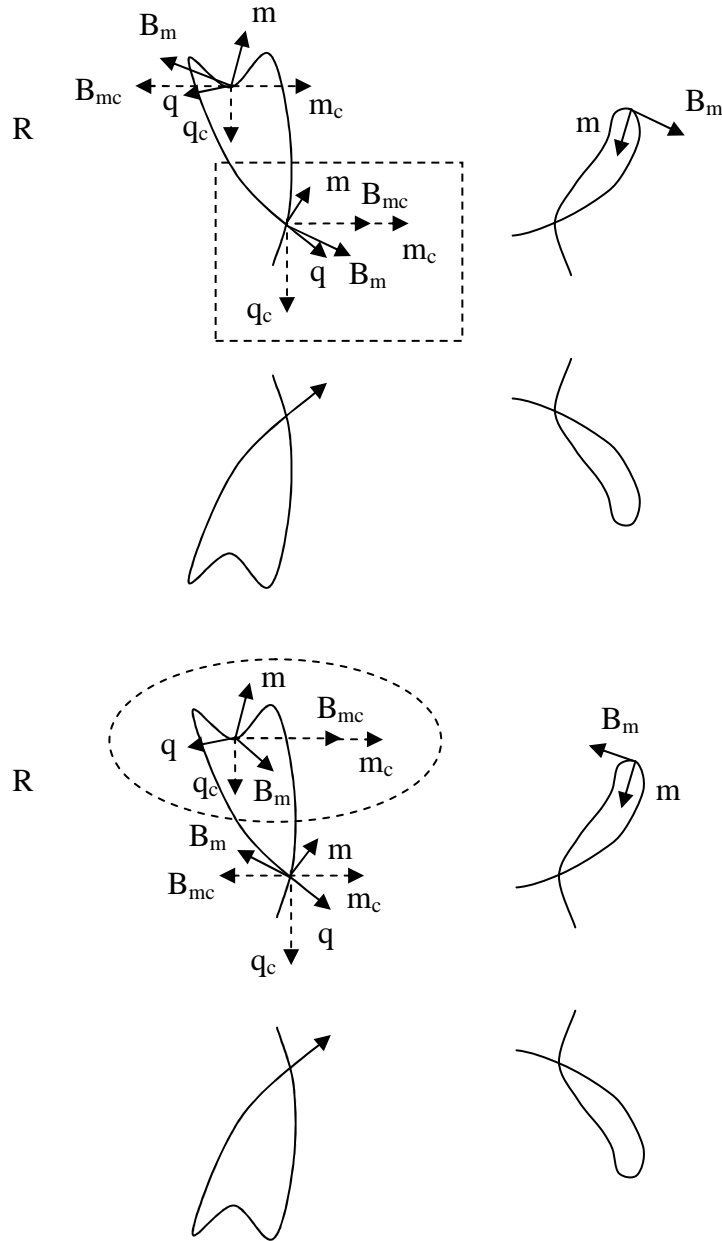
FIG. 28

Figure (29) shows how the microscopic magnetic spin vector component (B_{mc}) of a more bent virtual particle path (dashed oval) of the right hand screw side of an upright negatively charged particle propagating on the bottom is aligned parallel to the microscopic magnetic spin vector component (B_{mc}) of the coupling virtual particle path of the right hand screw side in the "nuclear region" (dashed rectangle) of an upright negatively charged particle which is propagating antiparallel on the top, thus causing magnetic repulsion. (Note that the spins of the propagating charged particles shown in figures (29) and (31), which include antiparallel mass components which attempt to turn the particles around, are considered to especially disclose the role they could play in a two-body problem.)
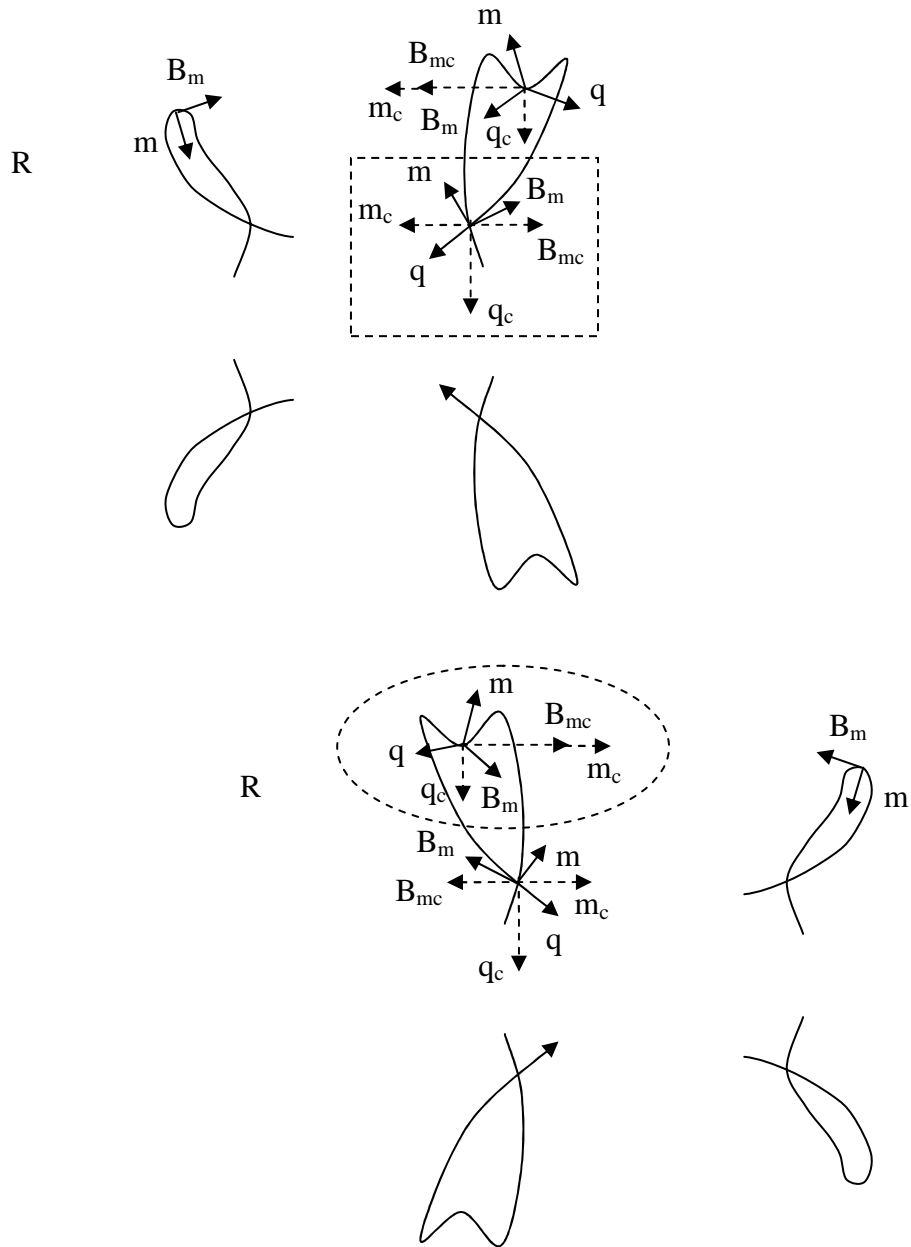
Here, the microscopic magnetic spin vector component (B_{mc}) of the more bent virtual particle path (dashed oval) of an upright negatively charged particle propagating out of the page on the bottom is aligned parallel in the horizontal plane to the microscopic magnetic spin vector component (B_{mc}) of the "nuclear region" (dashed rectangle) of an upright negatively charged particle propagating antiparallel into the page on the top, thus causing magnetic repulsion.
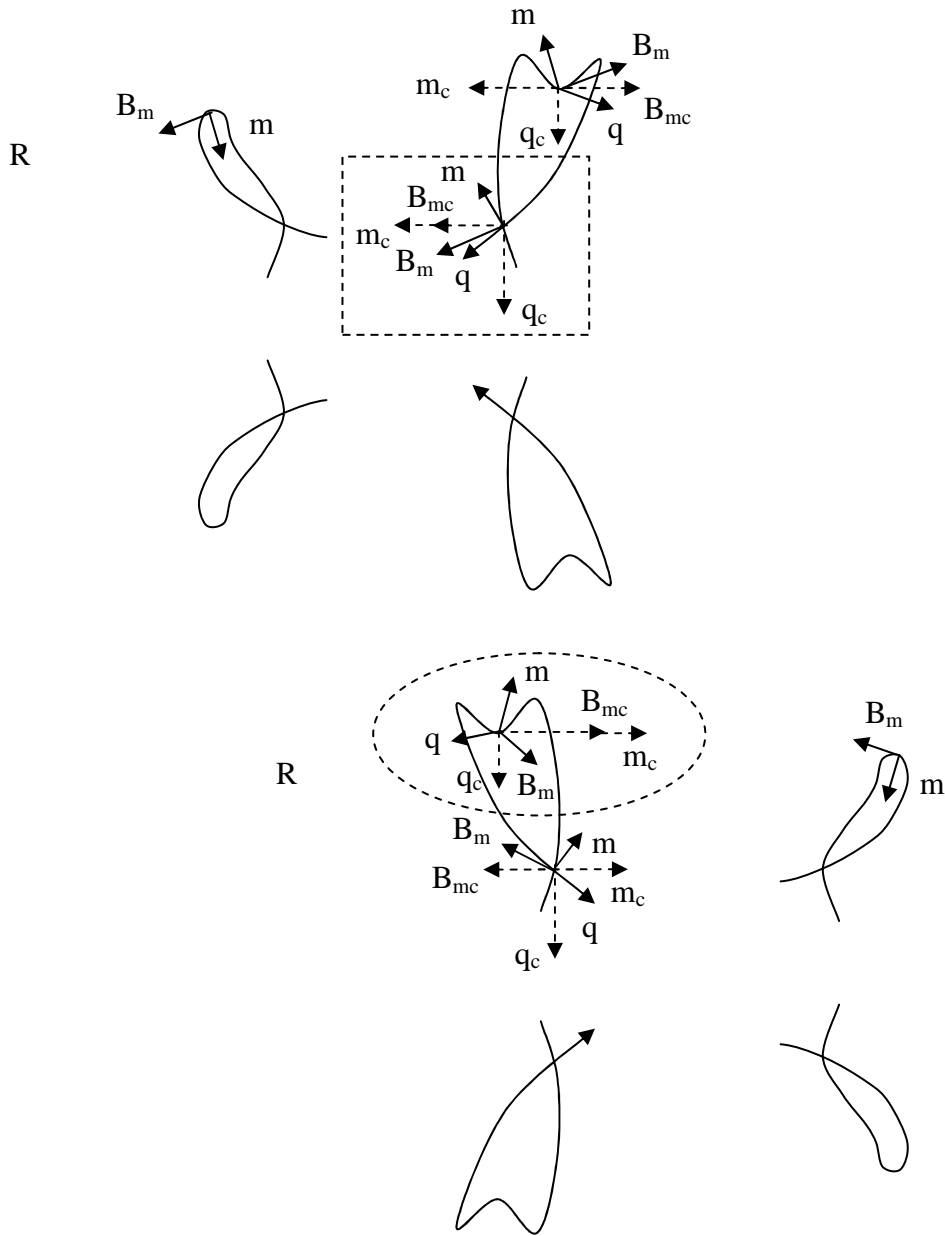
FIG. 29

Figures (30) and (31) show the arrangement for the interaction of negatively and positively charged propagating particles. Wherein, in figure (30), the microscopic magnetic spin vector component (B_{mc}) of the more bent virtual particle path (dashed oval) of the right hand screw side of the upright negatively charged particle propagating on the bottom is aligned parallel to the microscopic magnetic spin vector component (B_{mc}) of the coupling virtual particle path of the right hand screw side in the "nuclear region" (dashed rectangle) of the inverted positively electrically charged particle which is propagating in parallel on the top, thus causing magnetic repulsion.

Here, the microscopic magnetic spin vector component (B_{mc}) of the more bent virtual particle path (dashed oval) of an upright negatively charged particle propagating out of the page on the bottom is aligned parallel in the horizontal plane to the microscopic magnetic spin vector component (B_{mc}) of the "nuclear region" (dashed rectangle) of an inverted positively charged particle propagating in parallel out of the page on the top, thus causing magnetic repulsion.

FIG. 30

While, figure (31) shows how the microscopic magnetic spin vector component (B_{mc}) of the more bent virtual particle path (dashed oval) of the right hand screw side of the upright negatively charged particle propagating on the bottom is aligned antiparallel to the microscopic magnetic spin vector component (B_{mc}) of the coupling virtual particle path of the right hand screw side in the "nuclear region" (dashed rectangle) of the inverted positively electrically charged particle which is propagating antiparallel on the top, thus causing magnetic attraction.

Here, the microscopic magnetic spin vector component (B_{mc}) of the more bent virtual particle path (dashed oval) of an upright negatively charged particle propagating out of the page on the bottom is aligned antiparallel in the horizontal plane to the microscopic magnetic spin vector component (B_{mc}) of the "nuclear region" (dashed rectangle) of an inverted positively charged particle propagating antiparallel into the page on the top, thus causing magnetic attraction.

FIG. 31

VIRTUAL PARTICLES, SELF INTERACTION, AND SUPERLUMINAL VELOCITY:

Conventionally it has been difficult to detect and measure the parameters of particles thought to govern the internal structure of matter, e.g., due to the confinement of "quarks (the existence of which the present theory does not support)," etc. Herein, the theory of unification reuses the parameters of the unified field described previously for "everything" for structure, function, and simplicity, such that virtual particles constitute the internal structure of mass-energy, and such that each has a structure and function which is analogous to that of propagating electrically charged particles described previously (wherein virtual particles comprise "virtual-virtual particles," etc.).

Accordingly, "self interacting" virtual particle paths (which account for internal bonding) align in agreement with the alignment of their respective spin vectors so as to effectively produce the shape of the virtual particle paths, and consequentially the shape of a static or propagating particle as a whole. In which case, virtual particles on the top and bottom sides of negatively and positively charged particles are considered to self interact with virtual particles on the same side by way of the respective right-right and left-left hand spin vector interactions, such that parallel microscopic charge and mass spin vector interactions are attractive, and antiparallel microscopic magnetic spin vector interactions are attractive, etc. This is because virtual particles are also considered, in their own way, to comprise top and bottom sides which are either right or left hand screw, etc. Similarly, it is considered that virtual particles on the top and bottom sides interact with virtual particles on their opposing sides in self interaction by way of respective right-right and left-left hand spin vector interactions. Figure (32A) shows the virtual particles posited for the front side of example virtual particle paths on the top and bottom sides in the nuclear region of static negatively and positively electrically charged particles.
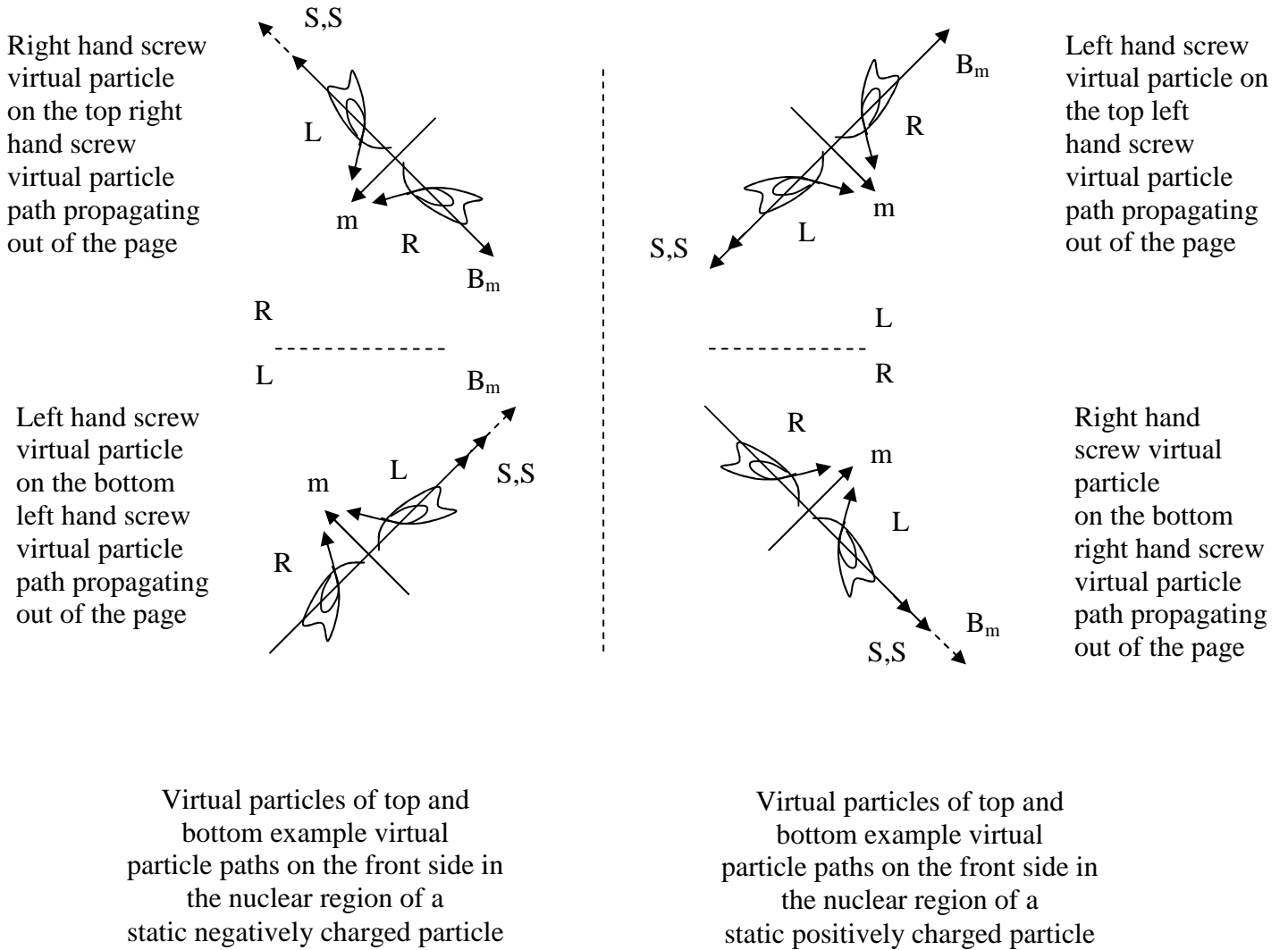
Right hand screw virtual particle on the top right hand screw virtual particle path propagating out of the page

Left hand screw virtual particle on the top left hand screw virtual particle path propagating out of the page

Left hand screw virtual particle on the bottom left hand screw virtual particle path propagating out of the page

Right hand screw virtual particle on the bottom right hand screw virtual particle path propagating out of the page

Virtual particles of top and bottom example virtual particle paths on the front side in the nuclear region of a static negatively charged particle

Virtual particles of top and bottom example virtual particle paths on the front side in the nuclear region of a static positively charged particle
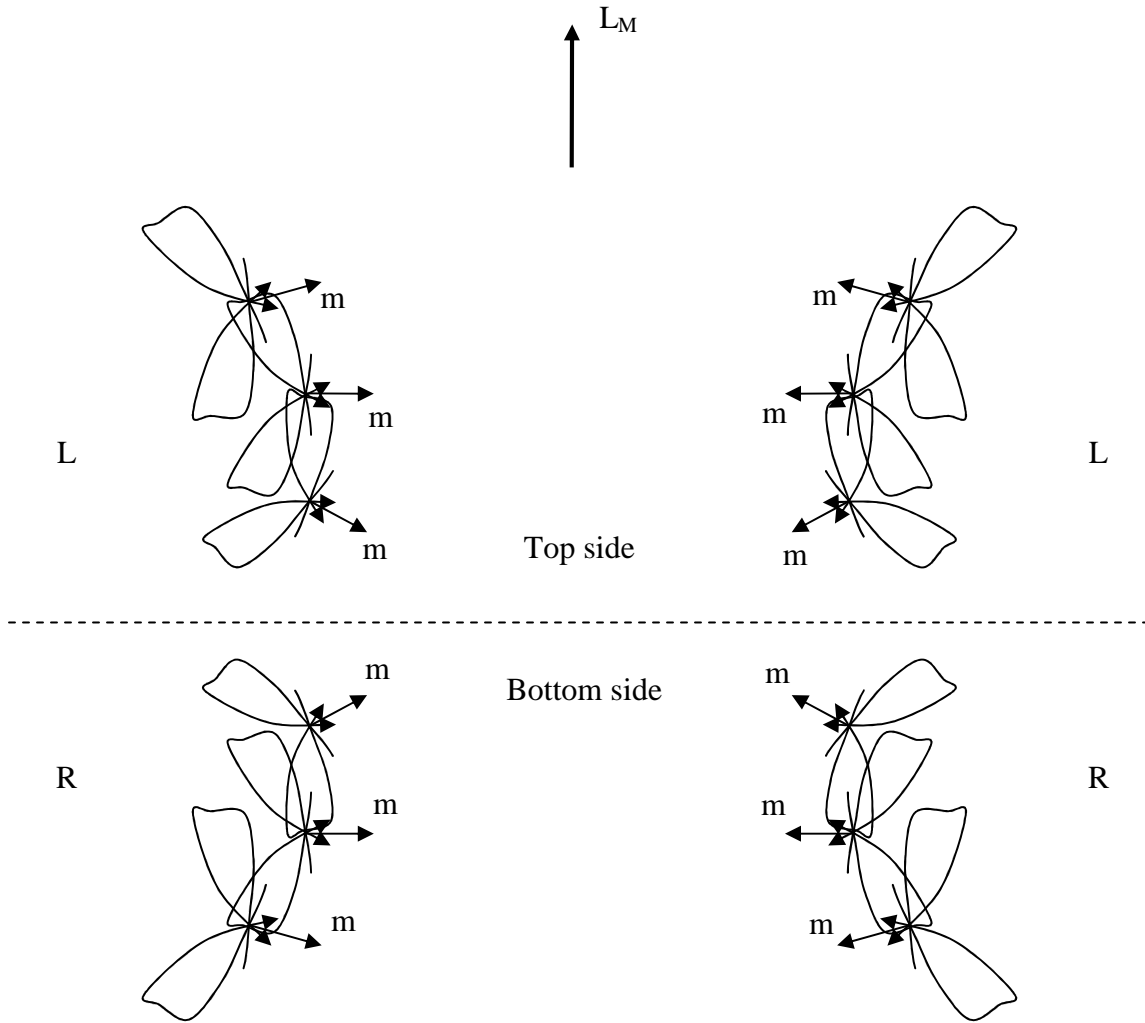
FIG. 32A

However, as shown in figure (32A), a virtual particle has a microscopic magnetic spin vector (B_m) which is aligned according to the screw (charge) of the particle in which it is comprised by switching hand rules. Wherein, a right hand screw virtual particle in a negatively charged particle and a right hand screw

virtual particle in a positively charged particle have oppositely aligned microscopic magnetic spin vectors (B_m) when their intrinsic spins are aligned parallel, and, similarly, a left hand screw virtual particle in a negatively charged particle and a left hand screw virtual particle in a positively charged particle have oppositely aligned microscopic magnetic spin vectors (B_m) when their intrinsic spins are aligned parallel.

For example, as described for propagating charged particle interaction before, "real" propagating electrically charged particles of, for example, opposite electric charge which are propagating in parallel with parallel intrinsic spins would magnetically repel because of virtual particles which are propagating on more bent extranuclear virtual particle paths on one real propagating particle with microscopic magnetic spins which are parallel to the microscopic magnetic spins of the virtual particles on virtual particle paths in the nuclear region of the other real propagating particle during interaction. Yet, conversely, the oppositely charged propagating particles would also electrically attract due to virtual particles which are propagating on less bent extranuclear virtual particle paths on one real propagating particle with microscopic magnetic spins which are antiparallel to the microscopic magnetic spins of the virtual particles on virtual particle paths in the nuclear region of the other real propagating particle during interaction. In which case, the differences in the microscopic magnetic spins of the virtual particles of the same spin in opposite screw particles (i.e., here, in oppositely electrically charged propagating real particles), and the respective magnetic repulsion and electric attraction are accounted for accordingly.

Still, in the process of mediating electromagnetic and gravitational interaction (as described before), virtual particles from electrically charged particles are considered to attract or repel analogous to the way propagating electrically charged particles attract or repel during interaction. While, virtual particles bonded in a band in a particle of opposing sides are also considered to interact analogous to the way propagating electrically charged particles interact. For example, virtual particles bonded in a band of virtual particle paths in the nuclear region of a static electrically charged particle are considered to interact analogous to the way in which

propagating electrically charged particles interact, but in a way in which they change in spacing (increasing vertically and horizontally in an outward manner from the center) and in a way in which they rotate (increasing in the less massive, or more decelerated, rotational direction in an outward manner from the center) as shown in figure (32B) (note that changes in the bends of the virtual particle paths are not shown). Wherein, such bonding in the nuclear region occurs in order to maximize attraction and minimize repulsion amongst virtual particles in agreement with the bends in their "virtual-virtual" particle paths (which function analogous to the more and less bent virtual particle paths of interacting propagating electrically charged particles described before), such that, in effect, virtual particles in the nuclear region contribute to the shape of the unified field along with the virtual particles in the remainder of the electrically charged particle as a whole.

L_M

Example virtual particles in virtual particle paths propagating out of the page
(left portion) and propagating into the page (right portion) on the top and
bottom front and back sides of the nuclear region of a static proton.

FIG. 32B

Now, as pertains to the geometry of virtual particle paths and velocity, it is considered in the present

theory that $h = 2\pi mcr \approx 2\pi(2.1765x10^{-8})\left(\frac{1.6162x10^{-35}}{5.3911x10^{-44}}\right)(1.6162x10^{-35}) = 6.6258x10^{-34}$. Wherein,

$2\pi mcr/2\pi = h/2\pi$ which is reduced Planck constant (h-bar); and Planck length (1.6162×10^{-35})/Planck time $(5.3911 \times 10^{-44}) = $ speed (c), which, given direction, represents a translational velocity. In which case, (h), i.e., unreduced Planck constant $(2\pi mcr)$, is applied herein in a context in which it relates to the geometry of the virtual particle paths of the unified field, such that $2\pi * 1.6162 \times 10^{-35}$ (i.e., 2π r) is "unreduced" Planck length when $r = 1.6162 \times 10^{-35}$, and is applied such that $2\pi * 1.6162 \times 10^{-35}$ (unreduced Planck length)/5.3911×10^{-44} (Planck time)$= 1.8835 \times 10^{+9}$ m/s, which, herein, is considered to be the superluminal velocity of virtual particles propagating over virtual particle paths.
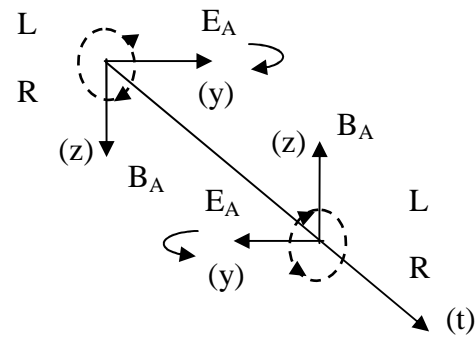
QUANTUM OF ELECTROMAGNETIC RADIATION ("MASSLESS" PARTICLES):

Consider that a "quantum of electromagnetic radiation" produces a conventional alternating electromagnetic field comprising an alternating electric field (E_A) aligned along the (y) axis which is perpendicular to the axis around which the top and bottom sides rotate, and perpendicular to the direction of propagation as shown in the perspective views in figures (33A) and (33B). Furthermore, consider that a quantum of electromagnetic radiation also produces a conventional alternating magnetic field (B_A), which is generated as the virtual particle paths helically propagate left and right, and which is aligned along the (z) axis perpendicular to the axis around which the top and bottom sides rotate, aligned perpendicular to the alternating electric field (E_A), and aligned perpendicular to the direction of propagation as also shown in figures (33A) and (33B).
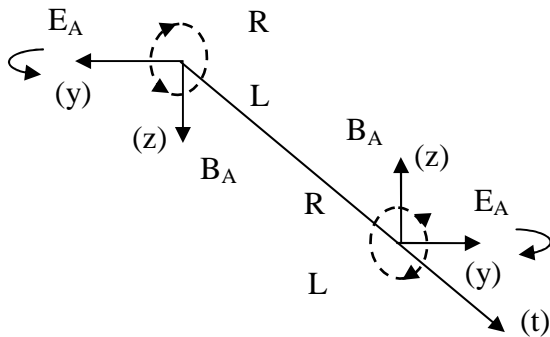
Matter quantum of
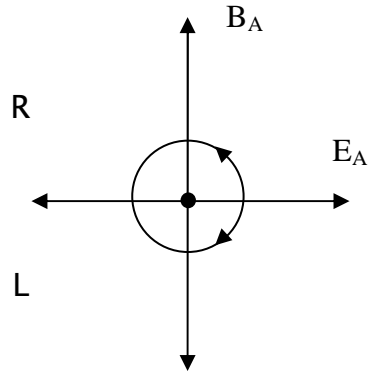electromagnetic
radiation

FIG. 33A

Antimatter quantum
of electromagnetic
radiation

FIG. 33B

The electric field (E_A) and magnetic field (B_A) axes are considered to be aligned as shown in the front

views for matter and antimatter quanta of electromagnetic radiation in figures (34A) and (34B), and also as

shown in perspective views in figures (35A) and (35B) (as they would also be aligned in an analogous manner,

and for similar reasons, for a negatively and a positively electrically charged particle, respectively). Note that

the top and bottom sides shown in figures (34A) and (34B) are propagating around a common central axis,

wherein the infinitesimally small separation of the top and bottom sides is not shown. In this regard, the spin of

a quantum of electromagnetic radiation is almost entirely eliminated when considered in the same context as

that of the spin of an electrically charged particle described before. Also, note that the helical geometry of the

virtual particle paths of a quantum of electromagnetic radiation in the present theory is supported by

conventional theory in which a photon is considered to comprise right and left helical components.

Furthermore, note that a conventionally polarized alternating electromagnetic field could be achieved by

rotating the spins of the virtual particle paths of a quantum (or equivalently an electrically charged particle) so

that together they follow an "elliptical" trajectory around their common center.
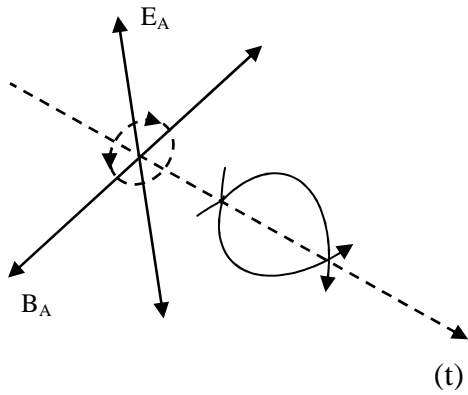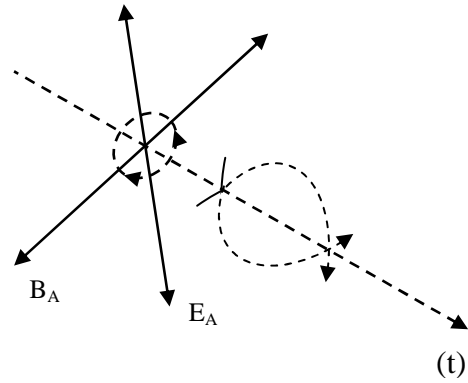

Matter quantum

FIG. 34A
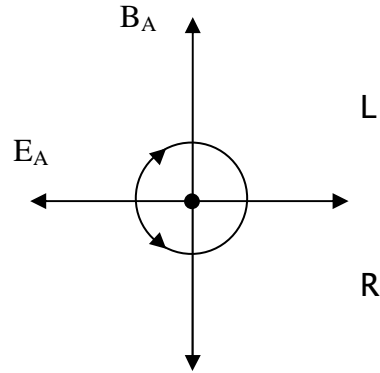
Antimatter quantum

FIG. 34B

E_A

B_A

(t)

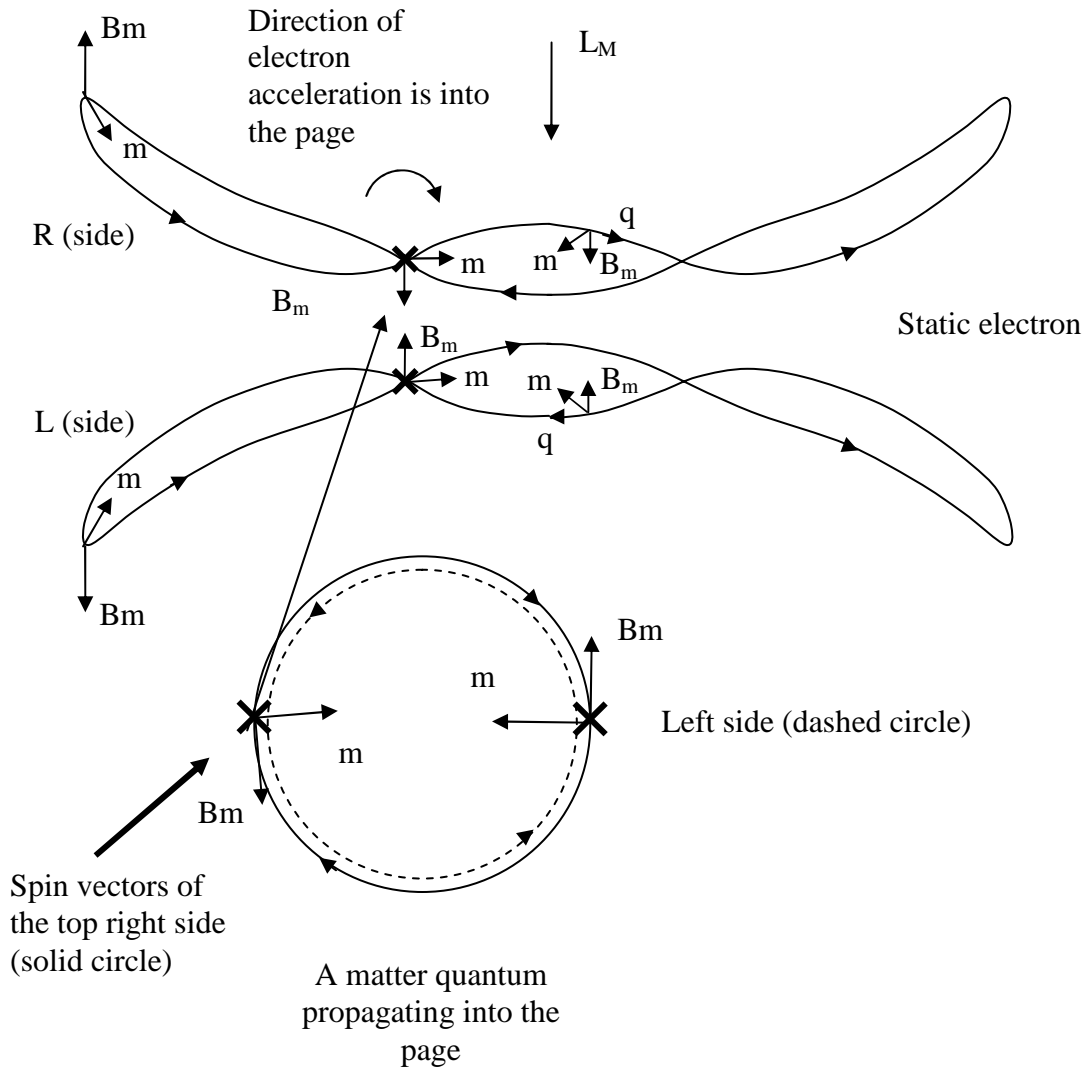Matter quantum

FIG. 35A

E_A

B_A

(t)

Antimatter quantum

FIG. 35B

It is also worth noting here that a matter quantum is considered to be emitted, for example, by an electron, and an antimatter quantum is considered to be emitted, for example, by a positron, and it will be shown later how an antimatter quantum can interact in a manner which is equivalent to a matter quantum, and vice versa.

The electric and magnetic fields of a quantum of electromagnetic radiation (or an electrically charged particle) are considered to be detected during measurement as a consequence of the affect that the virtual particle paths of a propagating quantum of electromagnetic radiation (or an electrically charged particle) have on another particle upon interaction. In figure (36), for example, consider that the right and left hand screw virtual particle paths of the matter quantum could align with, and be respectively absorbed by, the top and bottom sides of the electron shown. Wherein, the virtual particle paths of the quantum interact with the virtual particle paths of the electron, and thus cause the nuclear virtual particle paths of the electron to accelerate and project forward so as to establish the combined right and left elliptically helical top and bottom sides of a propagating electron along the direction of the propagating quantum (which is propagating into the page). Here,

consider that the quantum is also absorbed due to a lack of repulsion because of its field geometry (comprising a lack of eccentricity), and absorbed because of its corresponding field resonance, thus allowing the quantum's field to merge with the electron's field, and then become eccentric with the eccentric geometry of the electron's field upon deceleration (refer to the description later herein regarding the quantum's unified field spin vector geometry with respect to annihilation and pair production under the heading "PARTICLE TRANSMUTATION AND GENERATION").

Static electron acceleration during absorption of the energy of a matter quantum of electromagnetic radiation (only certain details of the absorption of top right side are shown)

FIG. 36

MAGNETIC INTERACTION:

Now, certain longstanding questions about magnetic fields can be addressed as they pertain to the present theory by examining the internal structure of the unified fields of static electrically charged particles as presented herein, e.g., the conclusion that the existence of magnetic monopoles is not supported by the present theory can be made. Wherein, in a description of a magnetic field produced by magnets herein, consider that certain more bent virtual particle paths from the top side of each of a number of electrons propagating in the north pole of one magnet, and certain more bent virtual particle paths from the bottom side of each of a number of electrons propagating in the south pole of an opposing magnet, respectively extend out to produce the virtual particle paths of the static magnetic field between the north and south poles of two magnets. In which case, the more bent virtual particle paths of electrons which are propagating in parallel with parallel intrinsic spins in atomic orbitals in one magnet would magnetically interact attractively with electrons which are propagating in parallel with parallel intrinsic spins in atomic orbitals in the opposing magnet as shown for the interaction of north pole electrons with south pole electrons in figure (37). Consequentially, in two such magnets, electrons in orbitals of protons in one magnet would be magnetically accelerated in an attractive manner towards parallel propagating electrons in orbitals of protons in the opposing magnet, such that the atoms in the opposing magnetic materials would accelerate towards each other.

South pole

North pole

Electrons in orbitals
propagating into the
page

Electrons in orbitals
propagating out of the
page
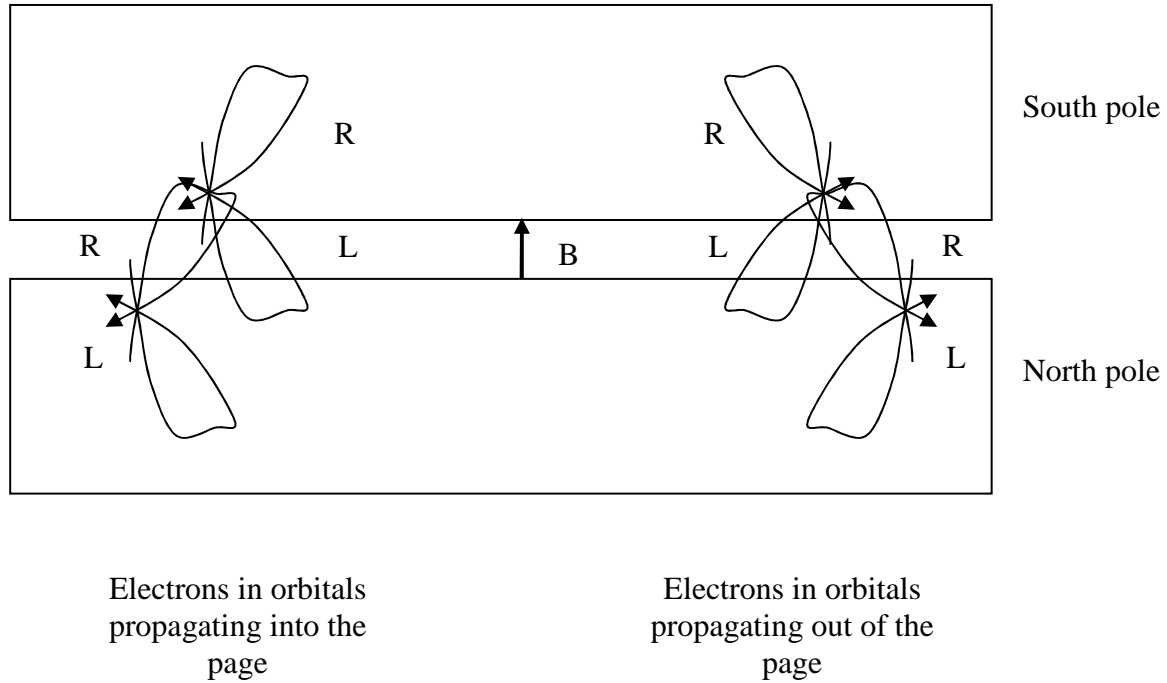
Here, example virtual particle paths extend out from parallel propagating
electrons in one magnetic (e.g., the north pole here) into the opposing
magnetic, and interact in a magnetically attractive manner with the nuclear
regions of parallel propagating electrons in the opposing magnet (as for the
interaction of propagating electrically charged particles described
previously).

FIG. 37

Figure (38A) shows the magnetic field produced between two magnets by the right and left hand

screw sides of certain more bent virtual particle paths extending out from electrons comprised in opposing

magnets. While, figure (38A) also shows how the virtual particle paths of the magnetic field would interact

with the top and bottom sides of negatively and positively charged particles which are propagating out of the

page while propagating in, and perpendicular to, the magnetic field, such that the top and bottom sides are

accelerated in a respectively curved path. Wherein, the negatively and positively charged particles turn to the

right and left, respectively (as shown looking into the page at figure 38A) due to the repulsion and attraction,

respectively, of, in particular, the microscopic magnetic spin vector components (B_{mc}) of the curved portions of

the more bent extranuclear virtual particle paths of the opposing magnets on the nuclear microscopic magnetic spin vector components (B_{mc}) of the negatively and positively charged propagating particles. Wherein, the propagating negatively and positively electrically charged particles are accelerated in a direction which is perpendicular to the direction of the magnetic field (B) according to conventional left and right hand rules, respectively.
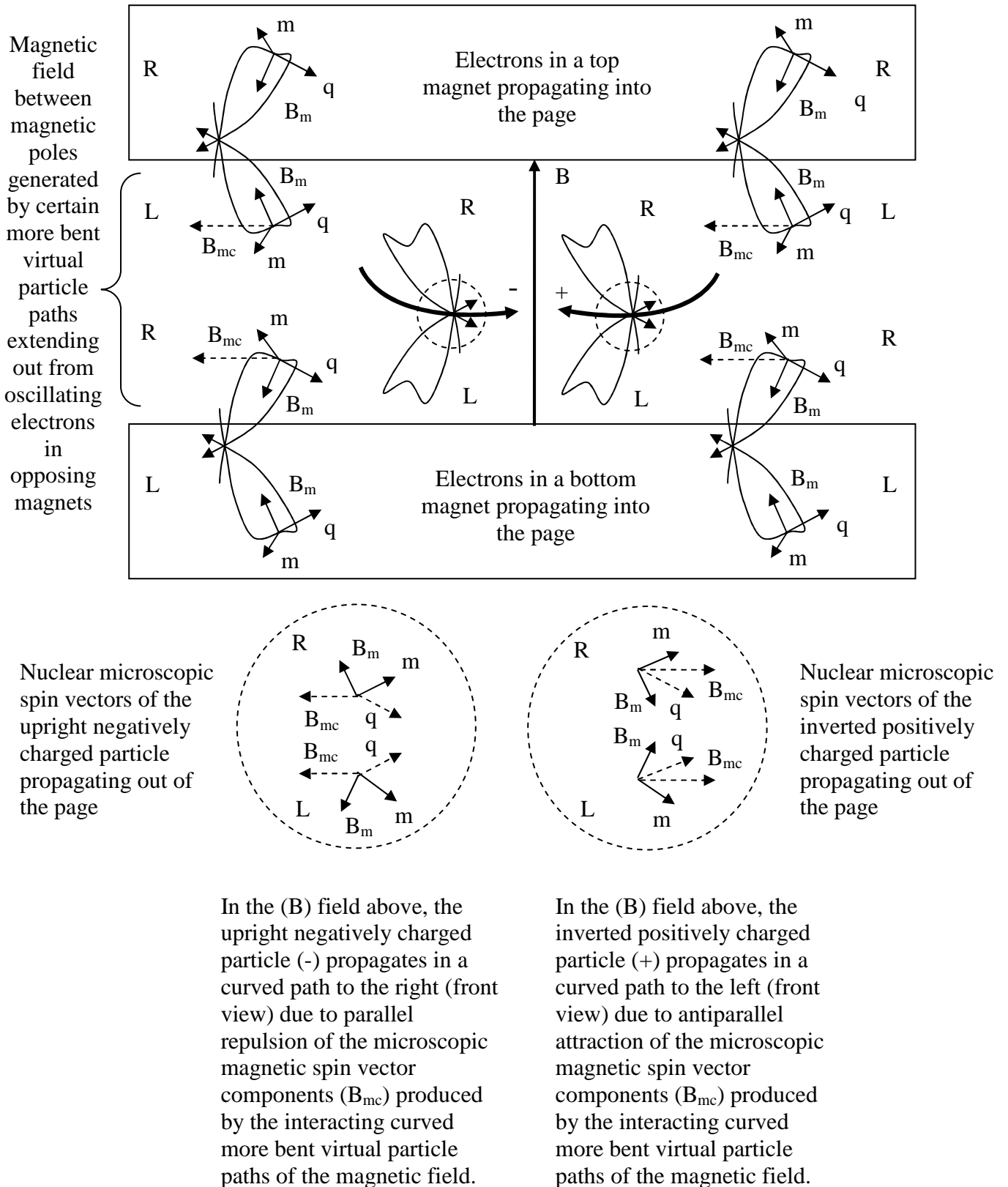
Magnetic field between magnetic poles generated by certain more bent virtual particle paths extending out from oscillating electrons in opposing magnets

Electrons in a top magnet propagating into the page

Electrons in a bottom magnet propagating into the page

Nuclear microscopic spin vectors of the upright negatively charged particle propagating out of the page

Nuclear microscopic spin vectors of the inverted positively charged particle propagating out of the page

In the (B) field above, the upright negatively charged particle (-) propagates in a curved path to the right (front view) due to parallel repulsion of the microscopic magnetic spin vector components (B_{mc}) produced by the interacting curved more bent virtual particle paths of the magnetic field.

In the (B) field above, the inverted positively charged particle (+) propagates in a curved path to the left (front view) due to antiparallel attraction of the microscopic magnetic spin vector components (B_{mc}) produced by the interacting curved more bent virtual particle paths of the magnetic field.

FIG. 38A

Figure (38B) shows the microscopic charge spin vector (q) and vertical microscopic charge spin vector component (q_c) of a right hand screw more bent virtual particle path of a portion of the magnetic field depicted in figure (38A) aligned with the charge spin vector (q) and vertical microscopic charge spin vector component (q_c) in the nuclear region of the right hand screw side of an upright negatively charged particle propagating in, and perpendicular to, the given portion of the magnetic field.

Magnetic field
portion

Upright negatively
charged particle
propagating to the
right
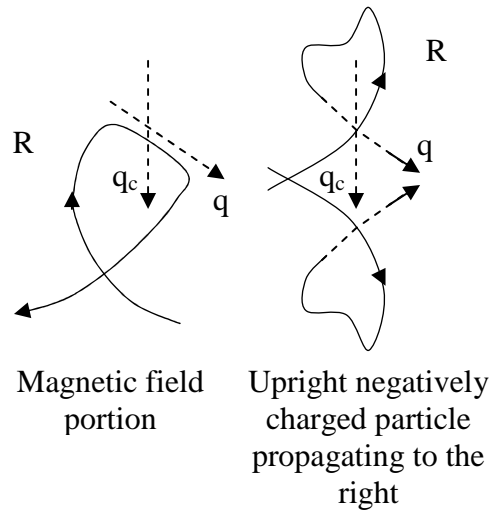
The microscopic charge spin vector (q) and
vertical component (q_c) of a portion of the
magnetic field shown in figure (38A) aligned
with the charge spin vector (q) and vertical
component (q_c) in the nuclear region of an
upright negatively charged particle propagating
to the right in, and perpendicular to, the given
portion of the magnetic field.

FIG. 38B

In application, for example, the spiral courses of negative and positive electrically charged propagating particles (and the undeflected course of neutral propagating particles) in, for example, a bubble chamber can be more

clearly understood.

NUCLEAR INTERACTION:

Figure (39) shows some orthogonal charge, mass, and magnetic microscopic spin vectors of example

virtual particle paths in the nuclear region of a static positively electrically charged particle, i.e., here, a static

proton. (Note that the distances which separate the virtual particle paths with respect to the origins of the spins

shown in figures 39-42B are arbitrarily drawn, and thus are not relevant in these cases.)
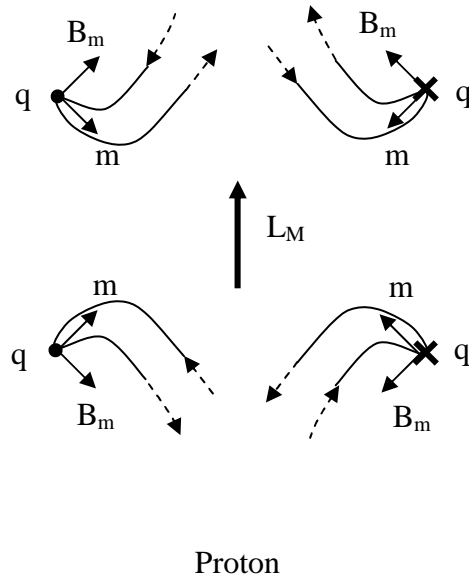

Proton

FIG. 39

Figure (40) shows some orthogonal charge, mass, and magnetic microscopic spin vectors of example virtual

particle paths in the nuclear region of a static negatively electrically charged particle, i.e., here, a static electron.
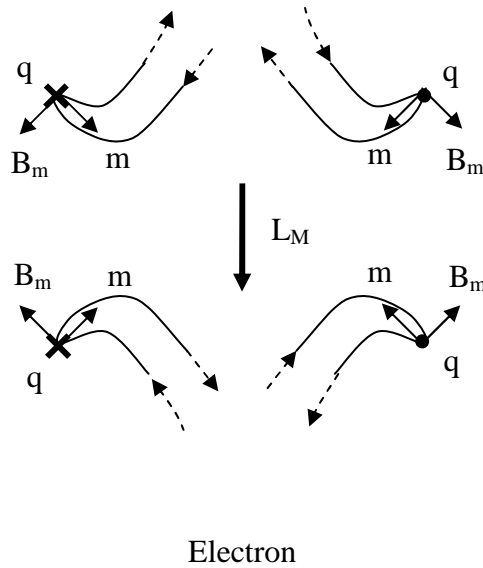
Electron

FIG. 40

Again, consider that the virtual particles in the virtual particle paths on the top, bottom, and top and bottom sides self interact as propagating electrically charged particles interact by way of the respective right-right and left-left hand (q), (m), and (B_m) spin vector interactions, and consequentially experience respective attractive, repulsive, or neutral alignment (internal bonding).

It is considered that a proton can bond with an electron to form a neutron as has been long argued by some in conventional physics. Figure (41A) shows the spin vectors which could exist for certain virtual particle paths of one side of an entirely isolated proton and electron before a possible "nuclear" interaction, and figure (41B) shows the alignment of the spin vectors of the virtual particle paths of one side of the proton and electron which could exist after forming a "nuclear bond" in the formation of a neutron.

Wherein, the microscopic spin vectors of the virtual particle paths of the proton and electron are considered to rotate around respective orthogonal rotational axes upon interaction for a proton-electron bond in the formation of a neutron as shown by the curved arrows in figure (41A), for example, for the microscopic magnetic and mass spin vectors rotating around the microscopic electric spin vector axes of the given example virtual particle paths. Accordingly, note how the accelerated condition of an electron in electron capture could facilitate the formation of a neutron.
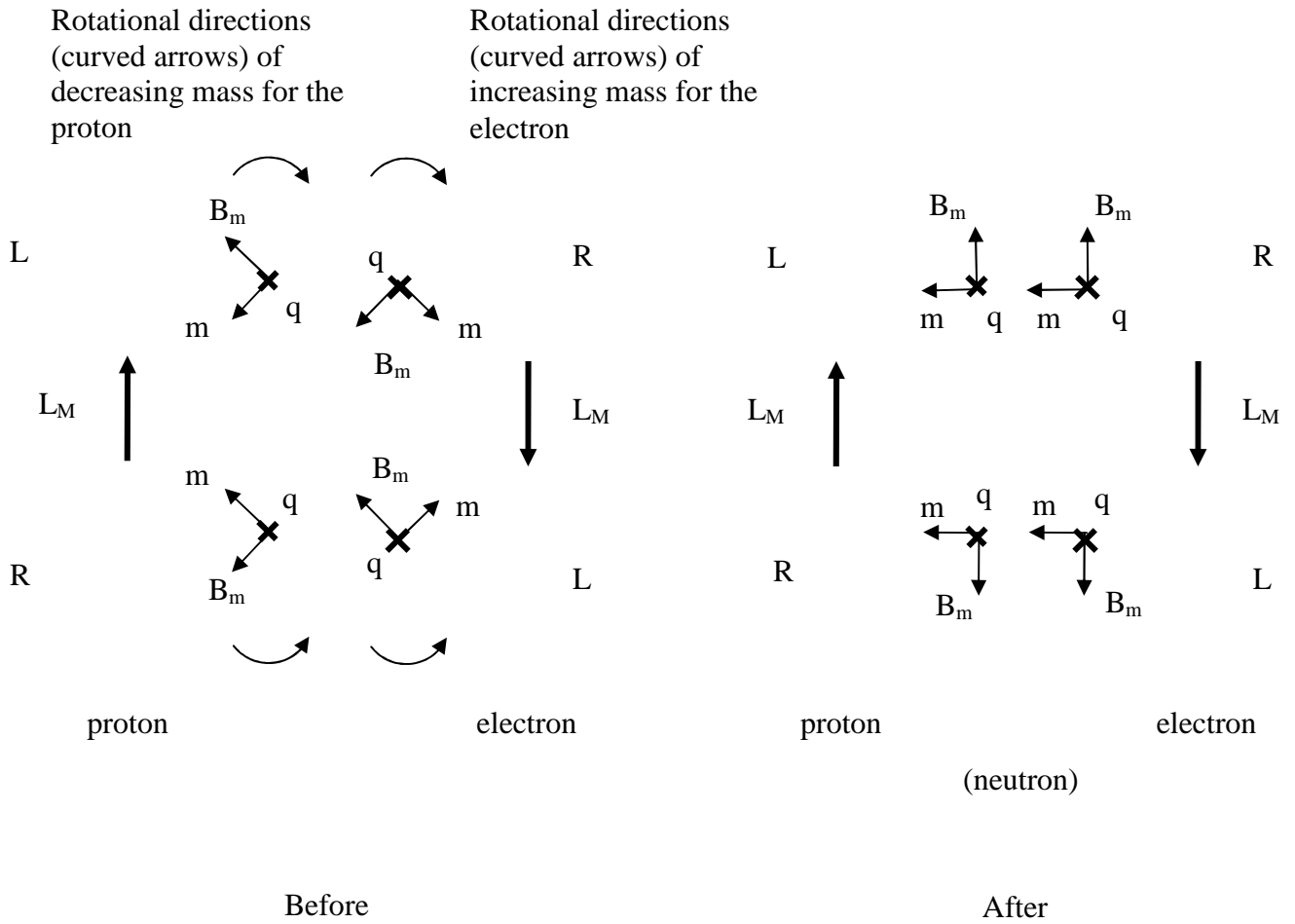
Rotational directions (curved arrows) of decreasing mass for the proton

Rotational directions (curved arrows) of increasing mass for the electron

FIG. 41A

FIG. 41B

Before

After

In the case of the proton-electron bond, the spin vectors are considered to rotate such that, in effect, there is a net increase in their total mass (an increase in mass for the electron and a lesser decrease in mass for the proton). In which case, for respectively interacting virtual particle paths positioned diagonally (right-right and left-left hand sides), the microscopic electric (q) and mass (m) spin vectors are respectively aligned parallel and attract, while the microscopic magnetic spin vectors (B_m) are aligned antiparallel and attract.

However, microscopic spin vectors of the virtual particle paths of a proton are considered to rotate around the orthogonal rotational axes upon interaction in the formation a proton-neutron bond as shown by the

curved arrows in figure (42A), for example, for the microscopic magnetic and mass spin vectors rotating around

the microscopic electric spin vector axes for the given example virtual particle paths.

Rotational directions (curved
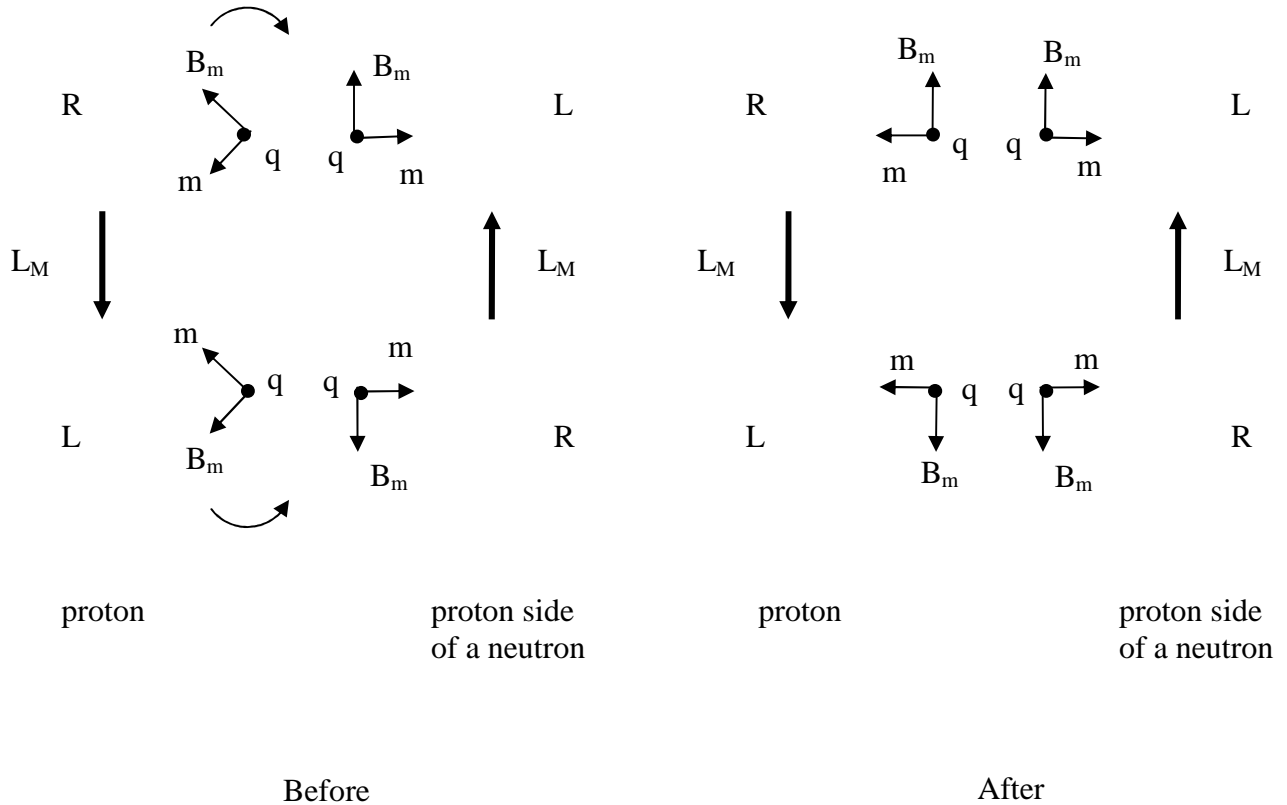arrows) of decreasing mass
for the proton

proton   proton side
                of a neutron

Before

FIG. 42A

proton   proton side
                of a neutron

After

FIG. 42B

In the case of the proton-neutron bond, the spin vectors of the newly bonded proton are considered to rotate to a less massive alignment such that, in effect, the total mass of the nuclearly bonded proton and neutron decreases so as to produce a mass defect. Wherein, for respectively interacting virtual particle paths positioned diagonally, the microscopic electric spin vectors (q) align parallel and thus attract, the mass spin vectors (m) align antiparallel and thus repel, and the microscopic magnetic spin vector (B_m) align antiparallel and thus attract.

Thus, the unified theory herein depicts the physical meaning of mass defect and binding energy.

Note that for the proton-neutron bond, microscopic spin vector alignments are equivalent to the alignments of the microscopic spin vectors during extranuclear interaction for the case of electromagnetic repulsion with gravitational "attraction" (in which case the respective gravitational attraction attempts to turn the particle around) for particles of the same electric charge as described for figure (18) before. This is considered the preferred alignment of such particles in both cases, but, in the case of nuclear bonding, this alignment of the microscopic spin vectors represents the electromagnetic attraction and the gravitational "repulsion" of nucleons, i.e., in the latter case, a form of mass repulsion or "antigravity" which, along with the other cases of mass repulsion described herein, addresses the essence of the longstanding issue in physics questioning the existence of the property of antigravity.

In this train of thought, the properties of the unified field, which include both attractive and repulsive aspects, the geometric distribution of the unified field, and the behavior of the unified field function, need to be considered when accounting for dark matter and dark energy. For example, consider starting with a sphere and a disk of the following dimensions:
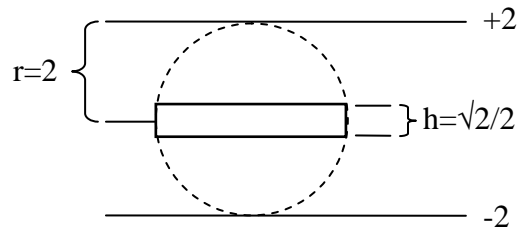

FIG. 16

such that the volume of the sphere is $\frac{4}{3}\pi r^3 = 33.49$ when r=2, and the volume of the disk is $\pi r^2 h = 8.88$ when r=2 and h=√2/2.

Accordingly, consider that the less bent virtual particle paths of the unified field of a galactic supermassive black hole occupy the volume of the disk, such that the galactic matter, which comprises ordinary matter potential and dark matter potential, amounts to 8.88/33.49=.265 or 26.5%, and this is 100% of the galactic matter potential (i.e., ordinary and dark matter potential). Wherein, 8.88*.1=.888 accounts for 10% of the galactic matter potential, which is galactic ordinary matter potential, and 7.992 accounts for 90% of the galactic matter potential, which is galactic dark matter potential comprising less bent virtual particle paths from the black hole. While, the remaining 73.5% is the dark energy potential comprises more bent virtual particle paths.

Respectively, consider, for example, a case in which a significant amount of less bent virtual particle paths from the top and bottom sides of a galactic supermassive black hole are concentrated along the event horizon, accretion disc, and beyond. Wherein, in effect, the electromagnetic and gravitational components of the virtual particle paths of the top and bottom sides of the black hole would present forces on ordinary matter (comprising positively and negatively charged ordinary matter), thus enabling the supermassive black hole to maintain the galaxy. In which case, the effective potential of the black hole would vary in geometry and magnitude radially from the center of the black hole, and would vary with the velocity of the orbiting matter. However, the attractive and repulsive aspects of the black hole, and their net outcome, would change as the spin vectors rotate in accordance with changes in the bends of the respective virtual particle paths of the black hole, such that the consumption of mass-energy by, and the expulsion of mass-energy from, the black hole would change the geometry, e.g., the more and less bent geometry, of the black hole, and therefore change the behavior of the black hole accordingly.

While still, it is considered that the black hole can have gravitational and electromagnetic interaction with another black hole according to the spin vectors of their respective virtual particle paths. In which case, the attractive and repulsive interaction between black holes as such needs to be considered when accounting for dark energy, the expansion of the Universe, etc. Here, regarding the accelerated expansion of the Universe, Big Bang theory, and figure (43), consider that as the unified field presented herein decreases in density, the virtual particle paths (gradients of the unified field) extend out farther, and, in the static form, bend more. Wherein, more bent virtual particle paths (dark energy) invert their respective microscopic mass and magnetic spin vectors, and more bent virtual particle paths can change their respective attractive and repulsive interactions, such that a decrease in the density of the unified field of a black hole can be associated with an increase in the expansion of the Universe which is expanding with momentum.

Nevertheless, continuing with the principles of nuclear bonding from before, the proton and electron in the neutron attract, and the sum of their masses is more than their resulting mass due to the rotations and realignments of their spin vectors. In which case, the electron is considered to "accelerate" (increase in mass) to a greater extent than the proton is considered to "decelerate" (decrease in mass) due to the disproportionate affect of the proton on the electron. While, the nuclearly bonded proton and neutron mutually attract, and yet, nevertheless, the sum of their masses is less than their resulting mass according to the rotations and realignments of the spin vectors of the decelerated proton.

As the spin vectors in a particle change alignment upon bonding, the virtual particle paths are redistributed in a denser manner for acceleration (resulting in an increase in mass), and are distributed in a less dense manner for deceleration (resulting in a decrease in mass). One geometric consequence of bonding, for example, is the occurrence of a certain amount of sideways bend that the extranuclear virtual particle paths experience in a nuclearly bonded proton in an atom comprising two or more nucleons due to the changes in the

trajectories of the virtual particle paths of a proton upon such vector realignments, such that, in result, the proper alignment for a respective orbital portion are produced.

Now, the energy of an electron antineutrino which is associated with the formation of a neutron is considered to be related to the acceleration ("compression") of the unified field of the bonded electron, and to the overall more massive condition which is respectively created due to changes in the electron's spin vector alignments and the redistribution of its respective virtual particle paths to an overall more dense condition. Wherein, when a neutron decays in the process of beta decay, the proton and electron separate, and the compressed unified field of the electron recovers to a respectively less compressed condition. In which case, it is considered that the energy of the electron antineutrino which is associated with beta decay corresponds to the release of the energy stored in the compressed unified field of the electron upon separation of the electron from the proton. Then, the antineutrino is produced from the resulting "accelerated" beta particle due to such changes (refer to the description of particle generation by acceleration later herein under the heading "PARTICLE TRANSMUTATION AND GENERATION").

ATOMS AND MOLECULES:

In conventional physics, the Pauli exclusion principle is considered to play a significant role in the structure and function of matter (or mass-energy) (e.g., in the stability of atoms). The present unified field theory shows how this is the case.

First, consider that the neutron assists in the bonding of protons according to the Pauli exclusion principle, which includes assisting in the manner of nuclear bonding described hereinbefore as required by the internal structure of electrically charged particles and the spin vector properties of their respective virtual

particle paths. In the example shown in figure (44), three protons can be bonded by the placement of an

electron between the two protons which have the same alignments of angular momenta. Wherein, one proton

and a respectively bonded electron act as a neutron. Note that the relative sizes of a proton and an electron in

figure (44) (and elsewhere) relate to mass not radius, and are for pictorial purposes.
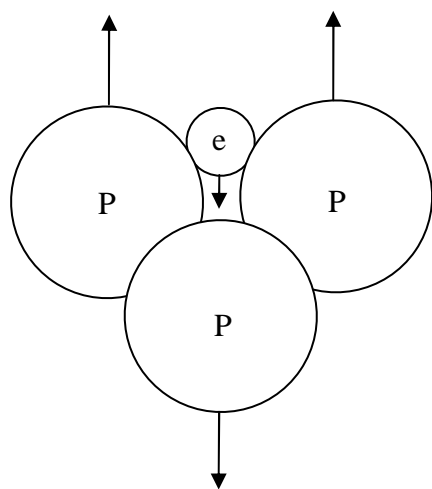
Bonding of protons with an electron according to the Pauli
exclusion principle (showing respective angular
momenta).

FIG. 44

Figures (45A) and (45B) show the nucleonic bonding in the (x-y) plane of a few nuclei in agreement

with the Pauli exclusion principle. In particular, in figure (45B), notice how, according to up and down

alignments, there is zero net angular momentum in terms of protons, and in terms of electrons, and also notice
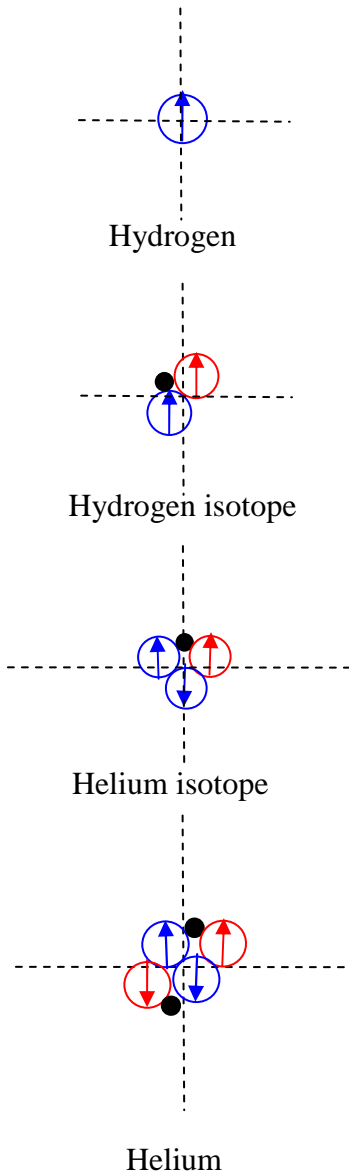
the respective quadrupole configuration of the protons.

Hydrogen

Hydrogen isotope

Helium isotope

Helium

FIG. 44A

(1s) and (2s) orbital
proton pairs (blue) along
the (x') and (y') axes,
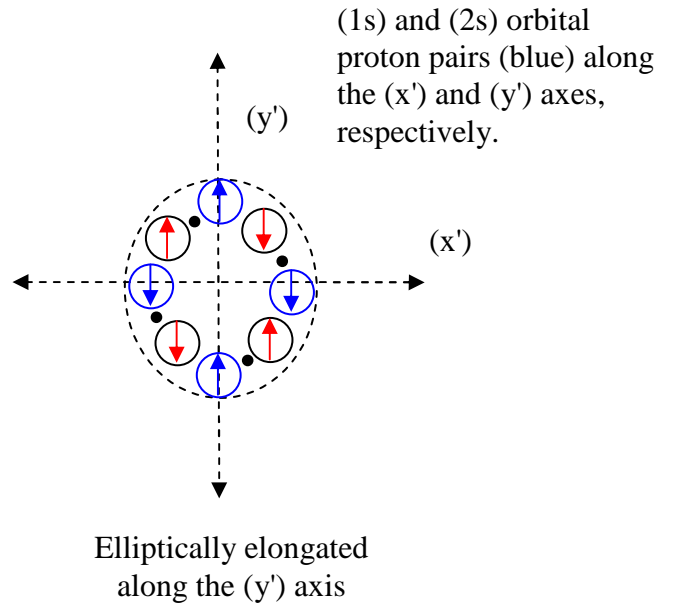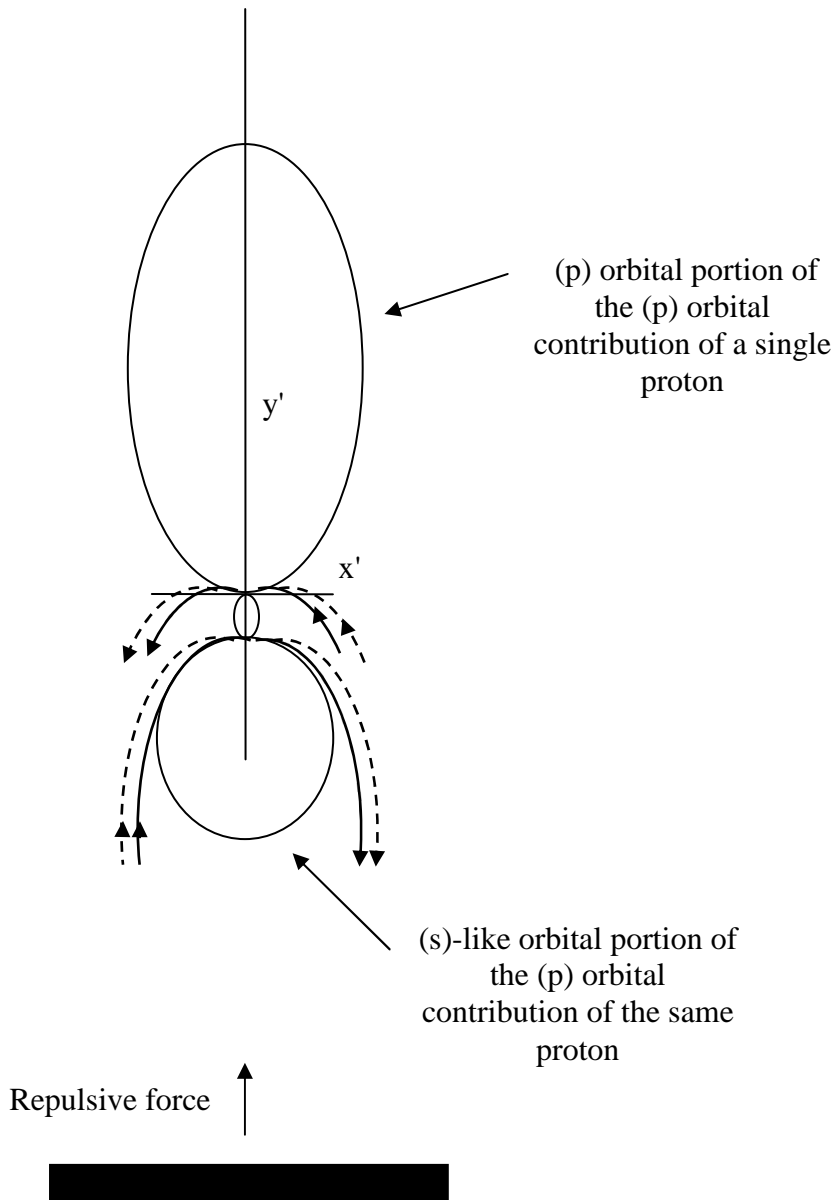respectively.

(y')

(x')

Elliptically elongated
along the (y') axis

FIG. 44B

Up proton (L_M directed out
of the page)

Up proton on proton side of neutron
(L_M directed out of the page)

Down proton (L_M directed
into the page)

Down proton on proton side of neutron
(L_M directed into the page)

● and • electron

Orbital proton and neutron positions are considered not only to be influenced by bond alignments, but are also considered to be influenced by nucleon proximity, in which case the repulsion of a proton by another proton or other protons, and the neutral presence of a neutron (or neutrons) are considered to affect proton positioning in the nucleus, and thus affect respective orbital positional potential energy. For example, in figure (45B) it is considered that the (1s) orbital is formed first with the (1s) protons along the (x') axis, and, subsequently, repulsion by the (1s) protons affect the potential (and respective spin vector angles) of the protons which attempt to form the (2s) orbital. In which case, repulsion rotates the spin vectors of the approaching protons, and they bond with neutrons at a slightly greater distance from the center than the (1s) protons (here, recall that microscopic spin vector alignments of a nuclearly bonded proton and neutron can be equivalent to the microscopic spin vector alignments, and the rotational directions thereof, of electromagnetic repulsion as described for figure 18, such that, here, electromagnetic repulsion and nuclear bonding can work together). Consequentially, an elliptically shaped octet of nucleons is formed. In result, the (2s) protons along the (y') axis have slightly greater positional potential energy than the (1s) orbital protons (as relates to their spin vector angles, virtual particle path distributions, position relative to the center of the nucleus, etc.), and thus fill after the (1s) orbital protons. Then, certain (p) orbital protons and neutrons form the next octet in the (x-y) plane, etc.

Now, orbital portions are considered to be affected asymmetrically by the repulsion of a proton (or protons) as shown in figure (46).

(p) orbital portion of
the (p) orbital
contribution of a single
proton

y'

x'

(s)-like orbital portion of
the (p) orbital
contribution of the same
proton

Repulsive force

Virtual particle paths of a proton experience acceleration and deceleration
rotations on opposite sides due to repulsion which correspond to a decrease
in mass and an increase in eccentricity on one side, i.e., the more eccentric
(p) orbital virtual particle paths on the top side in figure (46), and
correspond to an increase in mass and a decrease in eccentricity on the
opposing side, i.e., the less eccentric (s)-like orbital virtual particle paths on
the bottom side in figure (46). This process is equivalent to the process of
deceleration and acceleration on opposite sides of the nuclear region of a
positively charged particle due to electromagnetic repulsion by an irregular
distribution of positively charged particles as described with respect to
figure (18).

FIG. 46

With respect to figure (46), recall, still again, that the microscopic spin vector alignments of a nuclearly bonded proton and neutron can be equivalent to the microscopic spin vector alignments (and rotational directions thereof) of electromagnetic repulsion as described for figure (18). In this case, initially present protons (solid black rectangle) repel new protons, and thus a new proton bonds in an asymmetrical configuration, such that the virtual particle paths of each of the newly bonded protons experiences deceleration and acceleration rotations on opposite sides due to repulsion. Wherein, deceleration corresponds to a decrease in mass on one side (i.e., the top side in figure 46), and acceleration corresponds to an increase in mass on the other side (i.e., the bottom side in figure 46) as exemplified by the more eccentric (p) orbital virtual particle paths on one side (i.e., the less massive side) of the proton in contrast to those of the less eccentric (s)-like orbital virtual particle paths on the other side (i.e., the more massive side) of the proton, respectively.

Figure (47) shows (z) axis nucleon positioning.

(z) axis nucleon
positioning (shape per se
not shown)
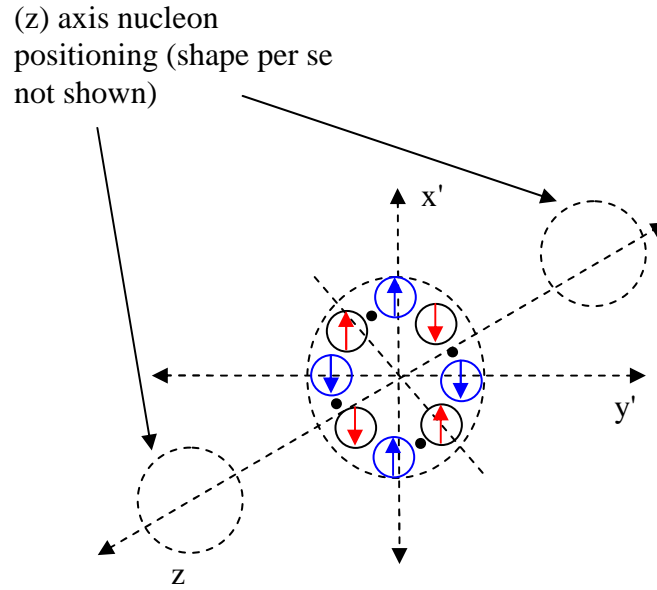
It is considered that in atoms with (z) axis nucleons, that nucleons along the
(z) axis establish certain terms which affect nucleon positioning in the
nucleus, such that, for example, certain (d) orbital bonding in the (x-y)
plane occurs along certain axes due to proton repulsion and neutral neutron
presence due to positioning of (d) orbital nucleons along the (z) axis.

FIG. 47

Figure (48) shows the (z) axis nucleon bonding of (p), (d), and (f) orbital nucleons on one side of the

(x-y) plane, while the configuration of the (z) axis orbital protons on the two sides of the (x-y) plane are

considered to symmetrically complement each other upon completion of a sub-shell. In which case, the

nucleonic bonding of (z) axis nucleons also occurs in agreement with the Pauli exclusion principle.

With respect to the (z) axis, as (s) and certain (p) orbital portions are constructed from the virtual

particle paths of two protons in the (x-y) plane, the central (z) axis orbital portions of (p), (d), and (f), etc.,

orbitals are constructed from (z) axis aligned versions of the same configuration of virtual particle paths as

those established by two opposing protons in the (x-y) plane, and certain other (d), (f), etc. orbital portions are

constructed from tilted versions (with respect to the z-axis) of the same configuration of virtual particle paths as those established by two opposing protons in the (x-y) plane. (Note that the "nesting" of orbital portions in the theory herein is considered to pertain to the ability of an electron to propagate in any orbital portion by switching virtual particle paths where virtual particle paths "combine.")
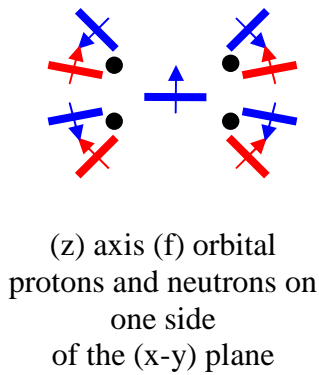
Central (z) axis (p) orbital
proton on one side of
the (x-y) plane
with a neutron on the same
side of the (x-y) plane and on
one side of the (y-z) plane

(z) axis (d) orbital
protons
which correspond to
tilted (z) axis (d) orbital
portions
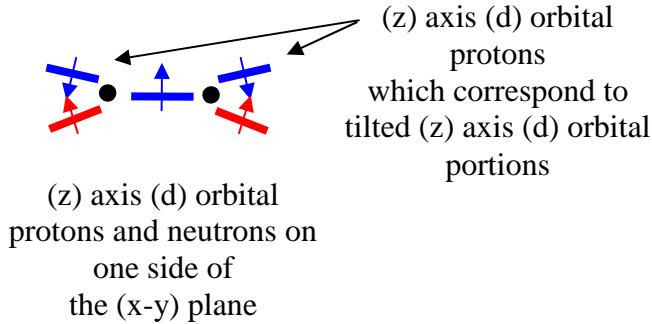
(z) axis (d) orbital
protons and neutrons on
one side of
the (x-y) plane

(z) axis (f) orbital
protons and neutrons on
one side
of the (x-y) plane

proton

Proton side of neutron

electron side of neutron

Here, the (z) axis nucleon bonding of (p), (d), and (f) orbital
nucleons is shown. As for the octets in the (x-y) plane, the (z)
orbital proton and neutron positions as shown are considered
not only to be influenced by bond alignments, but are also
considered to be influenced by the presence of protons and
neutrons along the (z) axis, and influenced by the presence of
protons and neutrons in the octets in the (x-y) plane.
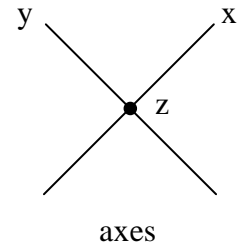
y   x

z

axes

FIG. 48

Figure (49) shows two (d) orbital nucleon configurations in the (x-y) plane which are considered to establish the $d_{x^2-y^2}$ and d_{xy} (d) orbitals.


$(d_{x^2-y^2})$ (d_{xy})

FIG. 49

It is considered that as atomic number increases so to does the repulsion and respective orbital eccentricity increase for newly bonded protons, and as the number of related nucleonic bonds increases for nucleons (i.e., as the number of sub-shell nucleons increases) so to increases the eccentricity of the resulting orbitals. While, the size of an orbital is considered to increase as the positional potential energy of an orbital increases according to its spin vector rotations (in the less massive direction) due to field repulsion and the number of related nucleonic bonds.

The (s) orbitals are considered to be bonded in nucleonic octets which are separate from the (p), (d), (f), etc. sub-shell protons bonded in nucleonic octets in the (x-y) plane which are considered to also have bonds with nucleons which are situated along the (z) axis (e.g., via the tilted alignment of the z-axis (d) orbital protons of a d-sub-shell extending virtual particle paths outward to respective nucleons of other (d) orbital sub-shell portions in the x-y plane). Wherein, in the example given, the (d) orbital nucleons bond while aligned so as to

pass over the relevant (s) orbital protons to some extent, i.e., (s) orbital protons are situated in field "pockets" so as to eliminate some repulsion. Thus, the (s) orbitals are considered to be less elliptical in shape, less asymmetric, and are considered to have less positional potential energy then, for example, (d) orbitals due to less field repulsion and a lesser number of related nuclear bonds, and fill first since they are produced by inner positioned nucleons with such attributes.

Next, the unified field theory shows in figure (50A) how the Pauli exclusion principle is involved in fine and hyperfine structure in a hydrogen atom. Figure (50A) shows a side view of one electron at any given time in the horizontal plane on the top or bottom side of the (s) orbital formed by a single non-nuclearly bonded proton (hydrogen atom). It is considered, for example, as shown in figure (50A), that the right hand screw virtual particle paths (top side) of a first inverted low energy electron could couple with (and be accelerated by) the less bent bottom right hand screw side virtual particle paths of the proton, such that the right hand microscopic magnetic spins (B_m) of the electron are antiparallel with right hand microscopic magnetic spins of the proton, and such that the electron would oscillate with its magnetic moment (u) antiparallel with the magnetic field (B_o) which it generates while orbiting (fine structure), and antiparallel with the macroscopic magnetic field (B_M) of the proton (hyperfine structure). While, as shown in figure (50A) at another time, an effectively upright high energy electron in the same (s) orbital could oscillate with its left hand (bottom side) microscopic magnetic spins (B_m) antiparallel with left hand microscopic magnetic spins of the more bent top left hand screw side virtual particle paths of the proton, and oscillate with its magnetic moment (u) parallel with the magnetic field (B_o) which it generates while orbiting (fine structure), and parallel with the macroscopic magnetic field (B_M) of the proton (hyperfine structure). Wherein, the more bent top left hand screw side virtual particle paths of the proton are considered to comprise higher positional potential energy than the less bent bottom right hand screw side virtual particle paths of the proton. (Note that the nuclear microscopic magnetic spins B_m of a propagating electron are relatively inverted due to spin vector rotations upon acceleration compared to those of a static electron.)

Upright electron (higher energy) propagating
into the page on a more bent orbital portion
on the top left hand screw side of the (s)
orbital of a hydrogen atom (shown in a plane
in a horizontally sectioned view). Note that
the direction of the electron is aligned by
factors including the bending of the virtual
particle paths of the proton.

B_M

u

B_o

B_m

B_m

left B_m

L (top)

R (bottom)

B_o

B_m

Right B_m

u

Inverted electron
(lower energy)
propagating out of
the page on a less
bent orbital
portion on the
bottom right hand
screw side of the
(s) orbital of a
hydrogen atom
(shown in a plane
in a horizontally
sectioned view).
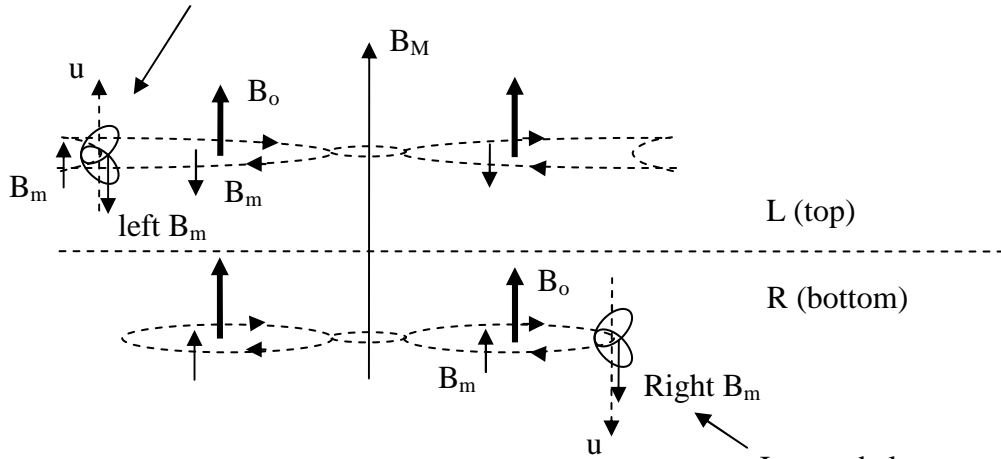
Electron at different times in more and
less bent orbital portions in the (s) orbital
of a hydrogen atom (shown in planes in a
horizontally sectioned view).

B_o Orbital magnetic field

u

R   L

L   R

u

Electrons with microscopic
magnetic spins (solid arrows)
and magnetic moments (u)
(dashed arrows)

and   Virtual particle path
microscopic magnetic spins (B_m)

FIG. 50A

A similar example of the role of the Pauli exclusion principle in the fine and hyperfine structure in the unified field is shown in an (s) orbital of an atom formed by two nuclearly bonded protons in figure (50B).

Upright electron (higher energy) propagating into the page on a top left hand screw orbital portion

Inverted electron (lower energy) propagating out of the page on a bottom right hand screw orbital portion

B_M B_M

B_o B_o

B_m B_m

B_m u

Left B_m

L (top)

R (bottom)

B_m B_o B_o B_m Right B_m

u
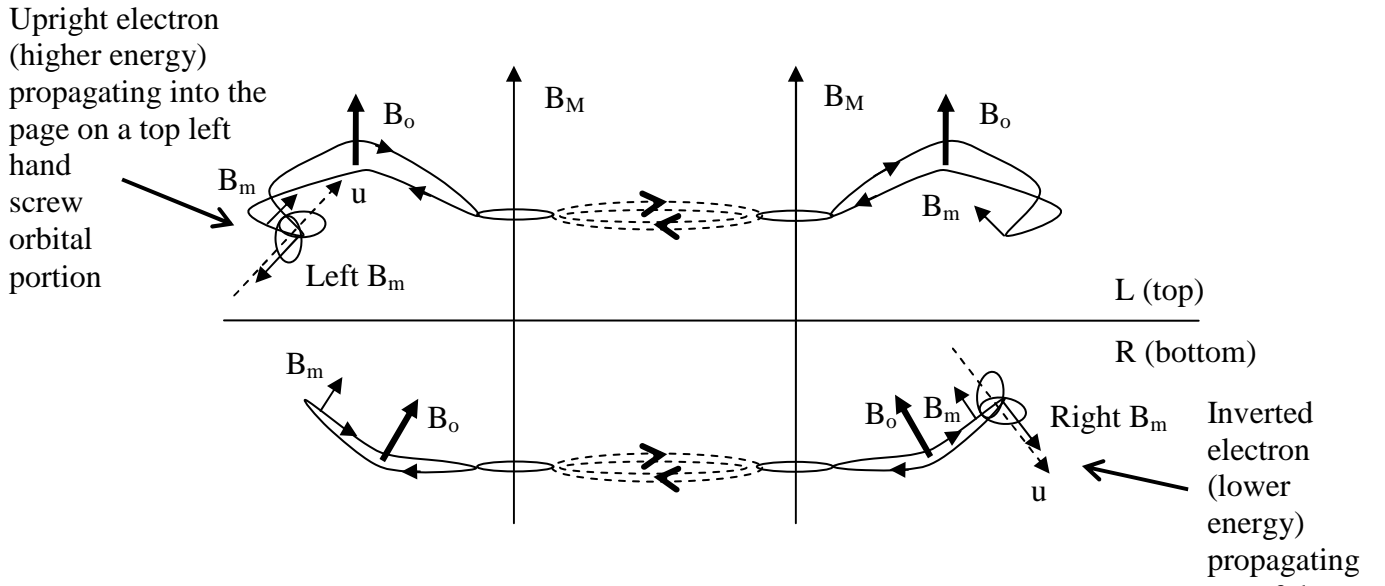
Electrons in orbital portions in an the (s) orbital produced from the combining of orbital virtual particle path portions from two protons. Wherein the combined portions, as in terms of "phase," include orbital portions extending out from each proton over combinable orbital portions of the other proton, in which case the interacting center portions are exclusively shown in duplicate in dashed line format. Note that the microscopic magnetic spins of the more bent virtual particle paths on the top left hand screw orbital portion invert the electron so that it is effectively upright, while the alignments of microscopic magnetic spins of the less bent virtual particle paths on the bottom right hand screw orbital portion effectively produce an inverted electron.

B_o Orbital magnetic field

u

R L

L R

and

Electrons with microscopic magnetic spins (solid arrows) and magnetic moments (u) (dashed arrows)

u

and Virtual particle path microscopic magnetic spins (B_m)
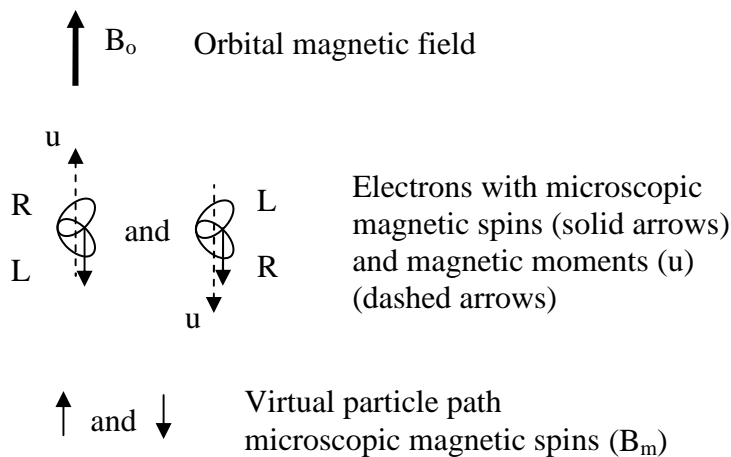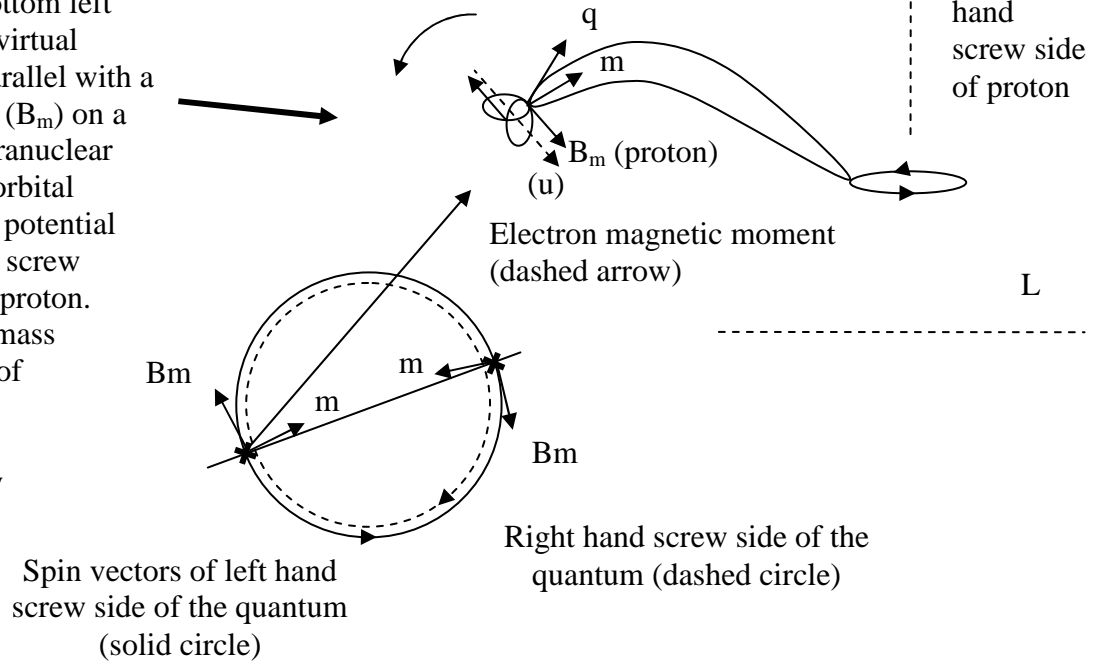
FIG. 50B

Still yet another example of the present unified field theory showing how electrons behave in atoms is illustrated in figure (51) which shows why electrons move outward from orbitals of lower to higher positional potential energy in atoms upon absorbing energy. In this case, figure (51) shows an electron oscillating with a left hand (bottom side) microscopic magnetic spin (B_m) antiparallel with the left hand microscopic magnetic spin of a "somewhat more bent" virtual particle path on the top left hand screw side of a nuclearly bonded proton (lower portion of the drawing), and shows the respective spin vector alignments of a quantum during absorption by the electron. Then, upon absorption, the quantum produces spin vector rotations in the electron so that the spin vectors of the electron rotate towards the alignment of the spin vectors of the "even more bent" virtual particle path of an orbital higher in positional potential energy, such that the electron then propagates on the respective orbital higher in positional potential energy. (Note that a similar process would occur for elevating an electron in a hydrogen atom, i.e., a non-nuclearly bonded proton.)

Inverted electron propagating into the page with a left hand microscopic magnetic spin (B_m) on a bottom left hand screw side "nuclear" virtual particle path aligned antiparallel with a microscopic magnetic spin (B_m) on an "even more bent" extranuclear virtual particle path on an orbital portion of greater positional potential energy on the top left hand screw side of the nuclearly bonded proton.
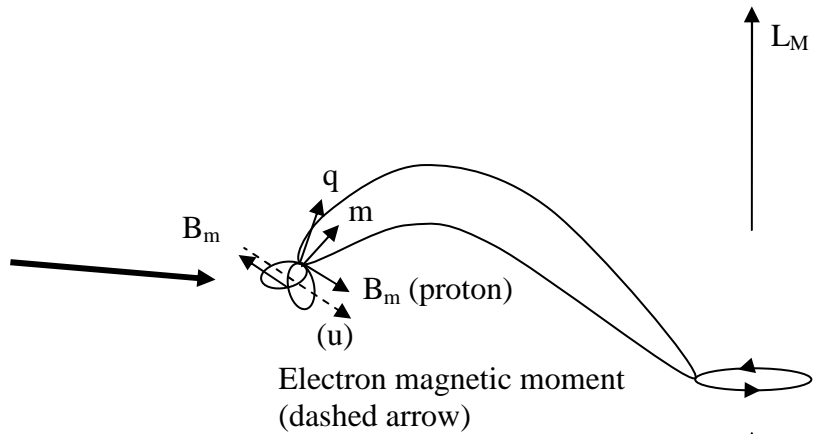
L_M

B_m

q

m

B_m (proton)

(u)

Electron magnetic moment (dashed arrow)

Inverted electron propagating into the page with a left hand microscopic magnetic spin (B_m) on a bottom left hand screw side "nuclear" virtual particle path aligned antiparallel with a microscopic magnetic spin (B_m) on a "somewhat more bent" extranuclear virtual particle path on an orbital portion of lesser positional potential energy on the top left hand screw side of a nuclearly bonded proton. Wherein, the microscopic mass and magnetic spin vectors of the electron are rotated in the direction of the curved arrow upon acceleration by the quantum.

Top left hand screw side of proton

q

m

B_m (proton)

(u)

Electron magnetic moment (dashed arrow)

L

Bm

m

m

Bm

Right hand screw side of the quantum (dashed circle)

Spin vectors of left hand screw side of the quantum (solid circle)

A matter quantum of electromagnetic radiation propagating into the page

Here, a quantum is absorbed by an electron in the extranuclear region of an orbital. Wherein, the directions of rotation for increases in positional potential energy for the virtual particle paths of the proton are in the same direction as the direction of rotation for an increase in mass for the electron. Thus, when the electron is accelerated by the quantum, and electron then couples with the virtual particle paths of an orbital at a different (greater) positional potential energy level, such that the electron propagates on the respective orbital higher in positional potential energy (wherein only certain details of the absorption of the left hand screw side of the quantum are shown).

FIG. 51

Next, the combinability of the virtual particle paths (in terms of "phases") of molecularly bonded protons is considered to occur according to the spin vector directions and effective interactions of their more and less bent virtual particle paths (which include electric repulsion). Figure (52A) (top view), and figure (52B) (side view), show (s) orbital sigma, and (p) orbital pi, molecular bonding and antibonding orbital localities of electrons (showing directions of electron propagation on respective molecular virtual particle paths (not shown). Wherein, the bonding and antibonding orbital localities are in agreement, in general, with convention.
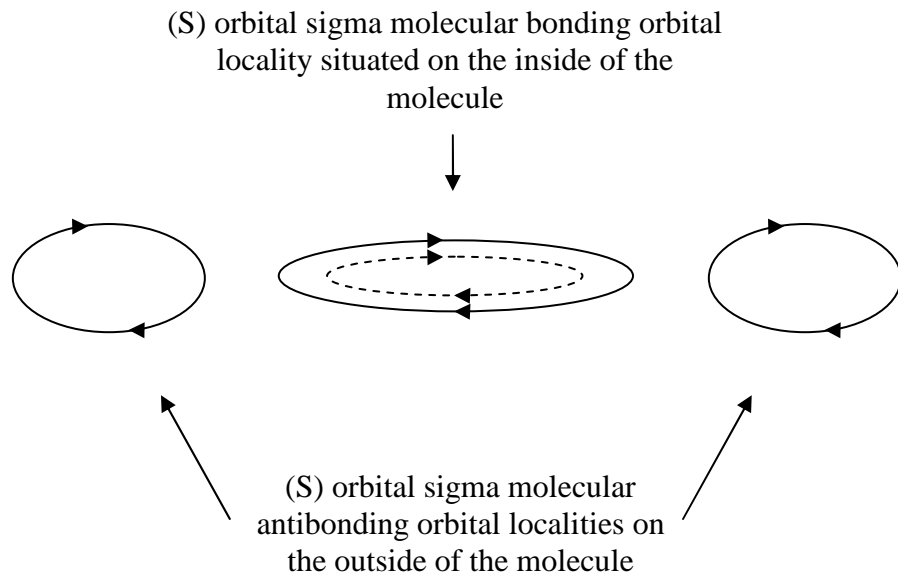
(S) orbital sigma molecular bonding orbital
locality situated on the inside of the
molecule

(S) orbital sigma molecular
antibonding orbital localities on
the outside of the molecule

FIG. 52A

Pi molecular bonding orbital
localities situated on the
inside of the molecule

Pi molecular antibonding orbital localities
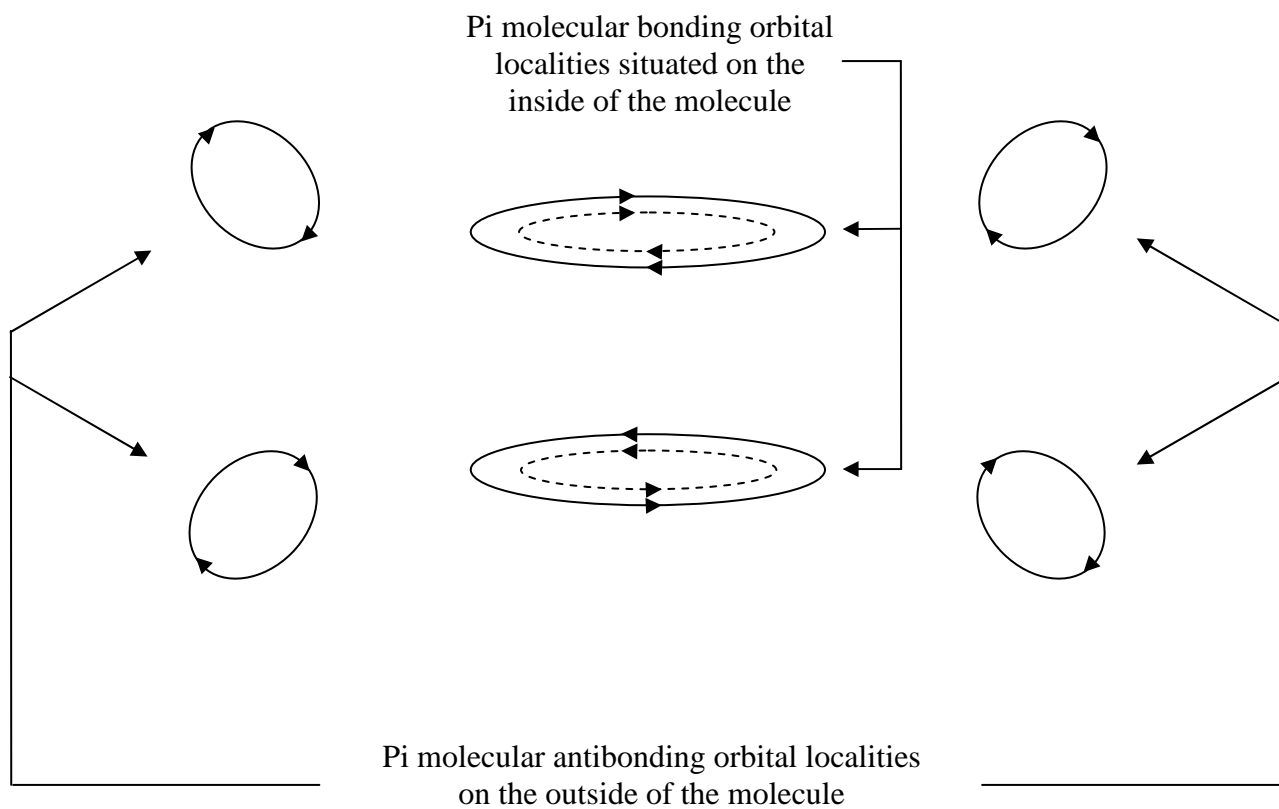on the outside of the molecule

FIG. 52B

It is worth noting here that a macroscopic collection of atoms is considered to produce virtual particle paths which extend out over a radial distance in direct proportion to their effective collective potential due to their respectively interacting virtual particle paths. While herein, similar to convention, electrons provide the means by which a collection of atoms, which comprises repelling protons, can group together.

PARTICLE TRANSMUTATION AND GENERATION:

Now, it is considered the vast diversity of particles which are produced in particle physics have a cause which transcends conventional theory which, if understood, would change the approach of conventional particle physics in its efforts to discover the underlying structure and function of mass-energy, and ultimately the Universe. Respectively, the cause of such a vast diversity of particles is considered to simply relate to the manifestations which are produced by the accelerations and decelerations of the mass-energy of the unified field presented herein.

Accordingly, first, in certain types of accelerations, a particle can transmute from one type of particle into another type of particle. For example, in one such type of "transmutational acceleration," the top and bottom sides of an electrically charged particle would rotate almost totally together so as to change into an electrically "neutral" particle. The transmutation of an electron and a positron into matter and antimatter quanta of electromagnetic radiation, respectively, upon annihilation is one example. In this case, the annihilating matter and antimatter are considered to interact in a symmetric manner so as to eliminate a significant extent of the eccentricities of their respective virtual particle paths, which includes the elimination of a significant extent of the bends in their respective virtual particle paths. Here, the annihilation process involves the effective rotation of each other's front and back virtual particle paths such that the front and back sides in each particle rotate in relatively the "same direction" with respect to its own internal structure (a process which is different

from the process described in figures 27A and 27B in which the front and back virtual particle path portions are effectively rotated in relatively opposite directions). Wherein, the virtual particle paths of the top and bottom sides of each electrically charged particle (e.g., the electron and positron in this example) internally converge, narrow, and project forward. In which case, the virtual particles on the top and bottom sides of the respectively produced quanta consequentially propagate away (while self interacting) with translational velocity (c).

It is considered that in another type of acceleration, that a neutral particle can produce two particles of opposite intrinsic spin and opposite electric charge while conserving electric charge, etc. as shown in figure (53). Wherein, for example, the top and bottom sides of an effectively electrically neutral gamma ray could, upon deceleration, open so as to produce an electron, in which case the top and bottom sides of the electron thus produced would split such that one portion would flip over so as to produce a positron of the opposite intrinsic spin and opposite electric charge, and the other portion would continue in the form of an electron, as in the case of pair production. Note that it is considered that a matter quantum differs from an antimatter quantum according to their different top and bottom side screw rotations, different top and bottom side microscopic magnetic spin (B_m) directions, etc., which is similar to how a negatively and a positively electrically charged particle differ. However, it is considered that an antimatter quantum can act in a manner which is equivalent to that of a matter quantum by the top and bottom sides flipping over upon being absorbed by, for example, an electron. Here, nevertheless, the production of oppositely charged particles (including the production of matter and antimatter) from an electrically neutral particle can be more profoundly understood by such a process.
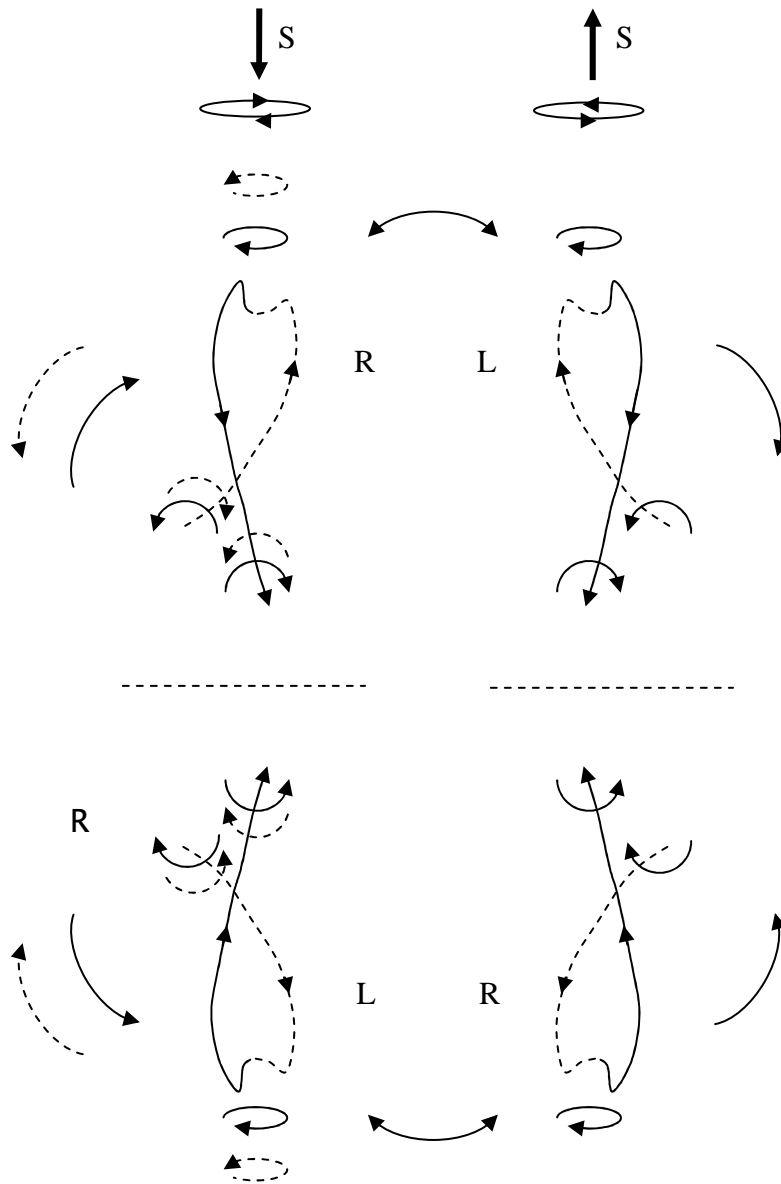
FIG. 53

In yet another type of acceleration, it is considered that a given electrically charged particle can emit another particle (e.g., during an oscillation).   Wherein, in one such acceleration, the top and bottom sides of the electrically charged particle would emit a particle from the nuclear region which would have top and bottom sides which are almost totally rotated together (e.g., as with a quantum of electromagnetic radiation).   In which

case, the top and bottom right and left hand screw sides of the emitted particle would be the same as the particle which emitted it, yet would comprise bands of virtual particle paths with spin vectors of different alignment (and eccentricity), such that the emitted particle would have neither an effective nuclear region nor an effective bend in its extranuclear field, and thus have neither an effective mass nor electromagnetically attract or repel in a effective manner (but electromagnetically, electrically, and gravitationally interact as mentioned previously).

In still yet another type of acceleration, the dipole pattern of electromagnetic radiation can be emitted by the virtual particles on the virtual particle paths of an accelerated electrically charged particle (e.g., a non-relativistically accelerated electron). Wherein, the structure and function of a virtual particle is considered to be analogous to that of an accelerated electrically charged particle as stated above. While, in even still yet another type of acceleration, the forwardly directed pattern of electromagnetic radiation from a relativistically accelerated electron in, for example, a synchrotron is considered to be produced by the virtual particles on the virtual particle paths of the forwardly aligned and somewhat rotated top and bottom sides of the respectively accelerated electron as the electron follows a helical course while effectively propagating forward in the magnetic field of the synchrotron.

CONCLUSION:

In conclusion, one unifying general function for a unified field has been provided with the application of Planck units which not only unifies all of the conventional fields and respective forces, but also unifies mass-energy and electric charge with "spacetime," and includes quantum field theory and relativity as well. Accordingly, the unifying principles were applied in a description of the geometry (including internal structure) and functionality of certain aspects of the unified field including certain aspects of the geometry and functionality of electromagnetic, gravitational, and nuclear interaction, certain aspects of the geometry and functionality of Lorentz transformations, and certain aspects of the structure and function of elementary particles (including antiparticles), atoms, molecules, and bodies of astronomical dimensions. In broadening, the resulting unified field theory proposes to also provide a basis for describing and solving problems in unified terms in other areas of physics which include subject matter which pertains to relevant "probabilistic" phenomena, chaos, big bang theory, and, in general, the Universe as a whole (including dark matter, dark energy, and the expansion of the Universe). While furthermore, it is proposed that the principles of the unified field theory presented are also applicable as a means of describing and solving problems in unified terms in other areas of the sciences.